

TWO QUADRANT CHOPPERS FOR DC MOTOR CONTROL

A Thesis Submitted
In Partial Fulfilment of the Requirements
for the Degree of
MASTER OF TECHNOLOGY

50858

by

SUDHANSHU SHEKHAR JOSHI

to the

DEPARTMENT OF ELECTRICAL ENGINEERING
INDIAN INSTITUTE OF TECHNOLOGY, KANPUR
AUGUST, 1982

JUN 1984

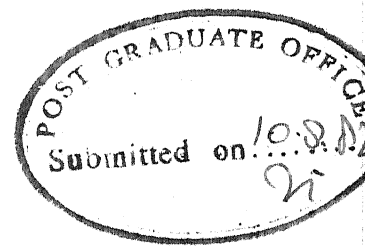
CENTRAL LIBRARY

Acq. No.

o. A 82867

EE-1982-M-305- TWO

82867



CERTIFICATE

Certified that this work 'Two quadrant Choppers for d.c. Motor Control' by S.S. Joshi is carried out under my supervision and is not submitted elsewhere for a degree.

Aug, 1982

— KJ —
(G.K. Dubey)
Professor
Department of Electrical Engineering
Indian Institute of Technology
KANPUR

गुरुचरणं समर्पयामि

आकर्षक अभिव्यक्ति

—धन्यवाद

ACKNOWLEDGEMENT

I am deeply indebted to adorable , magnanimous Dr. G.K. Dubey for making me to come out with best of my capabilities in the course of completion of the thesis. I can offer here only an inadequate acknowledgement of my appreciation.

I express my sincere gratitude to Dr. S.R. Doradla and Dr. A. Joshi for their very helpful and encouraging attitude.

I thank altruist Bhat, who always helped me at the cost of his own work, with all my sincerity. Thanks to Mr. Patel, Mr. Punacha, Prasad and Kumar for their contribution to this work. Thanks to all the young friends for being very kind to me.

I thank all the staff members of electrical engineering faculty, Sharma, Arora, Ghorpade and Imran Khan in particular for their help in carrying out this work smoothly.

I am very thankful to Arvind Ashwini and Aithani for their help in giving final shape to this thesis. Thanks are due to Mr. J.S. Rawat for his excellent typing and Mr. Gupta for his excellent drawings.

I acknowledge from the core of my heart to everybody around for creating a congenial atmosphere and making my stay at I.I.T. enjoyable as well as fruitful.

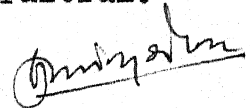

(Sudhanshu Shekhar Joshi)

TABLE OF CONTENTS

	Page
CHAPTER 1 INTRODUCTION	1.1
CHAPTER 2 A TWO QUADRANT CHOPPER WITH AN IMPROVED COMMUTATION CIRCUIT	2.1
2.1 Introduction	2.1
2.2 Commonly used commutation schemes	2.4
2.3 The developed chopper circuits	2.10
2.4 Analysis and performance of the proposed chopper	2.11
2.5 Design criteria	2.31
2.6 Analysis of the performance of the motor fed by the developed chopper	2.33
2.7 Experimental verification	2.51
2.8 Conclusion	2.51
CHAPTER 3 COMPARATIVE STUDY OF CHOPPERS	3.1
3.1 Introduction	3.1
3.2 Control approaches	3.3
3.3 Chopper performance analysis for a highly inductive load	3.5
3.4 Motor load	3.11
3.5 Comparison between the three different control approaches	3.44
3.6 Conclusion	3.57
CHAPTER 4 CONCLUSION	4.1
APPENDIX	
REFERENCES	

ABSTRACT

The present work deals with some aspects of two quadrant choppers for a dc separately excited motor.

A two quadrant dc chopper, with an improved commutation scheme has been developed for realising the forward motoring and regenerative braking operation. This chopper circuit has been analysed, designed, fabricated and tested for its performance. Equations have also been derived for the calculation of the motor performance. Calculated results are compared with the experimental results.

The next part of the thesis deals with the comparative study of three different schemes of dual chopper capable of providing positive current and voltage in either direction. Two types of loads have been considered - the one where current can be assumed ripple free and a dc separately excited motor. Both source and the load performance are critically examined. All the results are presented in terms of normalised variables, so that they can be used for a dc separately excited motor of any specification. Boundaries between the continuous and the discontinuous conduction are drawn for all the three cases, to facilitate the design of filter inductance.

NOMENCLATURE

V_L	instantaneous value of load voltage, volts
V	supply voltage, volts
T	time period of switches, seconds
t_{on}	on time of switches, seconds
δ	duty cycle of switches
V_{av}	average value of load voltage, volts
V_{rms}	rms value of output voltage, volts.
i_s	source current, A
T_1	on period of switches S_1 and S_2 for approach-2 under motoring operation, sec.
L	inductance of the motor armature, henery
R	resistance of the motor armature, ohms
i_a	instantaneous value of the armature current, A
I_{av}	average value of the armature current, A
E	back emf, volts.
I_{min}	minimum value of the armature current, A
I_{max}	maximum value of the armature current, A
τ	armature time constant, sec
T_p	T/τ , normalised time period
m	E/V , normalised back emf
K_T	torque constant
K_V	back emf constant

$I_{av(norm)}$	normalised value of I_{av}
$I_{min(norm)}$	normalised value of I_{min}
$I_{max(norm)}$	normalised value of I_{max}
E_c	critical value of back emf, volts.
m_c	normalised value of back emf
ω_c	critical speed, rps
T_{av}	average torque
L_c	commutation circuit inductor, H
C	commutation capacitor, F
ω	speed rps

CHAPTER 1

INTRODUCTION

Two quadrant choppers capable of providing forward motoring and regenerative braking operation find application in main line traction, battery operated vehicles and high performance speed control systems. Saxena [7] has done a comparative study of dual choppers capable of providing forward motoring and regenerative braking operation. He has shown that two quadrant chopper with simultaneous control does not give discontinuous conduction, and thus offers advantages in terms of good speed regulation and fast transient response at all loads. In this thesis, a two quadrant chopper circuit with simultaneous control, to provide forward motoring and regenerative braking operation, has been developed. This chopper circuit utilises the commutation scheme proposed by Sriraghvan, Pradhan and Revankar [1] for a half bridge inverter.

A two quadrant chopper capable of giving positive current and voltage in either direction is suitable for regenerative braking of a.c. drive using current source inverter, regenerative magnetic power supplies and the forward motoring and reverse braking of d.c. separately excited motor in crane applications. Three control schemes

are compared for two types of loads (a) when load current is ripple free and (b) a d.c. motor load. The results are presented in terms of the normalised variables so that they can be used for any load.

The new two quadrant chopper circuit with simultaneous control is described in Chapter 2. It has been analysed and design equations have been derived. Motor performance equations have also been derived. It has been fabricated and tested with a 3 h.p., 220V d.c. separately excited motor. Various theoretical deductions are verified experimentally.

In Chapter 3, three control approaches are described for the dual chopper capable of giving positive current and the voltage in either direction. The performances at the source and the load terminal have been compared for all the three approaches and two types of loads namely (a) a highly inductive load and (b) a motor load, are considered.

For the highly inductive load the comparison is done for source current ripple and output voltage ripple. For the motor load, comparison is based on the amount of armature current ripple, nature of torque speed characteristics, zone of discontinuous conduction and the amount of

source current harmonics. Armature current ripple is a measure of derating of the motor. Zone of discontinuous conduction in the torque-speed characteristic is the indicator of motor performance at light loads. The amount of source current harmonics tells about interference with the nearby communication system and possibility of generation of beat frequency. Number of commutation cycles per output cycle is also considered as it gives an idea of the switching losses. The results are presented in the normalised variables. Boundaries between zones of continuous and discontinuous conduction have been drawn, to facilitate the design of a filter inductance.

CHAPTER 2

A TWO QUADRANT CHOPPER WITH AN IMPROVED COMMUTATION CIRCUIT

2.1 Introduction:

A dual chopper with an improved commutation and capable of giving positive voltage and current in either direction is described here. Such a chopper circuit can be used for control of dc motor during forward motoring and regeneration. Some of the commutation schemes proposed in the past have been compared in brief for reference. All the half bridge inverters can be modified into a dual chopper, giving positive voltage and current in either direction. The commutation schemes of Mc-Murray - Bedford inverter and McMurray inverter are discussed in brief, in this context. The commutation scheme proposed by Sriraghvan, Pradhan and Revankar [1] incorporates merits of both the Mc-Murray- Bedford inverter, employing common bus complimentary impulse commutation method and the Mc-Murray inverter employing auxiliary parallel current commutation method. This half bridge inverter circuit has been modified into a dual chopper. Analysis of this chopper circuit has been carried out in detail.

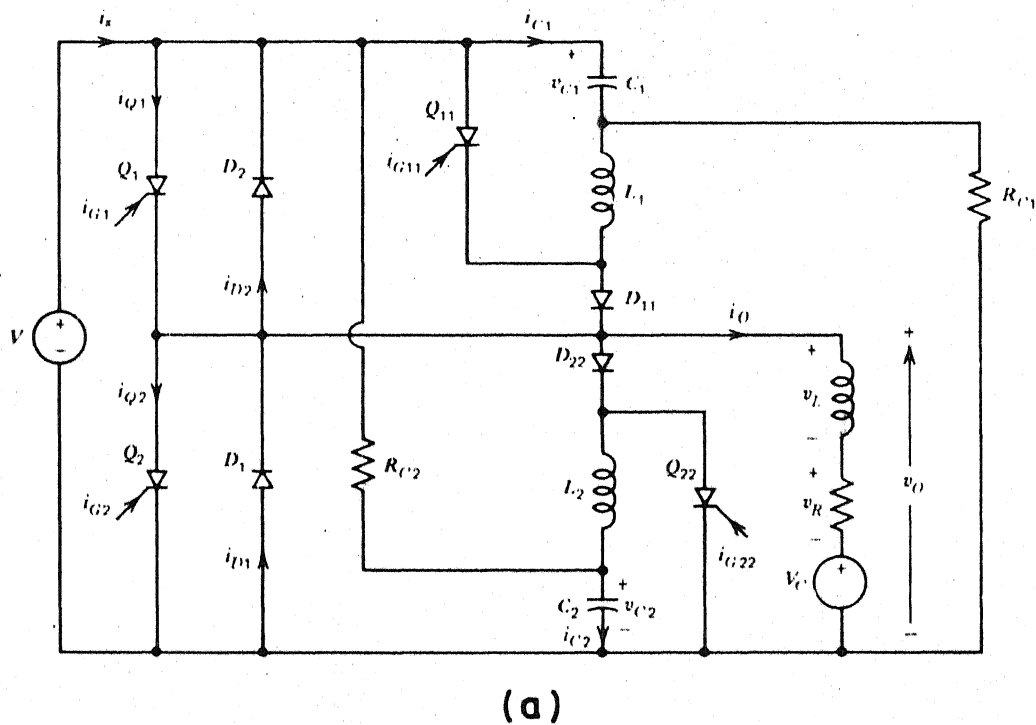
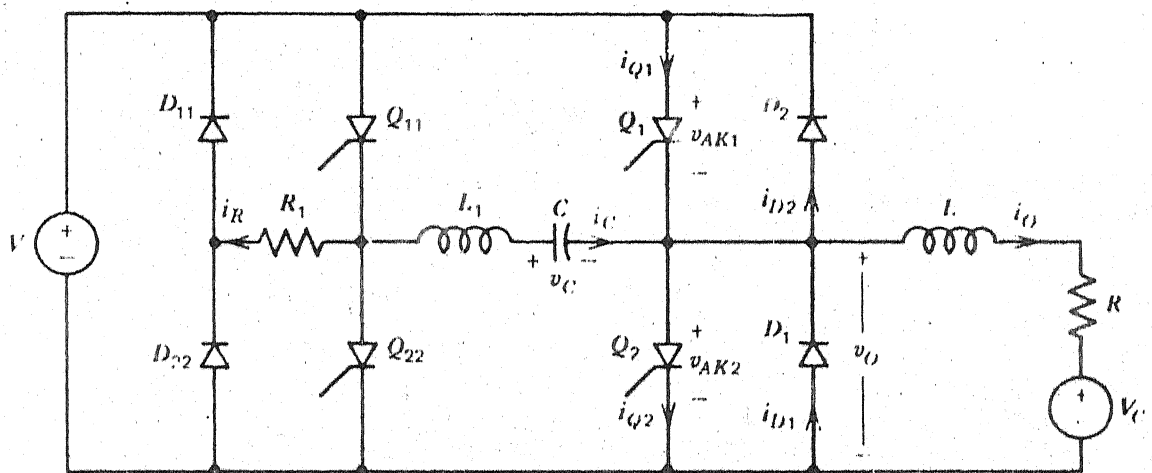


FIG. 2.1. COMMONLY USED COMMUTATION SCHEME.



(b)

Fig. 2.1 (contd.)

A dual chopper employing this commutation scheme has been designed for a 3 hp, 220V dc motor and its performance has been studied.

2.2 Commonly used Commutation Schemes:

Two commutation schemes for dual chopper, capable of giving first and second quadrant of operation are discussed in Reference [2]. First, the type-1 current commutation scheme (Ref. Fig. 2.1(a)) uses separate commutation circuits for main thyristors Q_1 and Q_2 . It has following drawbacks.

- a) Large number of semiconductor switches, capacitors and inductors are employed resulting in higher cost.
- b) Commutation method involves losses due to use of resistances.
- c) Circuit demands that delay equal in length to the commutation interval must elapse between the end of the gating signal for one main thyristor and the beginning of the gating signal for the other. This is a constraint over the maximum ^{obtainable} frequency.

Second scheme, the type-2 current commutation scheme or modified McMurray circuit for (Ref. Fig. 2.1(b)) chopper,

uses same L_1 , C and R_1 for both Q_1 and Q_2 . So cost and commutation losses are reduced.

Point (c) mentioned in the case of first scheme are valid here also.

Laha [5] proposed modifications in type-1 current commutation scheme (Fig. 2.1(c)). He used the same auxiliary parallel current commutation circuit for both T_1 and T_2 . Resistance used in type-1 current commutation scheme [2] is not used in the circuit proposed by him. Connections shown are for the motoring operation. To change-over to reverse regeneration, connections A-P and B-Q are changed to A-Q and B-R. At the same time pulses are withdrawn from T_1 and applied to T_2 after few chopping cycles. Pulses to T_3 are maintained as such. This scheme offers advantages in terms of reduction in cost, simplicity of the firing circuit and improvement in efficiency. But this scheme suffers from the drawback that there is no path for the overcharge on the capacitor to discharge and thus for a high Q circuit specially, indefinite charge build-up on the capacitor takes place. However with a proper design this feature can be used with an advantage.

The half bridge inverter circuits, can be modified into a dual chopper capable of providing forward motoring

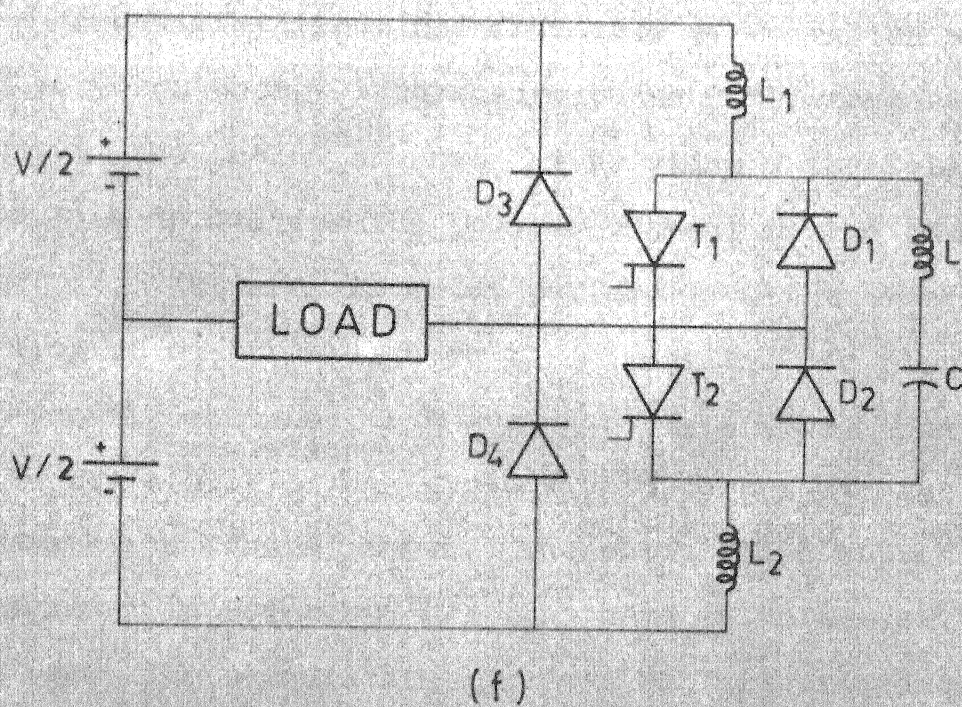
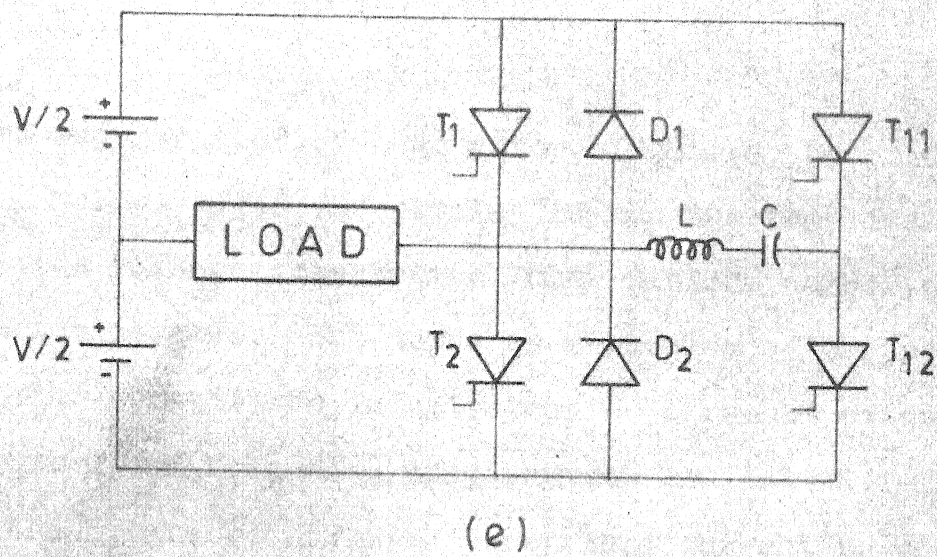


FIG. 2.1 (contd.)

and regeneration of a dc motor. McMurray-Bedford inverter (Fig. 2.1(d)) employing common bus complimentary series voltage commutation, uses minimum number of semiconductor devices. But there is a problem of trapped energy in the commutation inductances, as a result efficiency is reduced and frequency of operation is limited. Inductor L_1 and L_2 are required to carry load current on continuous basis and therefore their current rating is high.

McMurray inverter, using common bus auxiliary parallel current commutation as compared to McMurray Bedford inverter has higher efficiency and frequency of operation because of very low energy interchange between the commutation circuit and the dc source. It provides a local loop isolated from the dc bus for the impulse current in the commutation circuit. McMurray inverter suffers from the disadvantage of piling up of the charge on the capacitor. It also needs a special sequence for charging of capacitor. Modified McMurray/commutation scheme has already been described as 'type-2 commutation scheme' above. The commutation schemes discussed in Reference [2] also have advantage of low trap energy. The commutation loss can be further reduced by pumping back part of the excess energy in the commutation circuit to the dc supply.

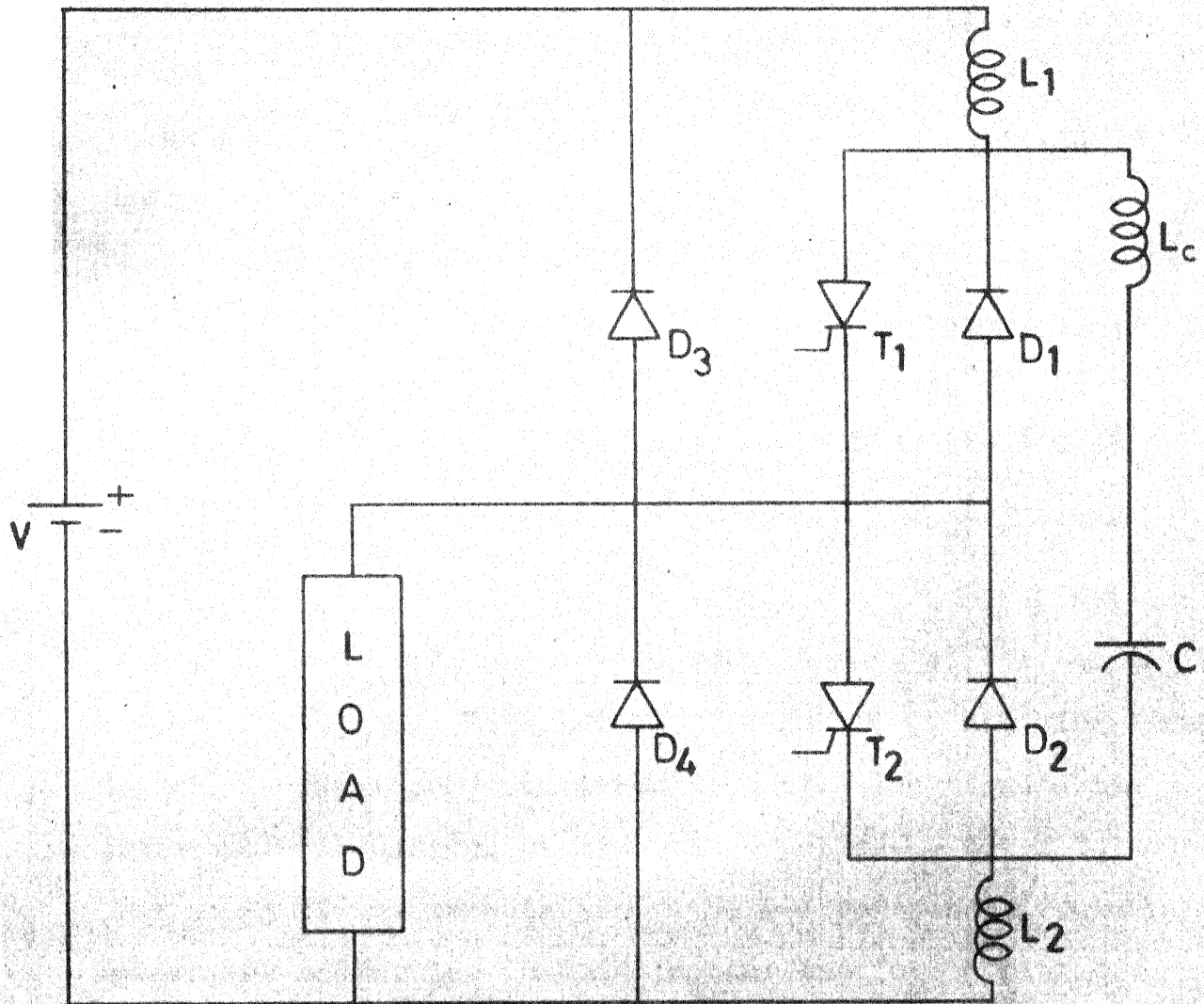


Fig.2.2 Proposed two quadrant chopper with simultaneous control.

The half bridge inverter proposed by Sriraghvan, Pradhan and Revankar [1] uses saturable inductors to support the dc bus voltage during the commutation and to reduce the trapped energy in the commutation circuits to a low value (Ref. Fig. 2.1(f)). It uses the thyristor T_1 and T_2 as main as well as the commutation thyristor. It does not need any special sequence for charging of capacitor as required in the case of McMurray inverter and commutation schemes discussed in reference [2] and [5]. Here this half bridge inverter has been modified into a dual chopper (Ref. Fig. 2.2),

2.3 The Developed Chopper Circuit:

Thyristor T_1 and T_2 act both as main as well as commutation thyristors. T_1 is fired to turn off T_2 and vice versa. L_c and C form the commutation circuit. The commutation capacitor C is always charged to dc voltage V prior to the beginning of any commutation. The L-C resonant circuit generates an impulse commutating current for turning off T_1 and T_2 . D_1 and D_2 are the commutation diodes. D_3 and D_4 are the feedback diodes.

L_1 and L_2 are saturable reactors which support the dc bus voltage during commutation and thus reduce the trapped energy in the commutation circuit. The saturable reactor in series with the conducting thyristor saturates

when carrying the load current and therefore offers negligible impedance during the major portion of the load current carrying interval. The other inductor in series with the nonconducting thyristor is unsaturated. When the blocking thyristor is fired, L_C -C commutation circuit forms local loop through T_1 and T_2 . The unsaturated inductor blocks the dc voltage throughout the commutation interval and isolates the commutation circuit from the dc bus.

The developed dual chopper is superior to the dual choppers discussed in reference [2] and [5] in terms of the ^{overall} cost and simplicity of the firing circuit. Discontinuous conduction does not exist, and hence speed regulation is good and faster transient response is obtainable at all loads. This is suitable for a battery operated vehicle [5] and main line traction application.

2.4 Analysis and Performance of the proposed Chopper:

Following assumptions are made for the analysis of the proposed chopper circuit.

1. Diodes and thyristors are ideal switches.
2. Length of the commutation interval is negligible in comparison to electrical time constant of the load, so load current during commutation interval is assumed constant.

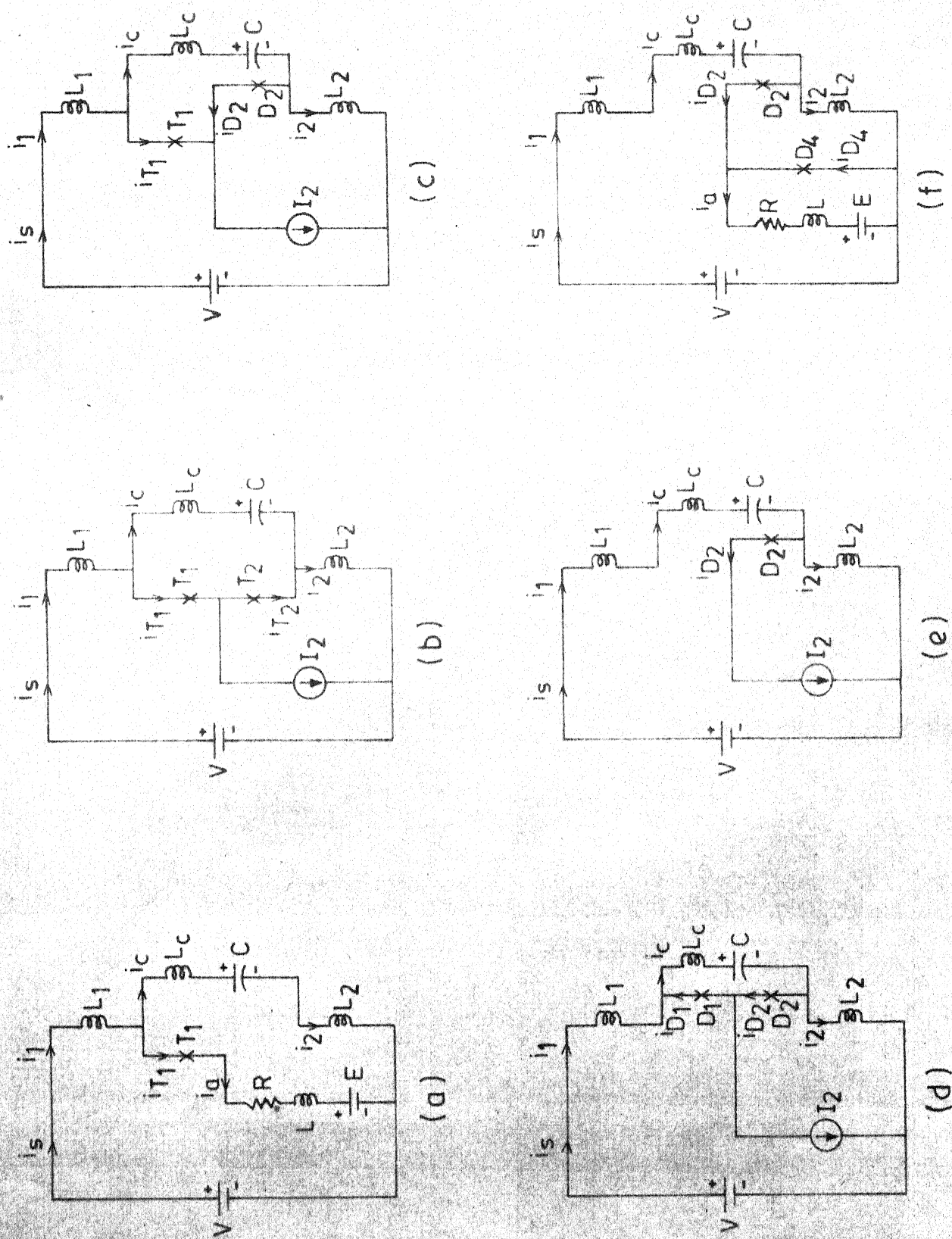


FIG. 2.3. MODES OF OPERATION PRESENT IN THE PROPOSED CHOPPER.

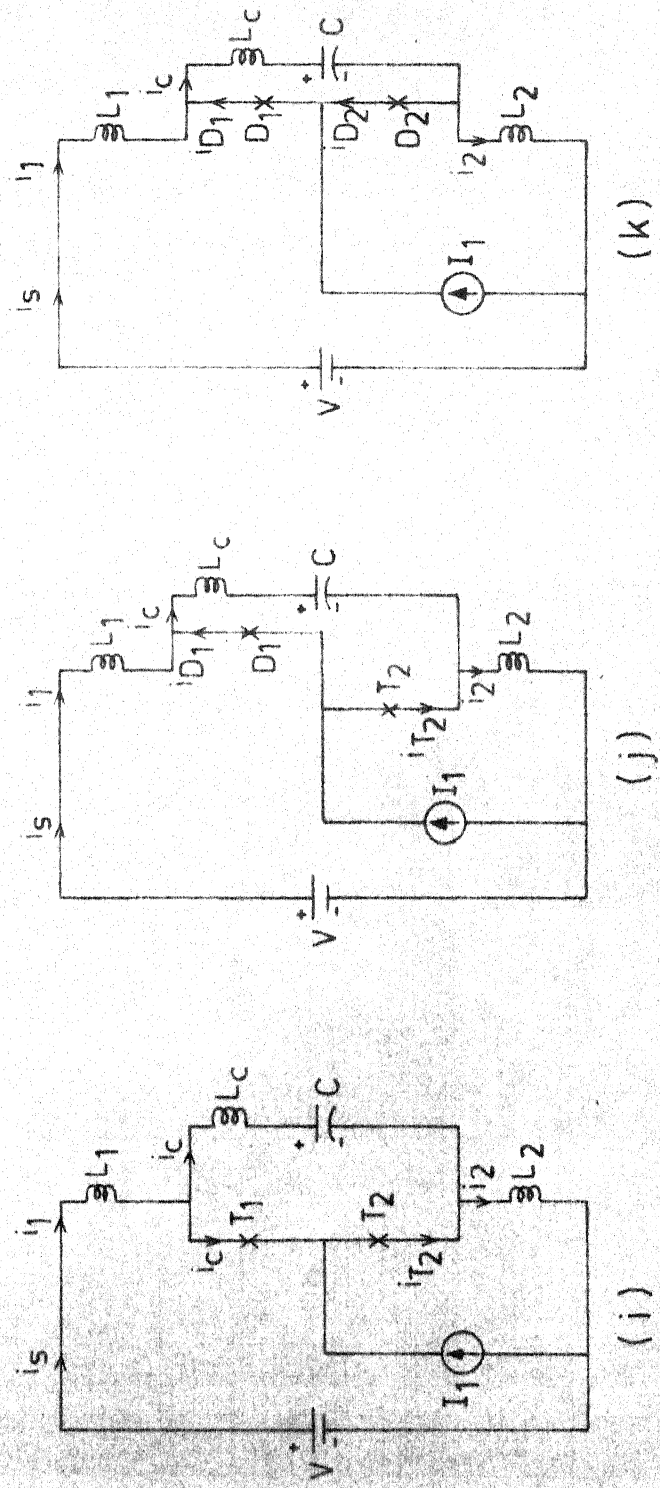
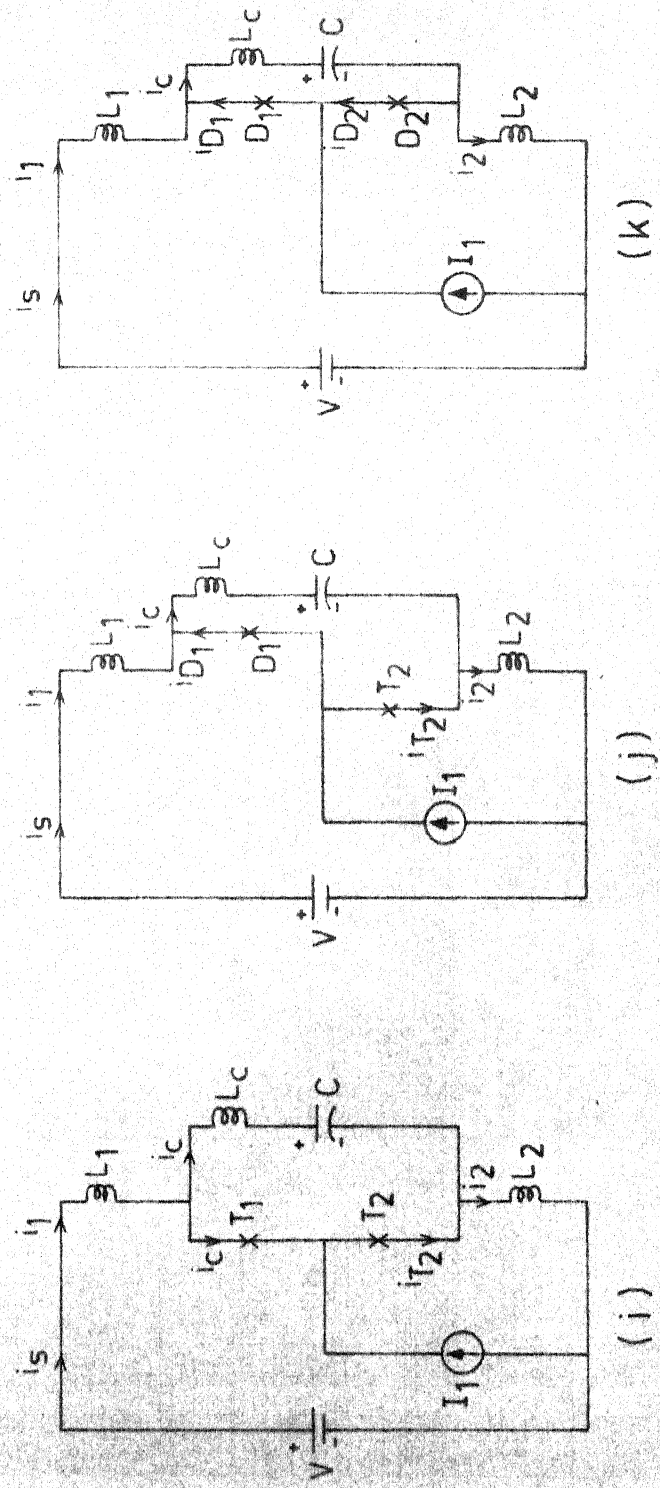
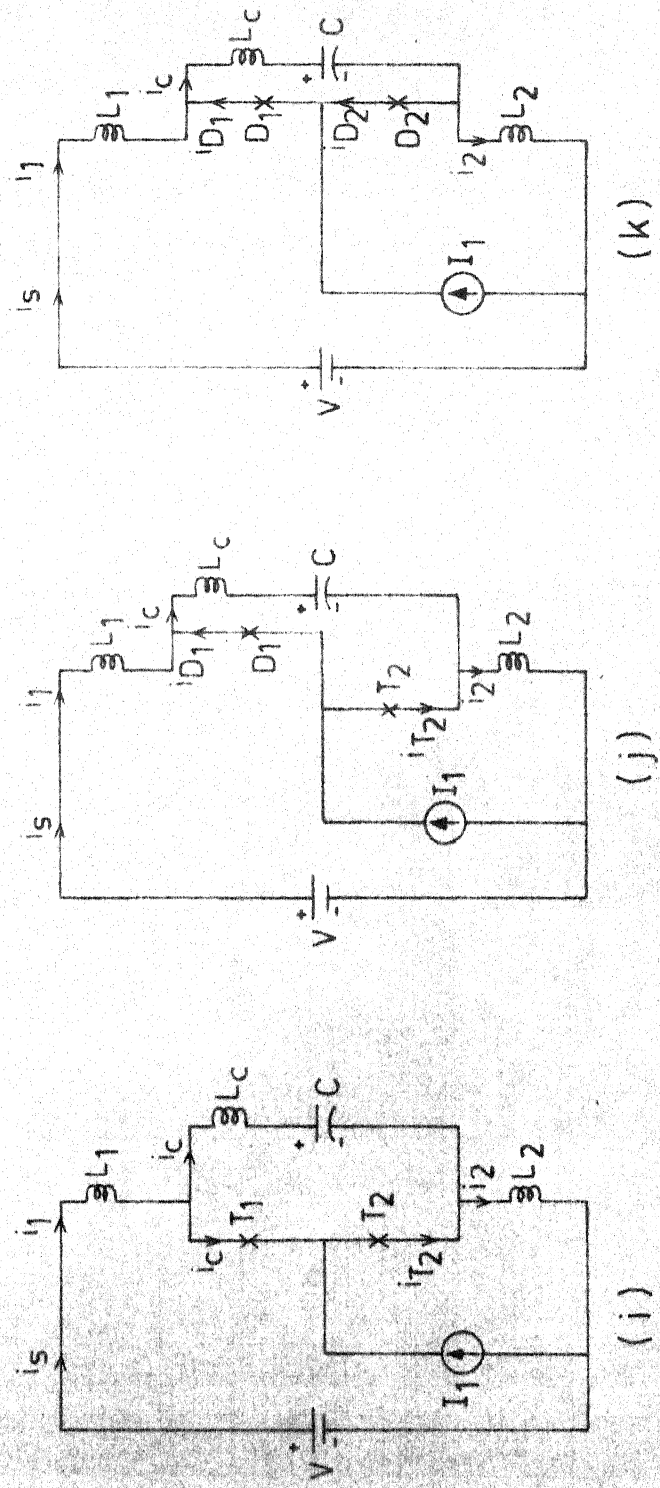
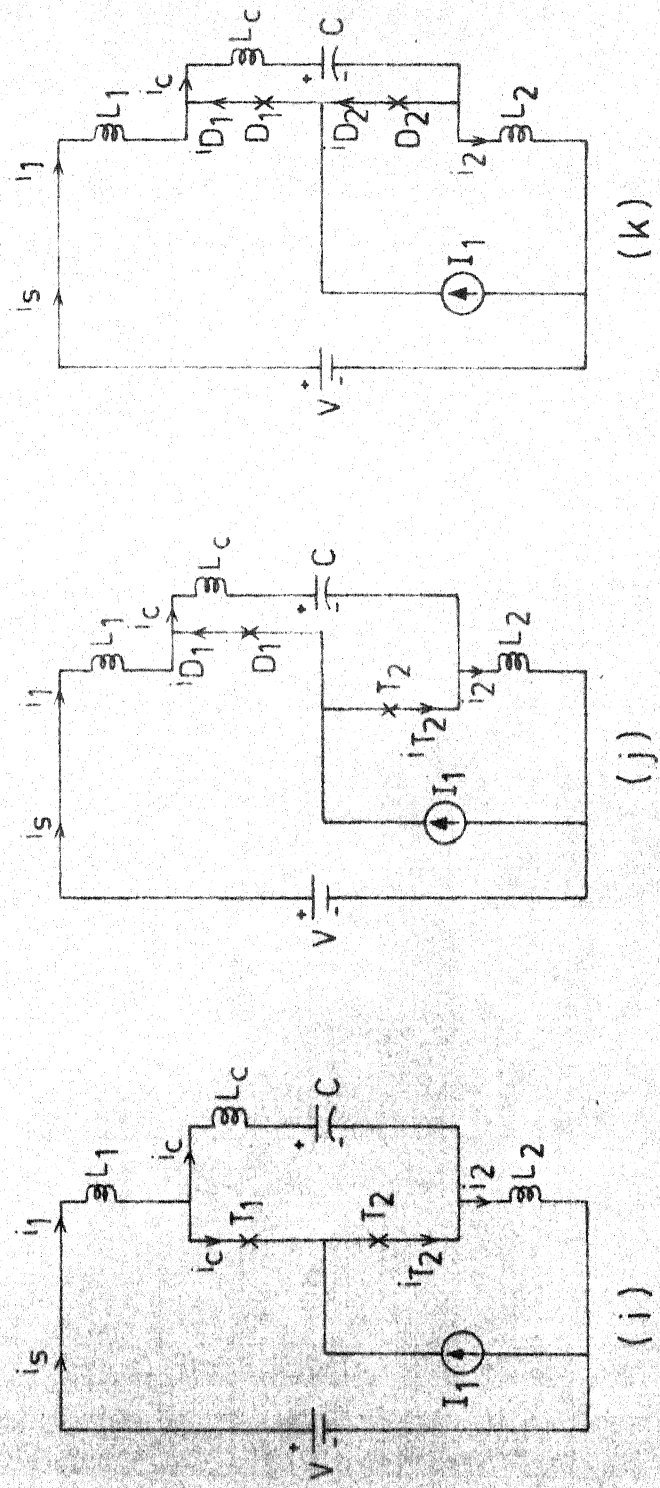
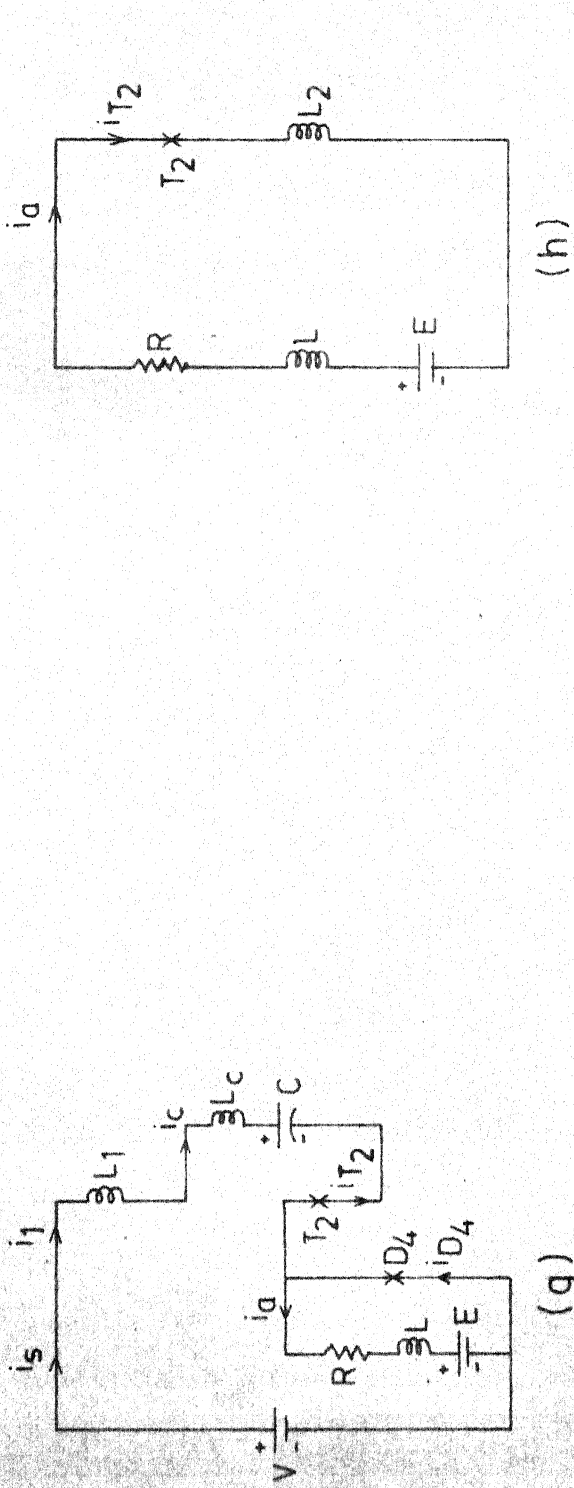


FIG. 2.3 (contd.)

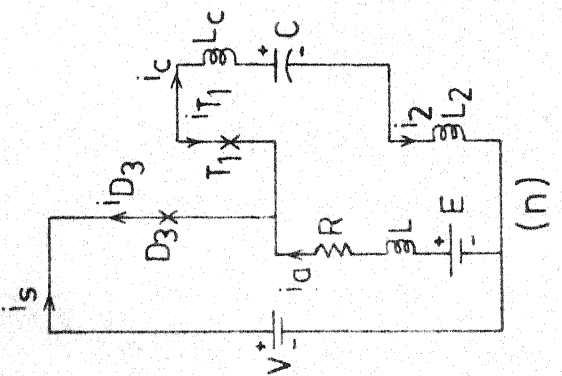
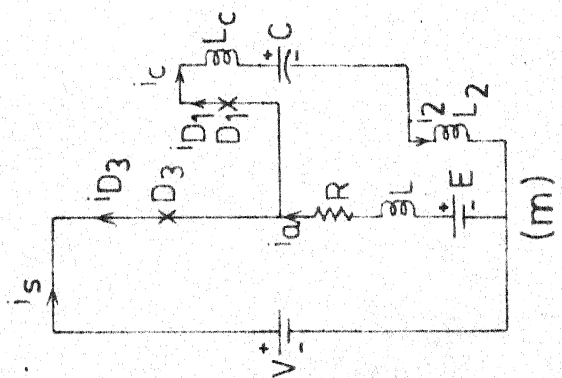
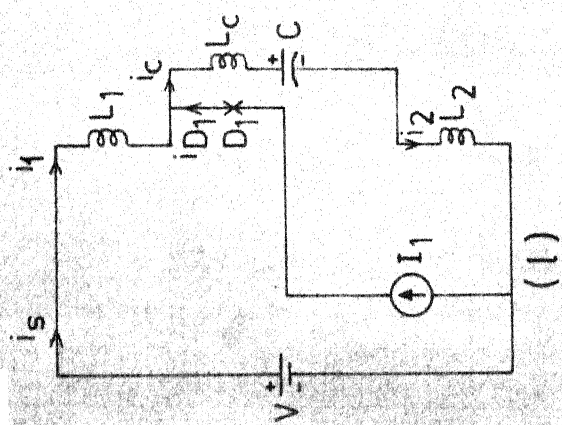


FIG. 2.3 (contd.)

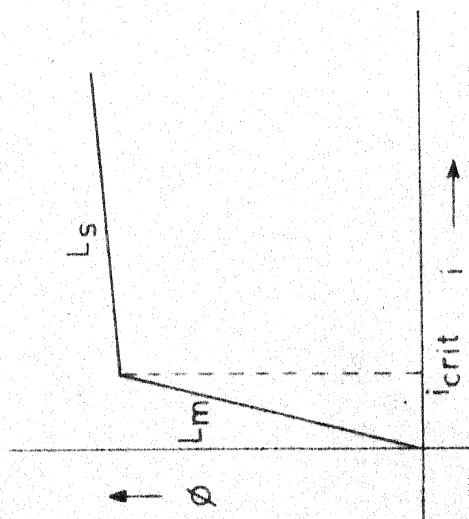


FIG. 2.4. ASSUMED MAGNETIC CHARACTERISTIC FOR THE SATURABLE REACTORS.

* L_s and L_m are slopes

3. Chokes L_1 and L_2 offer high inductance (L_m) while unsaturated and low inductance (L_s) when saturated.
4. Magnetic characteristic is assumed to be linear under ^{both} saturated and unsaturated conditions.

Assumed characteristic is shown in Fig. 2.4.

Operation of the proposed circuit can be divided explicitly in the following modes.

Mode-1: ($0 < t < \delta T$) capacitor charges to voltage V . Load current builds-up exponentially until commutation of thyristor T_1 is initiated. L_1 enters into saturation at low value of current and then has negligible (ideally zero) impedance (Ref. Fig. 2.3(a)).

$$V = (L_s + L) \frac{di_a}{dt} + R i_a + E \quad (2.1)$$

with initial conditions $i_a(0) = I_1$

Solution of eqn. (2.1) is given by

$$i_a = \frac{V-E}{R} (1 - e^{-t/\tau_1}) + I_1 e^{-t/\tau_1} \quad (2.2)$$

where, τ_1 = time constant of equivalent circuit = $\frac{L_s + L}{R}$

Commutation interval

Mode 2: ($0 < t' < t_1$) with $t = t' + \delta T$ thyristor T_2 is triggered to commutate thyristor T_1 off. This mode ends when current through thyristor T_2 reduces to zero. Equivalent circuit is shown in Fig. 2.3(b).

$$L_c \frac{di_c}{dt'} + r \cdot i_c + v_c = 0 \quad (2.3)$$

with initial conditions $V_c(0) = V, i_c(0) = 0$

$$i_a(0) = I_2$$

where r is the equivalent resistance of the loop formed by L_c, C, T_1 and T_2 , and

$$i_c(t') = -V \left(\frac{C}{L_c}\right)^{1/2} e^{-\omega_0 t'/2Q} \sin \omega_0 t' \quad (2.4)$$

$$v_c(t') = V e^{-\omega_0 t'/2Q} \cos \omega_0 t' \quad (2.5)$$

$$\omega_0 = \frac{1}{\sqrt{L_c C}}, \text{ natural frequency of oscillation} \quad (2.6)$$

$$Q = \frac{\omega_0 L_c}{r}, \text{ quality factor of inductor } L_c \quad (2.7)$$

In deriving equations (2.4) and (2.5), resistance r is assumed to be small. Thus the damped natural frequency

$$\begin{aligned} \omega_d &= \sqrt{1/L_c C - (r/2L_c)^2} \\ &\approx \omega_0 \end{aligned} \quad (2.8)$$

and Q being very large $1/4Q^2$ can be assumed much smaller than unity.

$$i_1(t') = I_2 + i_2(t') \quad (2.9)$$

where

$$i_2(t') = \frac{V}{(L_m + L_s)} t' \quad (2.10)$$

This mode ends at time $t = t_1$. So,

$$i_c(t_1) = i_2(t_1)$$

This becomes a transcendental equation and can be solved by iterative methods. However if L_m is large, $i_2(t_1) = 0$ and $t_1 = \pi/\omega_0$.

Mode-3: (Fig. 2.3(c)): When capacitor current equals to the load current, net current through T_1 is zero. Since T_1 prevents reversal of current through it, the mode ends at this time.

Eqns. (2.4) and (2.5) are valid in this mode also with initial conditions $i_c(t_1) = 0$, $V_c(t_1) = -V$. Let

$$i_c(t') \Big|_{t'=t_2} = I_2 \quad (2.11)$$

then,

$$t_2 = \sin^{-1} \left(\frac{I_2}{I_{c \max}(2)} \right) \quad (2.12)$$

where,

$$I_{c \max}(2) = V\sqrt{C/L_c} e^{-(\theta + \pi)/2Q} \text{ and } \theta = \pi/2 \quad (2.13)$$

If current through L_2 is also taken into account

$$\begin{aligned} i_c(t') \Big|_{t'=t_2} &= I_2 + i_2 \\ &= I_2 + \frac{V}{L_m + L_s} t_2 \end{aligned}$$

Mode 4 ($t_2 < t' < t_3$) (Fig. 2.3(d)): When i_c exceeds I_2 difference ($i_c - I_2$) flows through the diode D_1 till i_c falls to the value I_2 . A small reverse voltage equal to diode drop, appears across the thyristor T_1 and provides the turn off time for its recovery. Loop current in this mode flows through D_2 also, so both T_1 and T_2 are reverse biased. This feature makes circuit self healing, in case, nonrepetitive misfiring occurs due to a wrong gate pulse or due to dv/dt triggering. Further it is possible to turn off both T_1 and T_2 by withdrawing gate pulses from them during this mode.

$$\begin{aligned}
 t_{c1} &= \text{circuit turn off time for thyristor } T_1 \\
 &= t_3 - t_2 = 1/\omega_0 \left[\pi - 2\sin^{-1} \left(\frac{I_2}{I_{c \max}(2)} \right) \right]
 \end{aligned}
 \tag{2.14}$$

or,

$$t_{c1} = \frac{2}{\omega_0} \cos^{-1} \left(\frac{I_2}{I_{c \max}(2)} \right)
 \tag{2.15}$$

$$\begin{aligned}
 V_c(t_3) &= V_{c3} = V e^{-1/2Q(2\pi - \omega_0 t_2)} \left[\cos \omega_0 t_2 + \frac{1}{2Q} \sin \omega_0 t_2 \right] \\
 &= V_{c3} = V e^{-1/2Q(2\pi - \omega_0 t_2)} \cdot \cos \omega_0 t_2
 \end{aligned}
 \tag{2.16}$$

On taking i_2 also in to account, the circuit turn off time can be given as

$$t_{c1}, \frac{2}{\omega_0} \cos^{-1} \left(\frac{I_o + V/L_m + L_s (3\pi/2\sqrt{L_c C})}{V\sqrt{C/L_c}} \right) \quad (2.17)$$

Mode 5: ($t_3 < t' < t_4$) (Fig. 2.3(e)): R-C network across the $T_1 - D_1$ pair keeps dv/dt in the permissible limit when the capacitor voltage suddenly appears across the pair at the start of this mode. Capacitor charges at a constant rate upto voltage V , when D_4 starts conducting.

Initial conditions

$$i_c(t_3) = I_2, V_c(t_3) = V_{c3}$$

$$t_4 - t_3 = \left(\frac{V - V_{c3}}{I_2} \right) \cdot C \quad (2.18)$$

$$\begin{aligned} i_1(t_4) &= I_2 + i_2(t_4) \\ &\approx I_2 \end{aligned} \quad (2.19)$$

$$\begin{aligned} i_2(t_4) &= \frac{V}{L_m + L_s} \cdot t_3 + \frac{V - V_{c3}}{L_m} (t_4 - t_3) \\ &\quad - \frac{I_2}{C \cdot L_m} \left(\frac{t_4^2 - t_3^2}{2} \right) \end{aligned} \quad (2.20)$$

Mode 6: ($t_4 < t' < t_5$) (Fig. 2.3(f)): Load current is transferred gradually to the freewheeling diode D_4 . Capacitor current and the current through D_2 start decreasing. The capacitor charges to a voltage higher than V , thus reversing the voltage across L_1 . The flux in L_1 therefore starts decreasing. L_1 enters into the high impedance state. This mode ends when the current through D_2 becomes zero.

Negligible width of the hysteresis loop and piecewise linear model for saturable reactor are the assumptions taken in the following analysis. It is assumed that L_1 has inductance L_s upto the current zero and thereafter changes to unsaturated value L_m .

Assuming $i_2(t_4) \ll I_2$ as $L_m \gg L_s$, one gets

$$i_c(t') = I_2 \cos \frac{(t' - t_4)}{\sqrt{(L_s + L_c)C}} \quad (2.21)$$

$$V_c(t') = V + I_2 \sqrt{(L_s + L_c)/C} \cdot \sin \frac{t' - t_4}{\sqrt{(L_s + L_c)C}} \quad (2.22)$$

This mode ends when $i_c(t')$ reduces to zero. So,

$$V_c(t_5) = V + I_2 \sqrt{(L_s + L_c)/C}$$

and,

$$\text{overshoot } \Delta V = I_2 \sqrt{(L_s + L_c)/C} \quad (2.23)$$

Hence, in order to limit the overshoot voltage ΔV , it is essential to keep L_s and L as small as possible and C as high as possible.

Mode 7 ($t_5 < t' < t_6$) (Fig. 2.3(g)) : T_2 is getting sustained pulses, as soon as D_2 blocks, it starts conducting. The capacitor voltage is decreasing and reverse current through L_1 is increasing gradually.

The shifting of the flux point beyond the retentivity point in the negative direction takes place in this mode. As L_1 enters into the nonlinear range in the negative current direction, the capacitor voltage starts decreasing relatively fast. Thus the capacitor voltage ringing helps flux resetting in the saturable chokes, which would otherwise require airgaps in the construction of the core. Capacitor current in this mode can be written as follows.

$$i_c(t') = -\Delta V \sqrt{C/(L_c + L_m)} \sin \frac{(t' - t_5)}{\sqrt{(L_m + L_c)C}} \quad (2.24)$$

$$V_c(t') = V + \Delta V \cos \frac{(t' - t_5)}{\sqrt{(L_m + L_c)C}} \quad (2.25)$$

This mode ends when i_{T2} reduces to zero. Assuming i_2 to be negligible this corresponds to i_c reducing to zero. So

$$V_c(t_6) = V - \Delta V \quad (2.26)$$

At this instant mode-6 takes place again. Depending upon the circuit losses, modes 6 and 7 repeat alternately. However, since the half period $\pi\sqrt{(L_m + L_c)C}$ of capacitor ringing is large, the other circuit conditions like reversal of current or turning on of thyristor T_1 will make the mode change within one or two cycles of ringing.

It is clear from the equivalent circuits of mode 6 and 7 that the load voltage is free from any overshoot because of diode D_4 though the ringing capacitor voltage appears across the thyristor T_1 .

It is necessary that L_1 is unsaturated before the load current reversal through L_2 takes place. Otherwise when T_1 is triggered to commutate T_2 off, a dead short circuit will take place across the supply. For the flux to reset to zero value, the negative volt seconds absorbed during the resetting period should be greater than the volt-seconds absorbed by the commutation choke during 2-5. The voltage across L_1 remain negative for the duration $\pi/2\sqrt{(L_m+L_c)C}$ plus (t_5-t_4) . Since t_5-t_4 is very small in comparison to $\pi/2\sqrt{(L_m+L_c)C}$,

$$\Delta V \cdot \frac{\pi}{2\sqrt{(L_m+L_c)C}} > V \cdot 2\pi\sqrt{L_c C} \quad (2.27)$$

$$I_2 \left(\frac{L_s+L_c}{C} \right)^{1/2} \cdot \frac{\pi}{2} \sqrt{(L_m+L_c)C} > V \cdot 2\pi \sqrt{L_c \cdot C}$$

Since $L_m \gg L_c$

$$\left[\frac{L_m(L_s+L_c)}{L_c \cdot C} \right]^{1/2} > \frac{4V}{I_2}$$

$$K = \frac{L_m}{L_c} > \left(\frac{4V}{I_2} \right)^2 \left(\frac{C}{L_s+L_c} \right) \quad (2.28)$$

Eqn. (2.28) indicates that a large value of K is desirable. This however increases recovery time and is a constraint over high frequency operation.

Mode 8 ($t_{iv} + \delta T < t < t_7 + \delta T$)(Fig. 2.3(h)): T_2 is already getting pulses, as soon as the load current reverses T_2 takes over. Initially L_2 offers high inductance but soon it goes into saturation. Steady state condition for this mode will be represented by the following eqns. This mode continues, until T_1 is triggered to initiate the commutation of T_2

$$0 = (L_s + L) \frac{di_a}{dt} + R i_a + E \quad (2.29)$$

initial conditions

$$i_a(t_{iv}) = 0$$

So,

$$i_a = -\frac{E}{R} (1 - e^{-(t-t_{iv})/\tau_1}) \quad (2.30)$$

If L_2 is ideal then load voltage will remain zero in this mode also.

Mode 9 ($0 \leq t'' \leq t_8$) with $t'' = t - (t_7 + \delta T)$ (Fig. 2.3(i)): This mode ends when i_{T1} reduces to zero.

initial conditions

$$V_c(o) = V, i_c(o) = 0$$

$$i_a(o) = I_1$$

This mode can be analysed in the same way as mode 2.

Mode 10 ($t_8 \leq t'' < t_9$) (Fig. 2.3(j)): This mode ends when capacitor current equals to load current and thus current through T_2 is zero.

Mode 11 ($t_9 \leq t'' \leq t_{10}$) (Fig. 2.3(k)): In this mode, T_2 is kept reverse biased. t_{c2} , circuit turn off time for T_2 can be obtained by replacing I_2 by I_1 in eqn. (2.17). Points mentioned in mode 4 hold good here also. Capacitor voltage at the end of this mode is obtained from the modified version of eqns. (2.12) and (2.16), which are obtained by replacing I_2 by I_1 .

Mode 12 ($t_{10} \leq t'' \leq t_{11}$) (Fig. 2.3(l)): Capacitor is charged to voltage V by a constant current. The duration of this mode will depend upon the load current which is assumed constant here and the initial voltage of the capacitor. An equation similar to (2.18) can be written for the duration of this mode.

A R-C network across $T_2 - D_2$ pair keeps dv/dt within the permissible limits when the capacitor voltage suddenly appears across the pair.

Mode 13 ($t_{11} \leq t'' \leq t_{12}$) (Fig. 2.3(m)): As soon as the capacitor charges to voltage V , D_3 gets forward biased and starts conducting. Due to inductance present in the loop current transfer from D_1 to D_3 is not instantaneous.

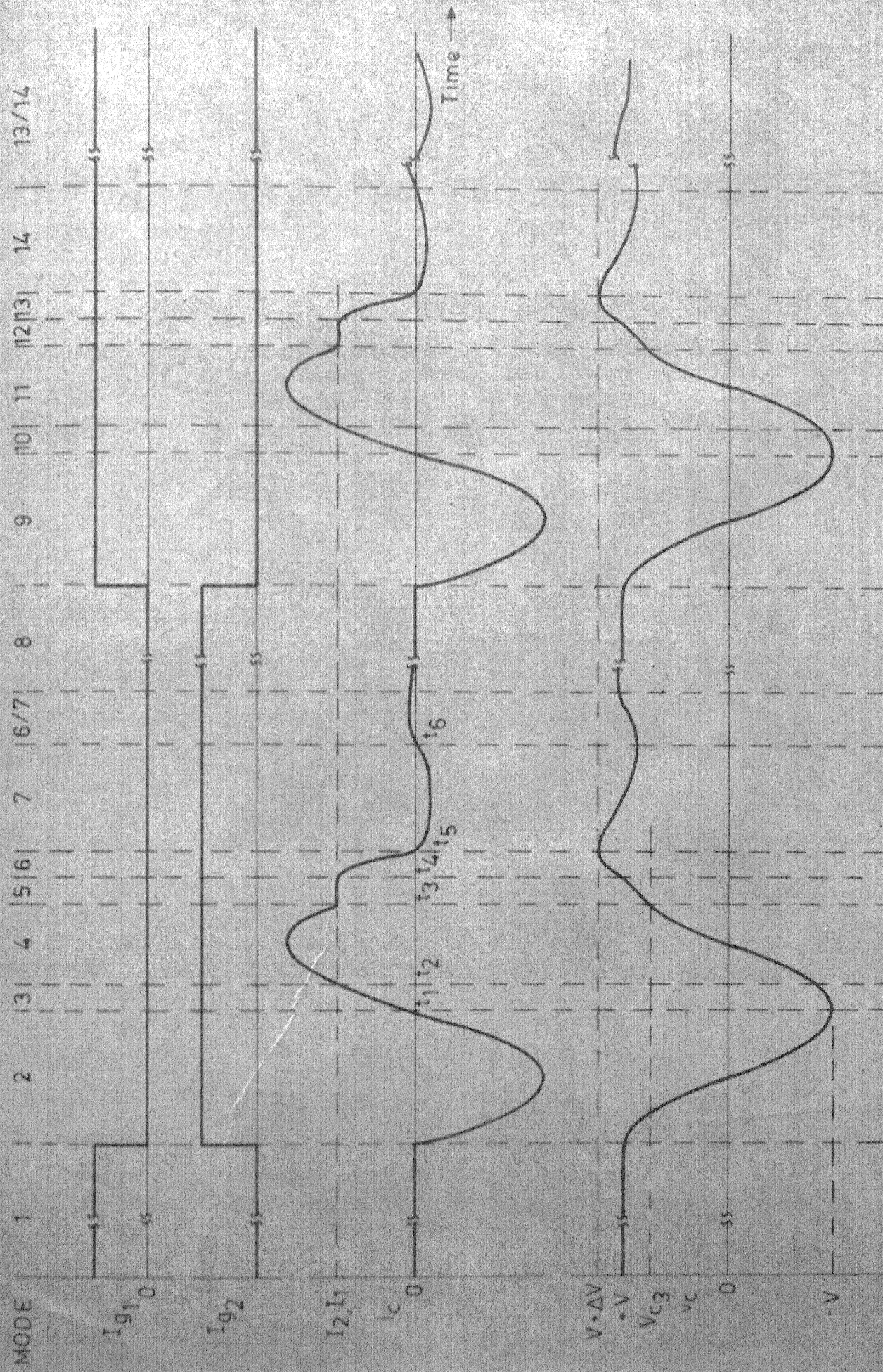


FIG. 2.5 TIME VARIATION OF CURRENT AND VOLTAGE IN THE PROPOSED CHOPPER CIRCUIT.

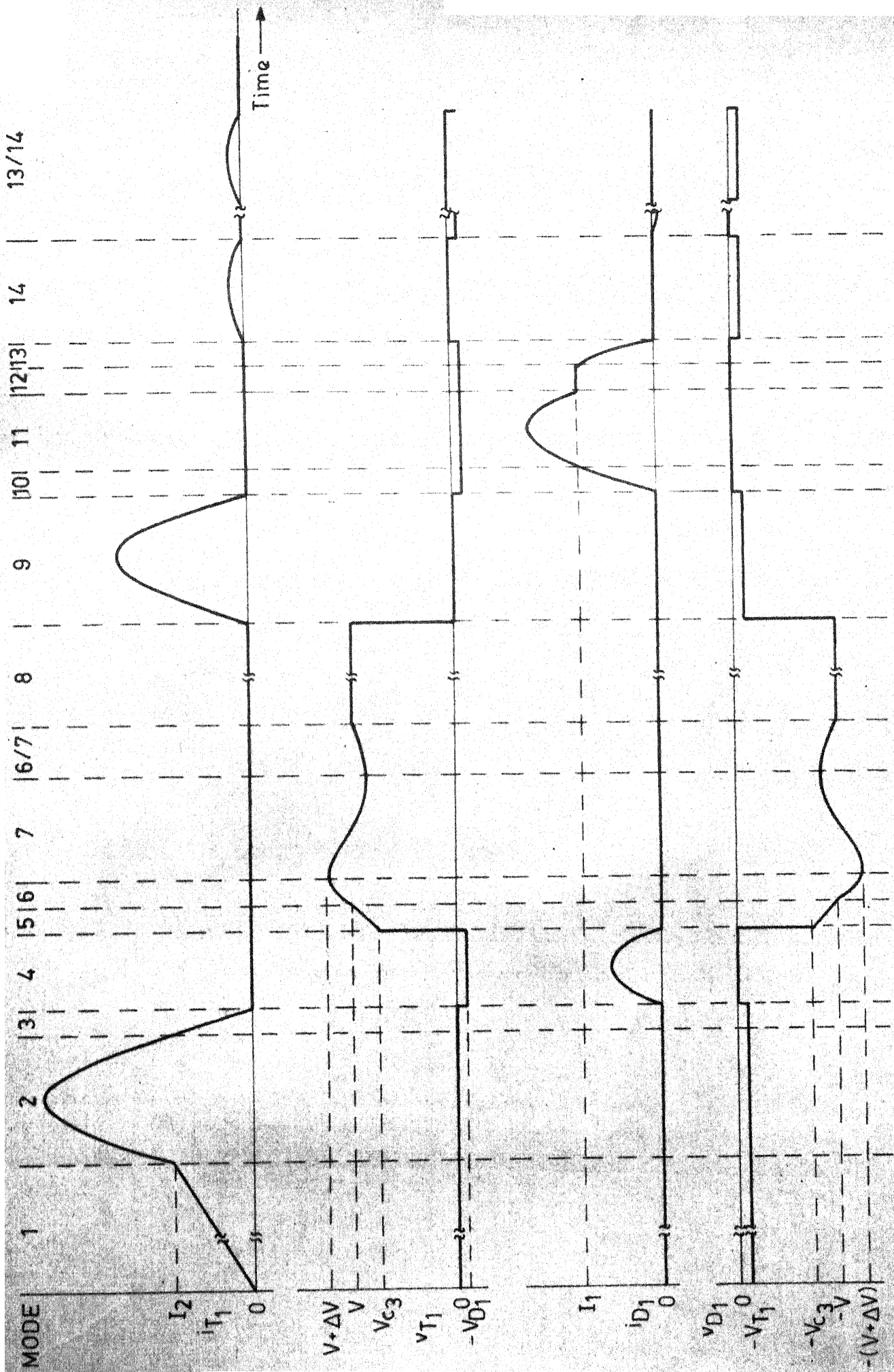


FIG. 2.5 (contd.)

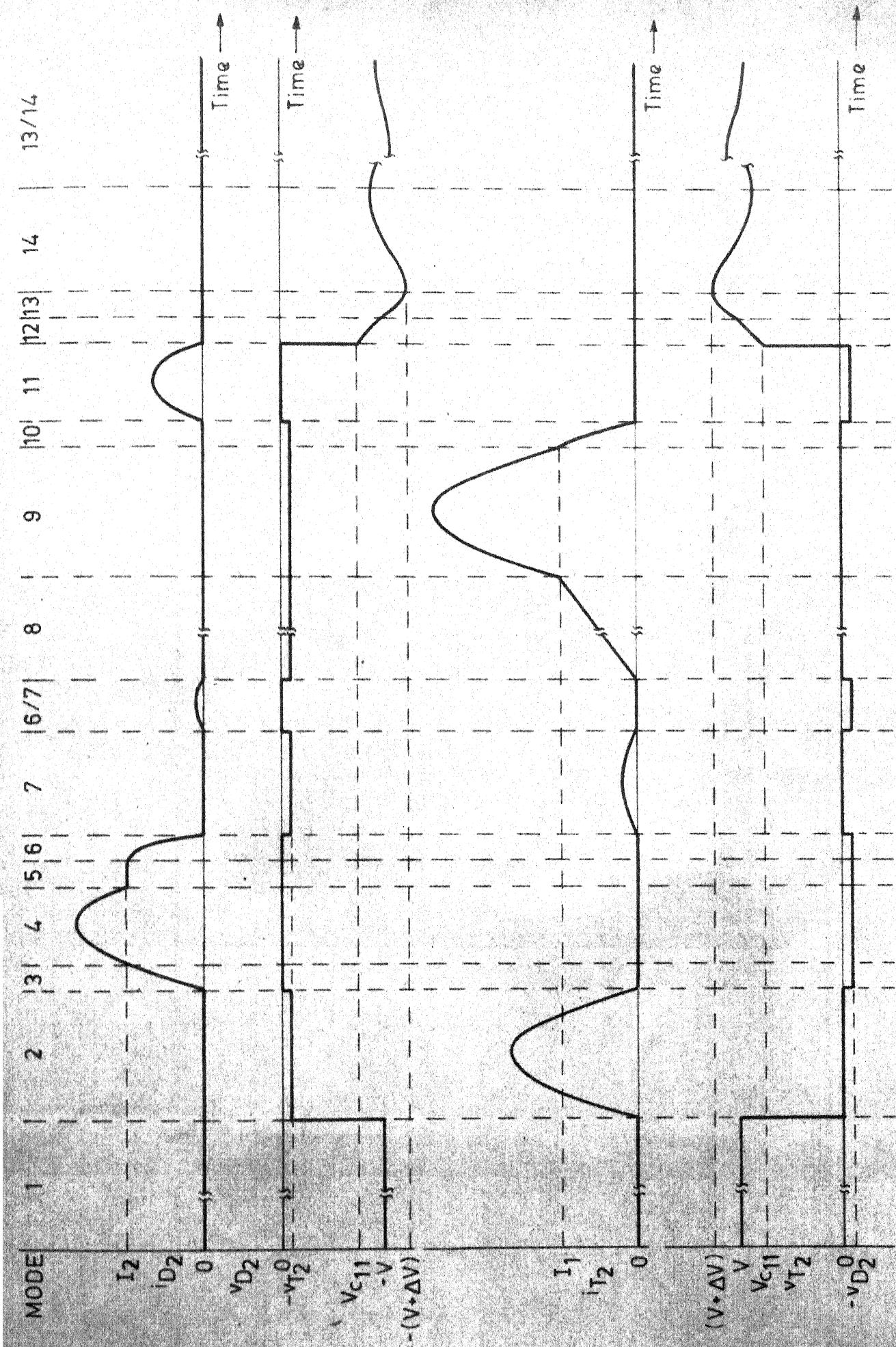


FIG. 2.5 (contd.)

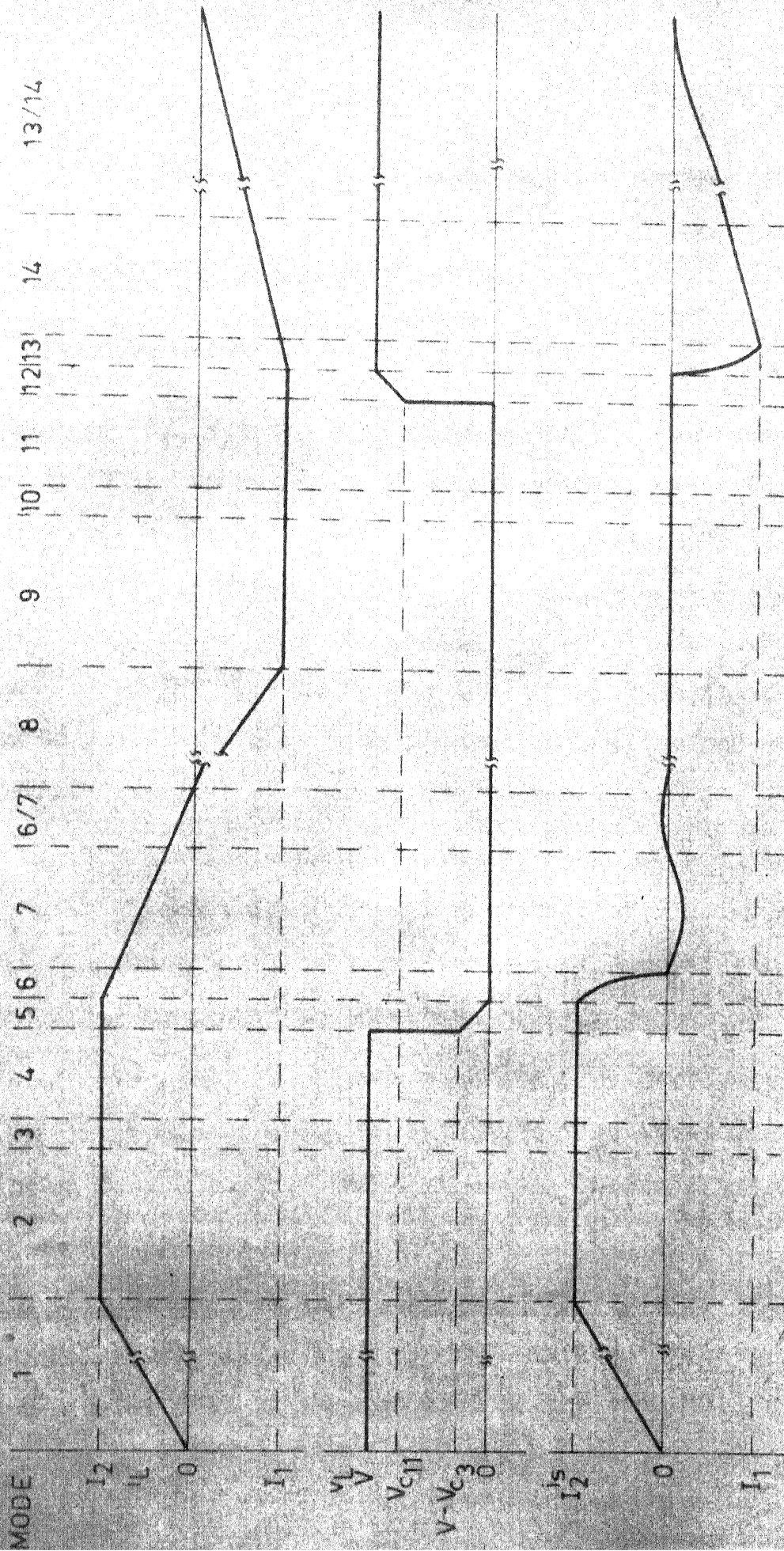


FIG. 2.5 (contd.)

Meanwhile the capacitor charges to an extra voltage ΔV_1 . Similar to eqn. (2.23) the following eqn. can be obtained for this case

$$\text{overshoot } \Delta V_1 = I_1 \sqrt{(L_s + L_c)} / C \quad (2.31)$$

Mode 14 ($t_{12} \leq t'' \leq t_{13}$) (Fig. 2.3(n)): Now the current through the commutation circuit reverses. This current reversal helps in the flux resetting process of L_2 which has already started in mode 13 when L_2 starts getting reverse biased. All the points mentioned in mode 7 can be similarly interpreted as per the circuit conditions in this mode. At the end of this mode charge on the capacitor remains $V - \Delta V$, so mode 13 starts again.

Depending upon the circuit losses, mode 13 and 14 repeat alternately. Since time period of ringing is large, it continues until either reversal of current takes place or T_2 is triggered to commutate T_1 off.

Voltage and current waveforms for different devices and the load are shown in Fig. 2.5. The waveforms are not drawn to the scale. The commutation interval has been expanded for the sake of clarity.

Minimum on time of the chopper and thyristors: Thyristor works as main as well as the commutation thyristor, so minimum on time will be decided by the commutation interval duration. The commutation interval

of thyristor T_1 , spans over mode 2 to mode 5. If we trigger T_1 again at this moment there will be high di/dt in the commutation circuit. So it is preferred not to turn on device T_1 again before the end of mode-6. Ofcourse there will be some extra voltage on the capacitor but that will die out through ringing.

So,

Minimum on time of the device T_1

= duration of mode 2 to mode 6

$$= \frac{1}{\omega_0} [2\pi - \sin^{-1}(\frac{1}{x})] + \frac{[V - V_c(t_3)]}{I_2} \cdot C + \frac{\pi}{2} \sqrt{(L_c + L_s) \cdot C}$$

$$= \sqrt{(L_c \cdot C)} [2\pi - \sin^{-1}(\frac{1}{x})] + \frac{V \cdot C}{I_2} [1 - \cos \theta]$$

$$\sin^{-1}(\frac{1}{x})] + \frac{\pi}{2} \sqrt{(L_c + L_s) \cdot C} \quad (2.32)$$

$$\text{where } x = I_c \max(2) / I_2$$

As the operation of the circuit is symmetrical, result of eqn. (2.32) holds good for T_2 also. Second term in eqn. (2.32) will be maximum for the lowest value of current. Maximum value of this term will be taken to calculate maximum on time.

For practical chopper minimum on time is calculated to be approximately 326.875 μsec .

Maximum frequency of operation: There are two such commutation intervals in one time period. So,

Minimum time period = 2* minimum on time of device

For practical chopper maximum frequency of operation 1.5 KHz.

Minimum voltage obtainable: Voltage waveform is not completely rectangular, so even when $\delta = 0$, voltage is not zero.

$$\text{Minimum average voltage} = \frac{V}{T} \left[\frac{1}{\omega_0} (2\pi - \sin^{-1}(\frac{1}{x})) + \frac{(V - V_c(t_3))}{2} (t_3 - t_2) + \left(\frac{V + V_c(t_{11})}{2} \right) (t_{11} - t_{10}) \right] \quad (2.33)$$

For practical chopper minimum obtainable voltage is found 7.5 percent of input voltage from eqn. (2.33).

2.5 Design Criteria:

2.5.1 Commutation circuit components:

Circuit turn off time provided in this chopper using parallel current commutation scheme is given by eqn. (2.15). For a high Q, commutation resonant circuit $I_{c \max(2)} = I_{c \max}$ so, eqn. (2.15) can be rewritten as

$$t_c = \frac{2}{\omega_0} \cos^{-1} \left(\frac{I_{\max}}{I_{c \max}} \right) \quad (2.34)$$

Operations of T_1 and T_2 are identical. A current through T_1 will be maximum when $t_{on} = T$ in first quad. while it will

be maximum through T_2 at $t_{on} = 0$ in second quadrant. So the same values of L_c and C will be appropriate for T_1 and T_2 . Following are the factors which should be considered at the time of deciding values of L_c and C .

(a) $1 < x < 3$, where $x = \frac{V}{I_{max}} \cdot \sqrt{C/L_c}$

(b) circuit turn off time > thyristor turn off time

(c) voltage overshoot on the capacitor $= I_o \cdot \left(\frac{L_s + L_c}{C} \right)^{1/2}$.

To reduce this, C should be higher and L_c should be lower.

Rewriting (2.34)

$$\frac{t_c}{\sqrt{L_c \cdot C}} = 2 \cos^{-1} \left(\frac{1}{x} \right) = g(x)$$

$$L_c = \frac{V(t_q + \Delta t)}{x \cdot g(x) \cdot I_{max}} \quad (2.35)$$

$$C = \frac{x \cdot I_{max} \cdot (t_q + \Delta t)}{V \cdot g(x)} \quad (2.36)$$

2.5.2 Saturable chokes L_1 and L_2 :

Following points should be taken into account, when designing L_1 and L_2 .

1. Critical value of current should be less than $V \cdot \left(\frac{C}{2L_m + L_c} \right)^{1/2}$, so that capacitor charging through L_1 , L_2 and L_c at the instant of switching on the chopper should take place fast.

2. L_1 and L_2 are required to block the dc voltage for approximately $2\pi/\omega_0$ seconds. There will be some current build up through them, but that should not drive them into saturation

$$\frac{V}{L_m} \cdot \frac{2\pi}{\omega_0} < i_{\text{critical}}$$

where i_{critical} is the current corresponding to the knee point of the magnetisation characteristic.

3. Voltage overshoot on the capacitor is $\Delta V = I_0 \sqrt{(L_s + L_c)}/C$. So as to reduce the ΔV , L_s should be as low as possible.

4. Overcharge on the capacitor forces a reverse current through the saturable reactor. This current should not drive choke into saturation in another direction. So peak value of sinusoidal current flowing through it in reverse direction i.e. $I_0 \sqrt{(L_s + L_c)}/L_m$ should be less than i_{critical} .

2.6 Analysis of the performance of the Motor fed by the Developed Chopper:

Following assumptions are taken in the analysis of the performance of the motor fed by the proposed chopper.

(a) The saturable inductors offer very high inductance when unsaturated and zero inductance when saturated. Saturable reactors are assumed to go into saturation even for negligibly small current.

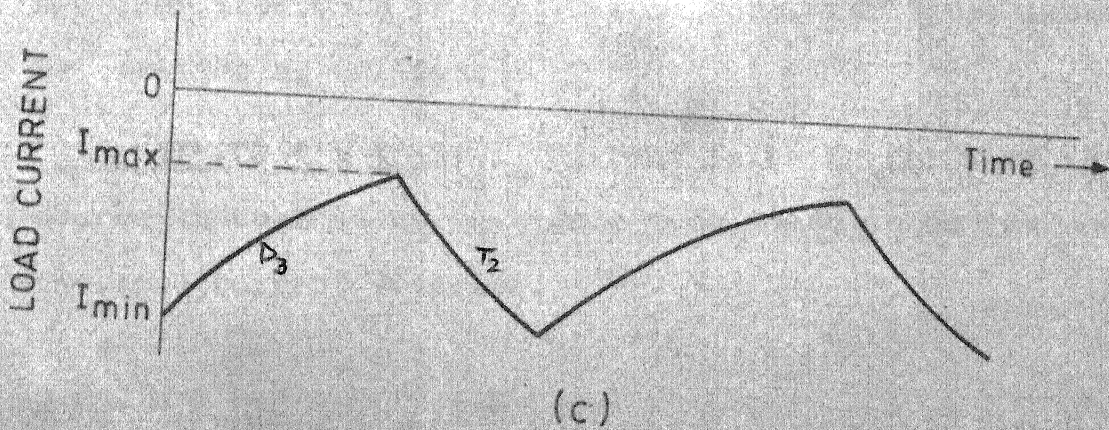
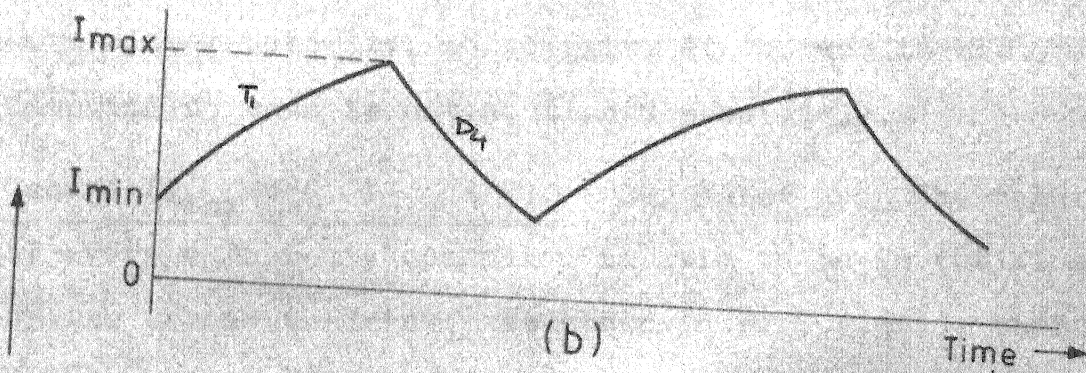
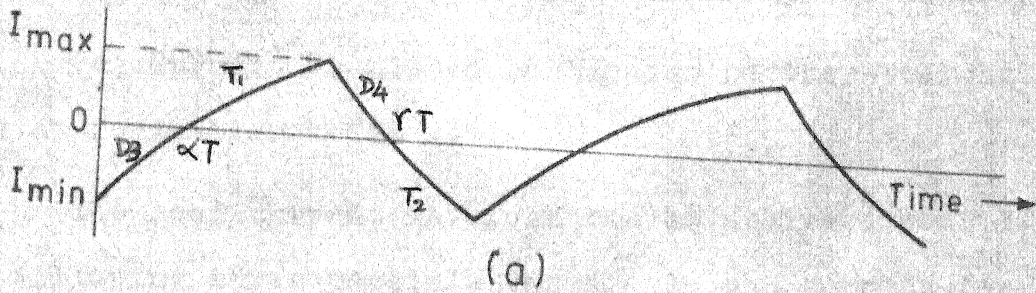
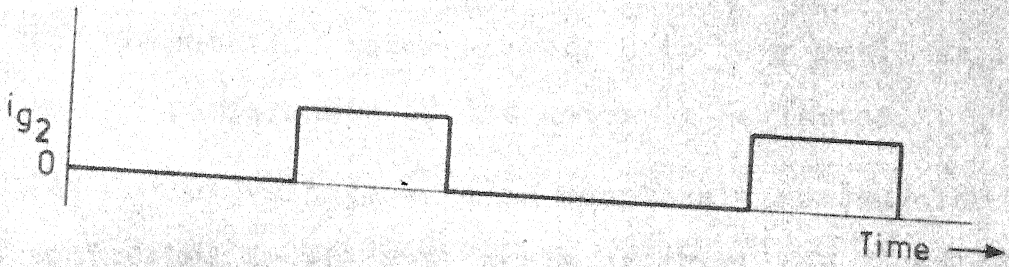
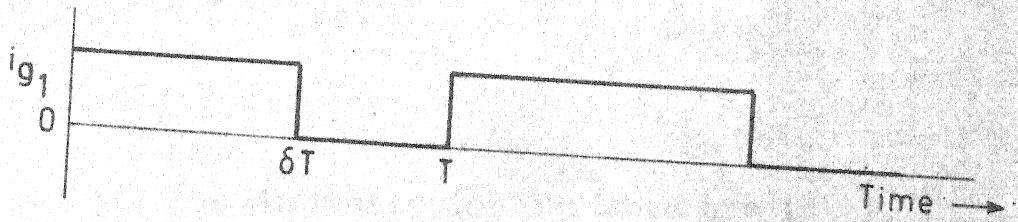


FIG. 2.6. LOAD CURRENT WAVEFORMS.

(b) All the semiconductor switches are ideal.

(c) Commutation interval length is very small so its effect on the performance of the motor is neglected.

(d) Output voltage wave is completely rectangular and is controlled by the duty cycle of thyristor T_1 only.

(e) Current is always continuous so the straight line approximation holds good.

The load current waveform can be analysed considering the following three possible cases. As the current can have either polarity, so polarity of current in any specific interval or case is not mentioned separately.

Case 1 ($I_{\max} > 0, I_{\min} < 0$) : Depending upon the magnitude of average current, operation is said to be in the first or the second quadrant. As shown in Fig. 2.6(a), there are four intervals present. Mesh eqns. for these intervals are written as follows.

Interval-1 ($0 \leq t \leq \alpha T$) : Current is being fed back to the source through diode D_3 . This mode comes to an end when the load current reverses.

$$V = L \frac{di_a}{dt} + R i_a + E \quad (2.37)$$

$$i_a(0) = I_{\min}$$

Solution of eqn. (2.37) is given as

$$i_a = \frac{V-E}{R} (1 - e^{-t/\tau}) + I_{\min} e^{-t/\tau} \quad (2.38)$$

$$\text{where } \tau = L/R$$

Since $i_a \Big|_{t=\alpha T} = 0$; α can be obtained from eqn. (2.38) as,

$$\alpha = \frac{\tau}{T} \ln \left[1 - \frac{I_{\min} \cdot R}{V-E} \right] \quad (2.39)$$

Interval-2 ($\alpha T \leq t \leq \delta T$): Motor is being fed through thyristor T_1 and saturable choke L_1 . Resistance of the choke is taken into account.

$$V = L \frac{di_a}{dt} + (R+R_1) i_a + E \quad (2.40)$$

$$i_a(\alpha T) = 0$$

where R_1 = resistance of this saturable choke.

Solution of eqn. (2.40) is,

$$i_a = \frac{V-E}{(R+R_1)} (1 - e^{-(t-\alpha T)/\tau_2}) \quad (2.41)$$

$$\text{where } \tau_2 = L/(R+R_1)$$

Since,

$$i_a \Big|_{t=\delta T} = I_{\max}$$

So from eqn. (2.41)

$$I_{\max} = \frac{V-E}{(R+R_1)} (1 - e^{-(\delta-\alpha)T/\tau_2}) \quad (2.42)$$

Interval-3 ($\delta T \leq t \leq \gamma T$): Load current freewheels through diode D_4 , until it reduces to zero.

$$0 = L \frac{di_a}{dt} + R i_a + E \quad (2.43)$$

$$i_a(\delta T) = I_{\max}$$

Solution of eqn. (2.43) is obtained as

$$i_a = -\frac{E}{R} (1 - e^{-(t-\delta T)/\tau}) + I_{\max} e^{-(t-\delta T)/\tau} \quad (2.44)$$

Since $i_a \Big|_{t=\gamma T} = 0$

So,

$$\gamma = \delta + \frac{\tau}{T} \ln \left(1 + \frac{I_{\max} \cdot R}{E} \right) \quad (2.45)$$

Interval-4 ($\gamma T \leq t \leq T$): Load current builds up in the reverse direction through the thyristor T_2 and the saturable inductor L_2 .

$$0 = L \frac{di_a}{dt} + (R+R_1) \cdot i_a + E \quad (2.46)$$

$$i_a(\gamma T) = 0$$

so, i_a can be written as,

$$i_a = -\frac{E}{(R+R_1)} (1 - e^{-(t-\gamma T)/\tau_2}) \quad (2.47)$$

$$i_a \Big|_{t=T} = I_{\min} = \frac{-E}{(R+R_1)} (1 - e^{-(1-\gamma)T/\tau_2}) \quad (2.48)$$

By straight line approximation,

$$I_{av} = [I_{\min} (1 + \alpha - \gamma) + I_{\max} (\gamma - \alpha)] / 2 \quad (2.49)$$

Case 2 ($I_{\max} > 0, I_{\min} > 0$) : It is a first quadrant operation. (Fig. 2.6(b)). There will be only two interval in this case.

Interval-1 ($0 \leq t \leq \delta T$): Current is fed through the thyristor T_1 and saturable reactor.

$$V = L \frac{di_a}{dt} + (R+R_1) i_a + E \quad (2.50)$$

$$i_a(0) = I_{\min}$$

on solving eqn. (2.50), one gets

$$i_a = \frac{V-E}{(R+R_1)} (1 - e^{-t/\tau_2}) + I_{\min} e^{-t/\tau_2} \quad (2.51)$$

Interval-2 ($\delta T \leq t \leq T$): In this interval load current freewheels through diode D_4 .

$$0 = L \frac{di_a}{dt} + R i_a + E \quad (2.52)$$

$$i_a(\delta T) = I_{\max}$$

Thus,

$$i_a = -\frac{E}{R} (1 - e^{-(t-\delta T)/\tau}) + I_{\max} e^{-(t-\delta T)/\tau} \quad (2.53)$$

Since, $i_a|_{t=\delta T} = I_{\max}$ and $i_a|_{t=T} = I_{\min}$, one can write from eqn. (2.51) and eqn. (2.53)

$$I_{\max} = \frac{1}{(1 - e^{-\delta T/\tau_2} \cdot e^{-(1-\delta)T/\tau})} \left[\frac{V-E}{(R+R_1)} (1 - e^{-\delta T/\tau_2}) - \frac{E}{R} (1 - e^{-(1-\delta)T/\tau}) e^{-\delta T/\tau_2} \right] \quad (2.54)$$

and

$$I_{\min} = \frac{1}{(1-e^{-\delta T/\tau_2} e^{-(1-\delta)T/\tau})} \left[-\frac{E}{R}(1-e^{-(1-\delta)T/\tau}) + \frac{V-E}{(R+R_1)} (1-e^{-\delta T/\tau_2}) e^{-(1-\delta)T/\tau} \right] \quad (2.55)$$

Taking the straight line approximation,

$$I_{av} = \frac{1}{2} (I_{\max} + I_{\min}) \quad (2.56)$$

Case 3 ($I_{\max} < 0, I_{\min} < 0$): It is a second quadrant operation. The load current waveform for this case is shown in Fig. 2.6(c). Mesh eqns. for the two intervals present in this case, are given below.

Interval-1 ($0 \leq t \leq \delta T$) The current is fed into the source through diode D_3 .

$$V = L \frac{di_a}{dt} + R \cdot i_a + E \quad (2.57)$$

$$i_a(0) = I_{\min}$$

On solving eqn. (2.57)

$$i_a = \frac{V-E}{R} (1 - e^{-t/\tau}) + I_{\min} e^{-t/\tau} \quad (2.58)$$

Interval-2 ($\delta T \leq t \leq T$): Load current builds up in reverse direction through the thyristor T_2 and saturable inductor L_2 .

$$0 = L \frac{di_a}{dt} + (R+R_1) i_a + E \quad (2.59)$$

$$i_a(\delta T) = I_{\max}$$

From eqn. (2.59)

$$i_a = -\frac{E}{(R+R_1)} (1 - e^{-(t-\delta T)/\tau_2}) + I_{\max} e^{-(t-\delta T)/\tau_2} \quad (2.60)$$

Since $i_a \Big|_{t=\delta T} = I_{\max}$ and $i_a \Big|_{t=T} = I_{\min}$, so from eqns.

(2.58) and (2.60), one can write

$$I_{\max} = \frac{1}{(1 - e^{-(1-\delta)T/\tau_2}) e^{-\delta T/\tau}} \left[\frac{V-E}{R} (1 - e^{-\delta T/\tau}) - \frac{E}{(R+R_1)} (1 - e^{-(1-\delta)T/\tau_2}) e^{-\delta T/\tau} \right] \quad (2.61)$$

and

$$I_{\min} = \frac{1}{(1 - e^{-(1-\delta)T/\tau_2}) e^{-\delta T/\tau}} \left[\frac{V-E}{R} (1 - e^{-\delta T/\tau}) e^{-(1-\delta)T/\tau_2} - \frac{E}{R+R_1} (1 - e^{-(1-\delta)T/\tau_2}) \right] \quad (2.62)$$

Taking the straight line approximation, I_{av} can be calculated from eqns. (2.56), (2.61) and (2.62).

Torque and speed for different values of on time of thyristor T_1 can be obtained with the help of the following eqns.

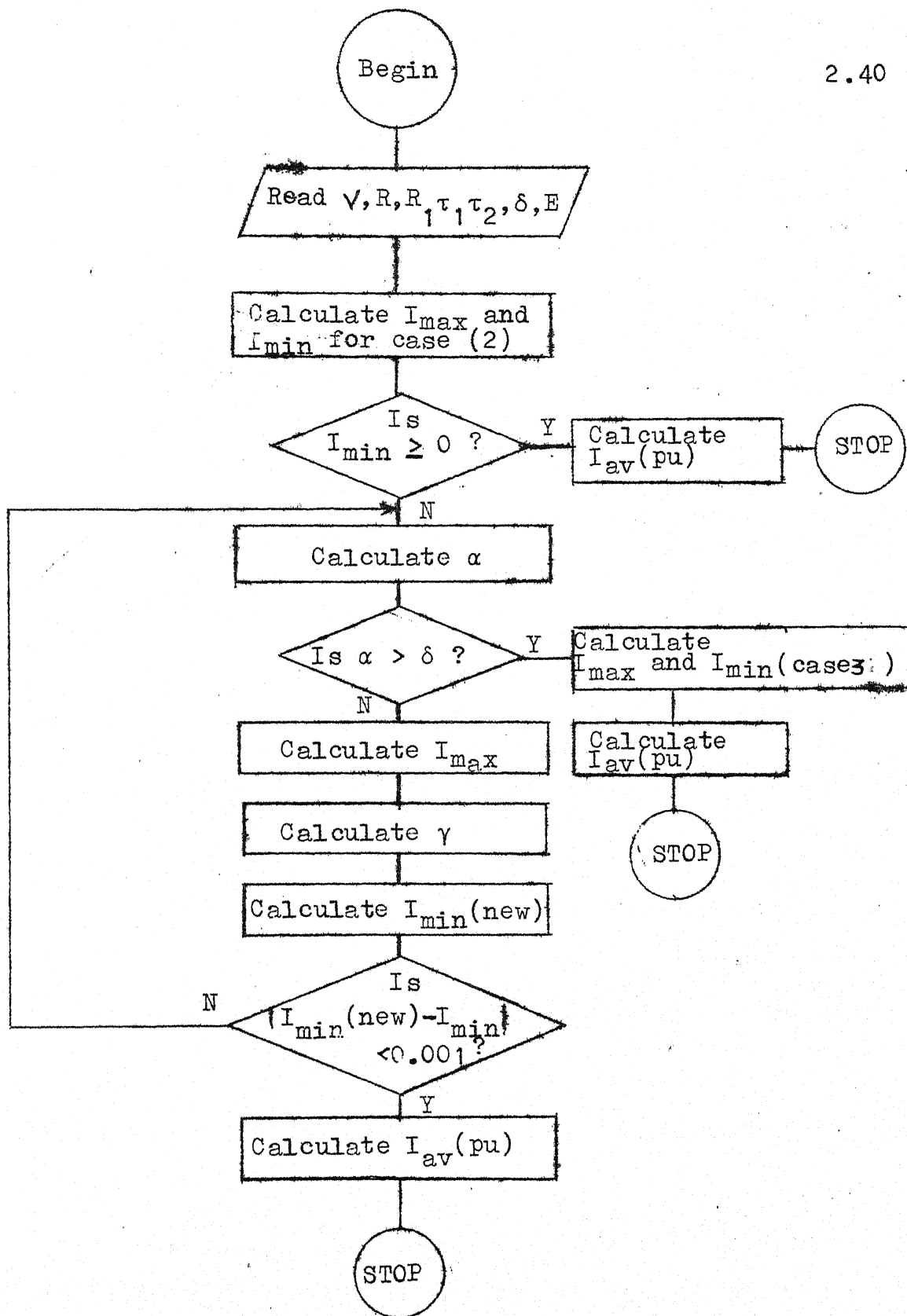


Fig. 2.7: Flow chart for computation of p.u. average current for different values of δ and back emf.

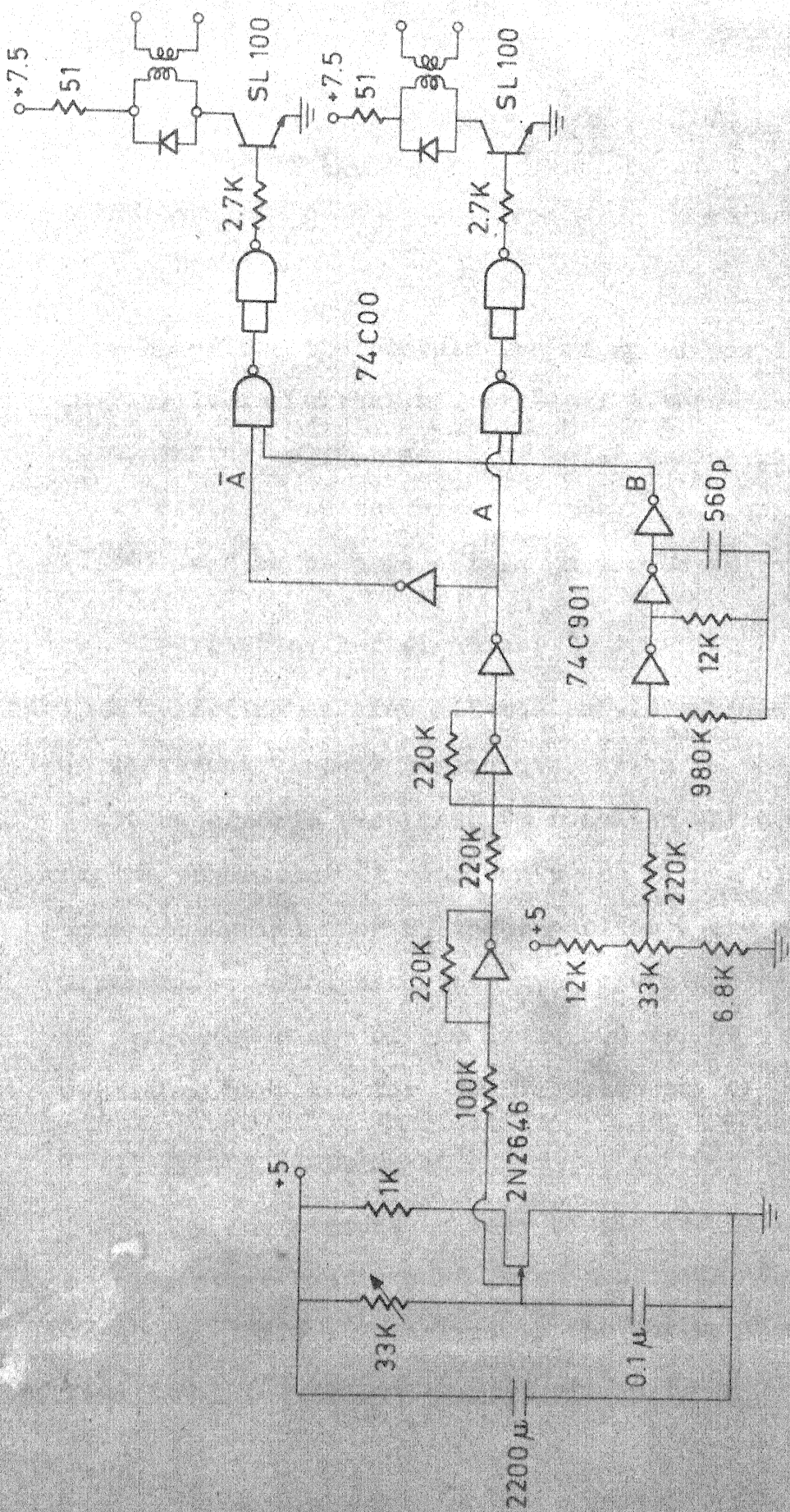


FIG. 2.8. FIRING CIRCUIT FOR THE DEVELOPED CHOPPER.

$$\text{Torque} = T_{av} = K_T \cdot I_{av} \quad (2.63)$$

and

$$\text{Speed} = \omega = \frac{E}{K_V} \quad (2.64)$$

Flow chart for the computation of speed and torque is given in Fig. 2.7. Current and back emf afterwards put in pu form, taking rated current of motor as the base current and input voltage, as the base voltage. Now eqns. (2.63) and (2.64) can be used to obtain pu torque and speed respectively.

2.7 Experimental Verification:

Keeping in view all the considerations for the design of different circuit components, given in the previous section, efforts were made to reach an optimum design. Ratings of the power circuit components and values of L_1 and L_2 , commutation inductor L_c and capacitor C are mentioned in Appendix B. Though chopper was operated satisfactorily in frequency range of 200 Hz to 600 Hz, all the results mentioned here are for 400 Hz frequency of operation.

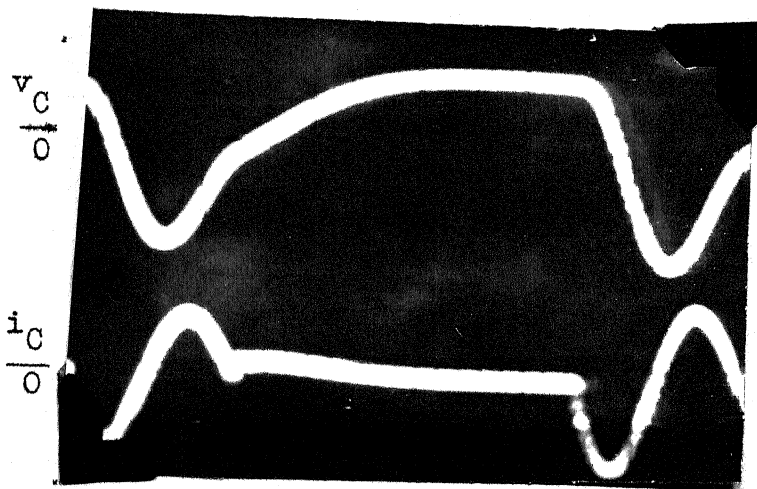
2.7.1 Firing circuit:

Firing circuit is very simple for this chopper. Two complimentary continuous pulse trains for T_1 and T_2 are required. This is obtained by the firing circuit shown in Fig. 2.8. UJT 2N2646 is used as the variable frequency

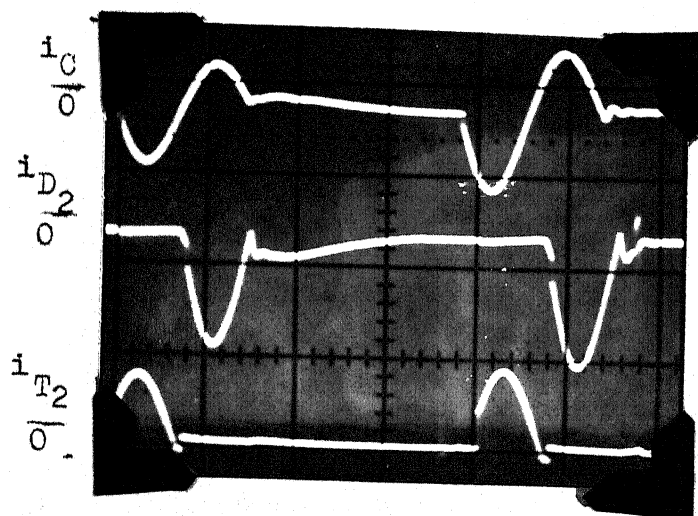
ramp generator. Inverters are used to realise the comparator and to generate the high frequency modulating signal. NAND gates are used for ANDing because of the nonavailability of AND gates. SL100 is used for the amplification of pulse train and is provided with the separate supply so that pulse strength can be varied if required. All the resistance are in ohms in Fig. 2.8.

2.7.2 Chopper performance verification:

Waveform across all the components of the circuit were examined. Their nature was close to those drawn in Fig. 2.5. Oscillograms of the waveforms are shown in Fig. 2.9. Capacitor voltage and current are shown in Fig. 2.9(a). Overcharging of capacitor and constant current interval can be easily identified in this. Capacitor current and current through D_2 and T_2 are shown in Fig. 2.9(b). The deviation from the ideal behaviour is clear here. The current through T_2 flows for more than half of the cycle of capacitor current. There are two commutation pulses shown in Fig. 2.9(a) and Fig. 2.9(b), corresponding to commutation of T_1 and T_2 . Current waveform for D_1 and D_2 are shown in Fig. 2.9(c). These give idea of the thyristor turn off time provided by the circuit. Constant current through D_2 corresponding to charging of capacitor is also

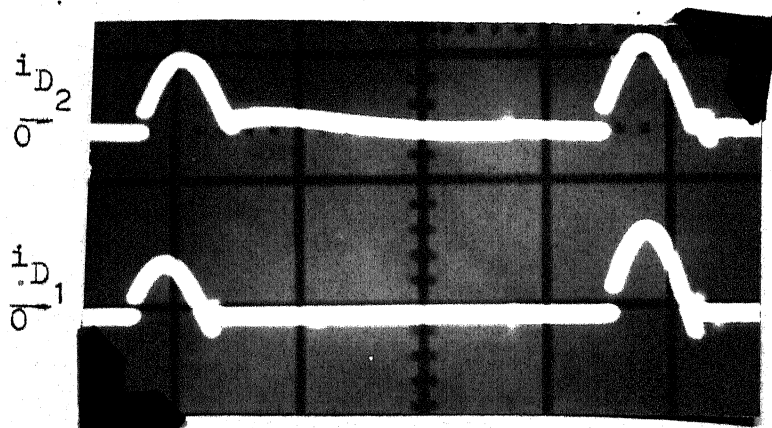


(a) Capacitor voltage and current waveforms
 Scale Voltage 200V/div.
 Current 100 A/div.
 Time 0.1 msec/div



(b) Current waveforms of capacitor, D_2 and T_2 .

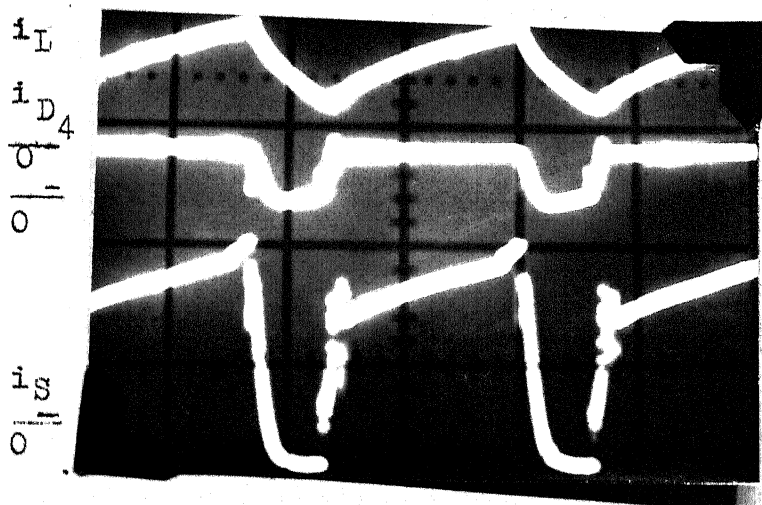
Scale
 i_c - 100 A/div
 i_{D_2} - 50 A/div.
 i_{T_2} - 100 A/div.
 time - 0.25 msec/div.



(c) Current waveforms of D_2 and D_1 .

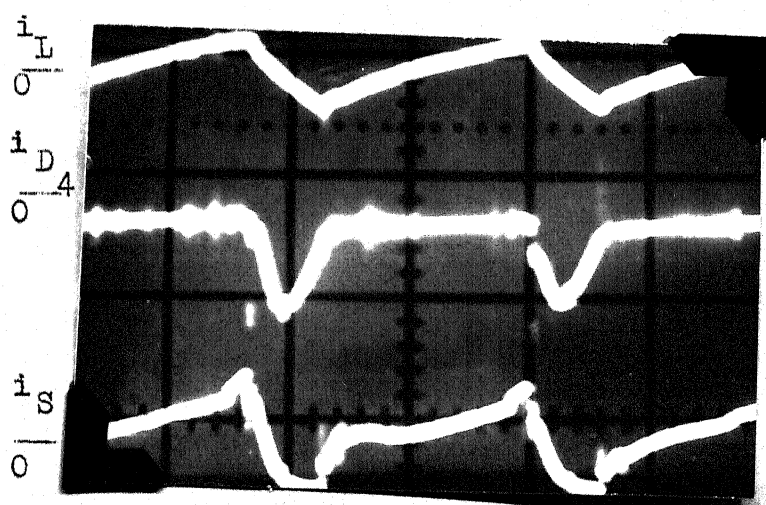
Scale
 i_{D_2} 100 A/div
 i_{D_1} 100 A/div.
 time 0.25 msec/div.

Fig. 2.9



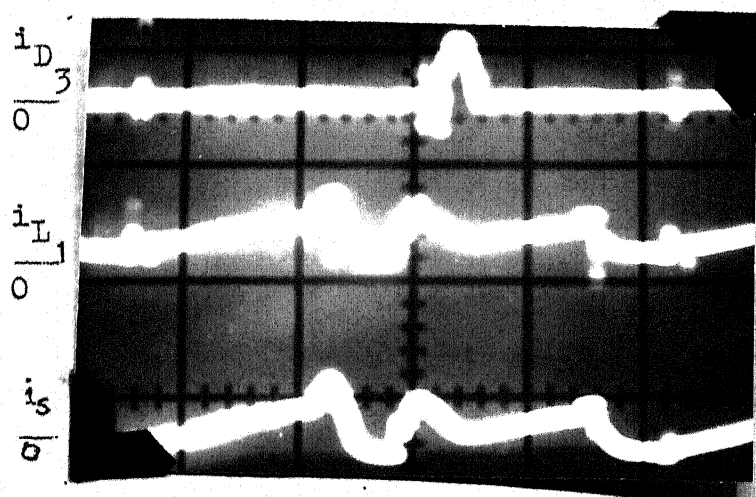
(d) Current waveform of load, D_4 and source. for $i_L = 0.434$ pu.

scale
 i_L - 10 A/div.
 i_{D_4} - 20 A/div.
 i_S - 2.1 A/div.
 time - 1 msec/div.



(e) Current waveform of load, D_4 and source. for $i_L = 0.09$ pu.

scale
 i_L - 10 A/div.
 i_{D_4} - 20 A/div.
 i_S - 2.1 A/div.
 time - 1 msec/div.



(f) Current waveforms of D_3 , L_1 and source

scale
 i_{D_3} - 0.84 A/div.
 i_{L_1} - 20 A/div.
 i_S - 20 A/div.
 time - 1 msec/div.

Fig. 2.9 (contd.)

$$\delta = 0.16$$

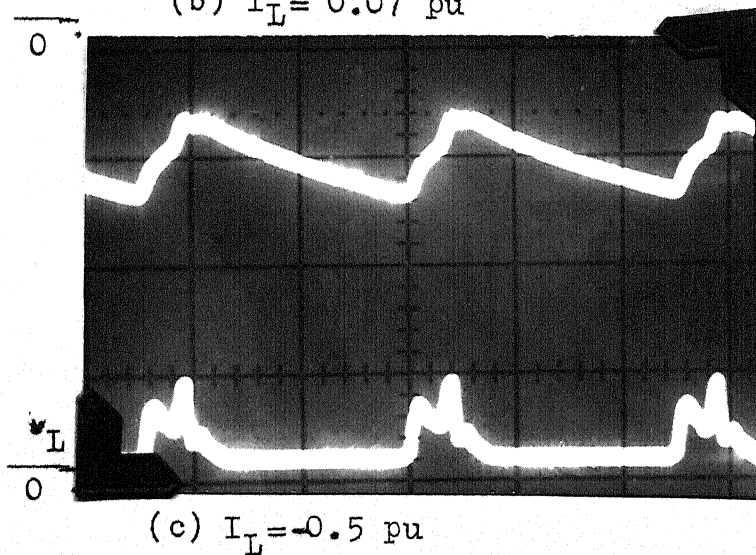
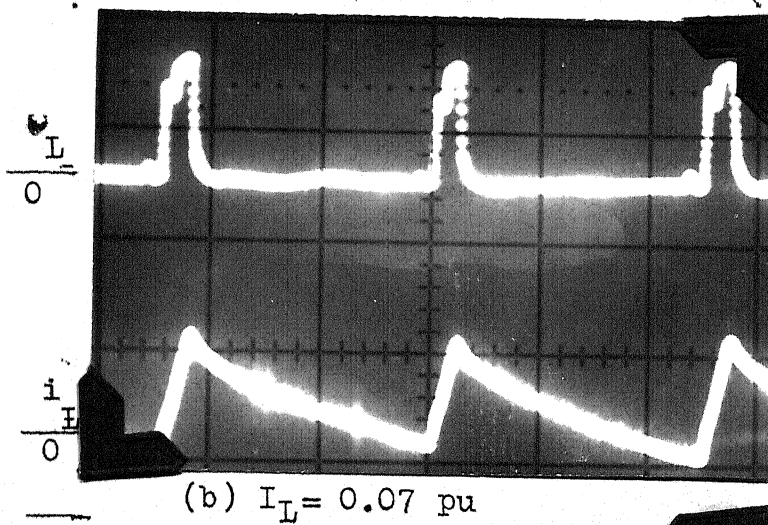
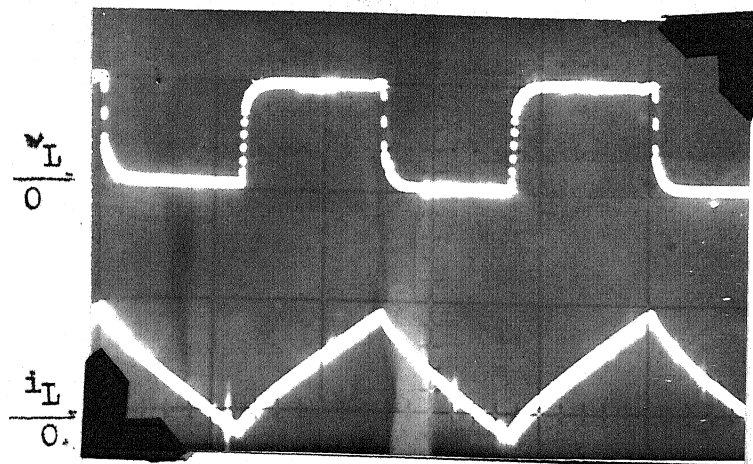


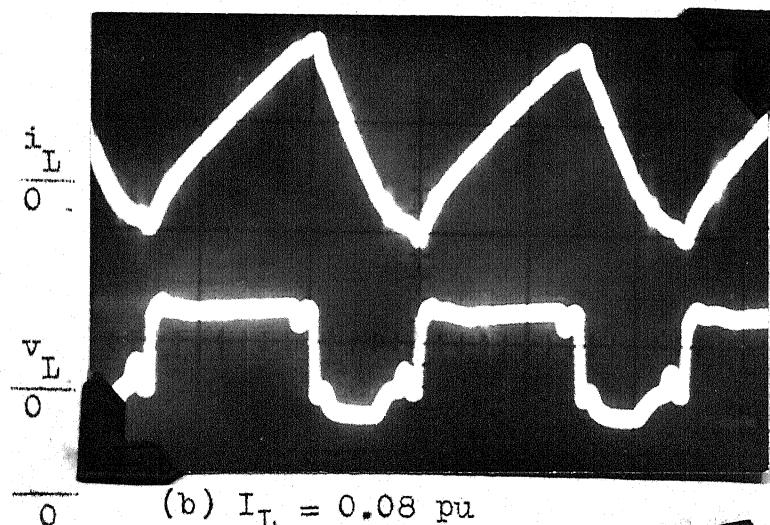
Fig. 2.10 Load voltage and current waveforms

$$\delta = 0.5$$

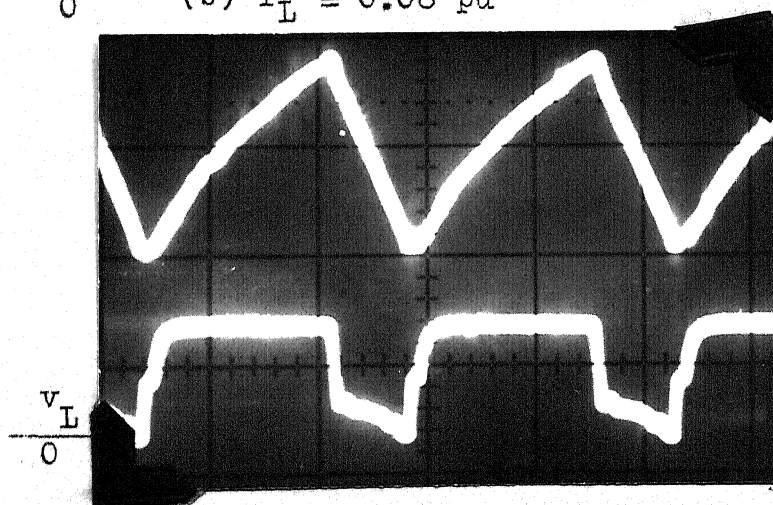
2.47



(a) $I_L = 0.65$ pu



(b) $I_L = 0.08$ pu



(c) $I_L = -0.345$ pu

Fig. 2.10 (contd.)

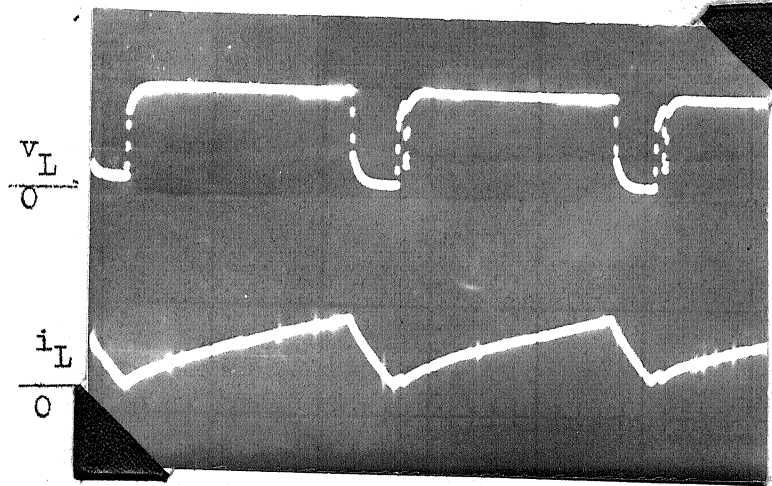
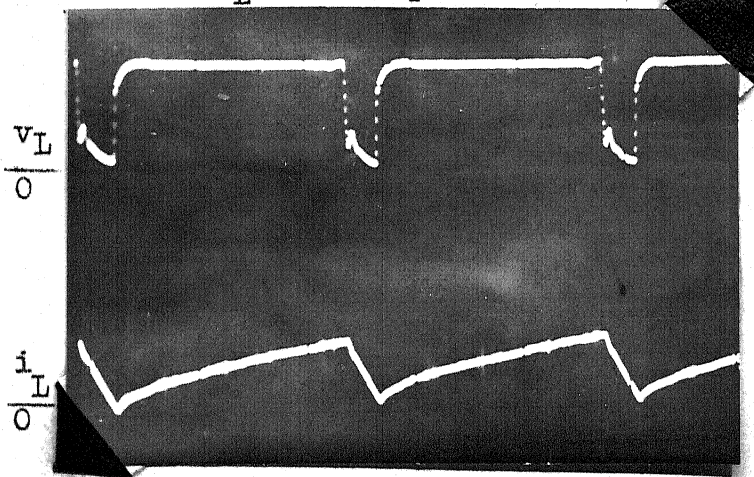
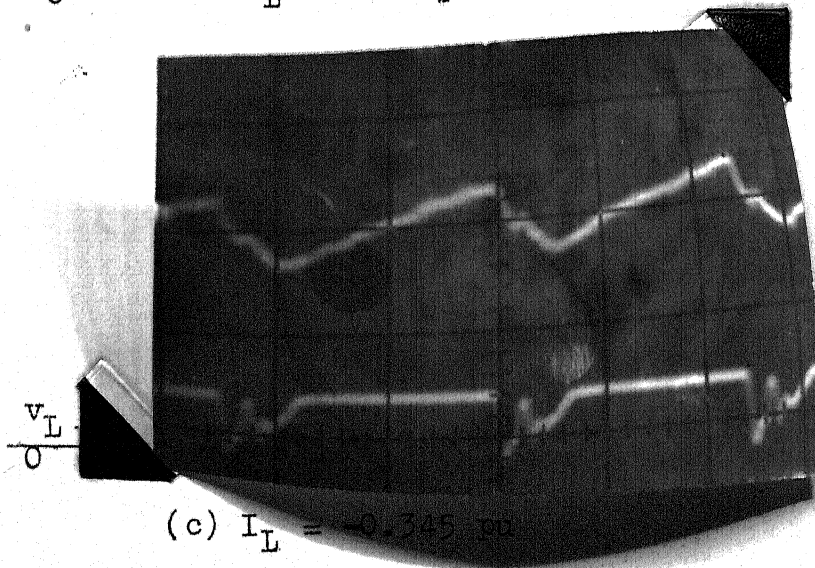
(a) $I_L = 0.65$ pu(b) $I_L = 0.08$ pu(c) $I_L = -0.345$ pu

Fig. 2.10 (contd.)

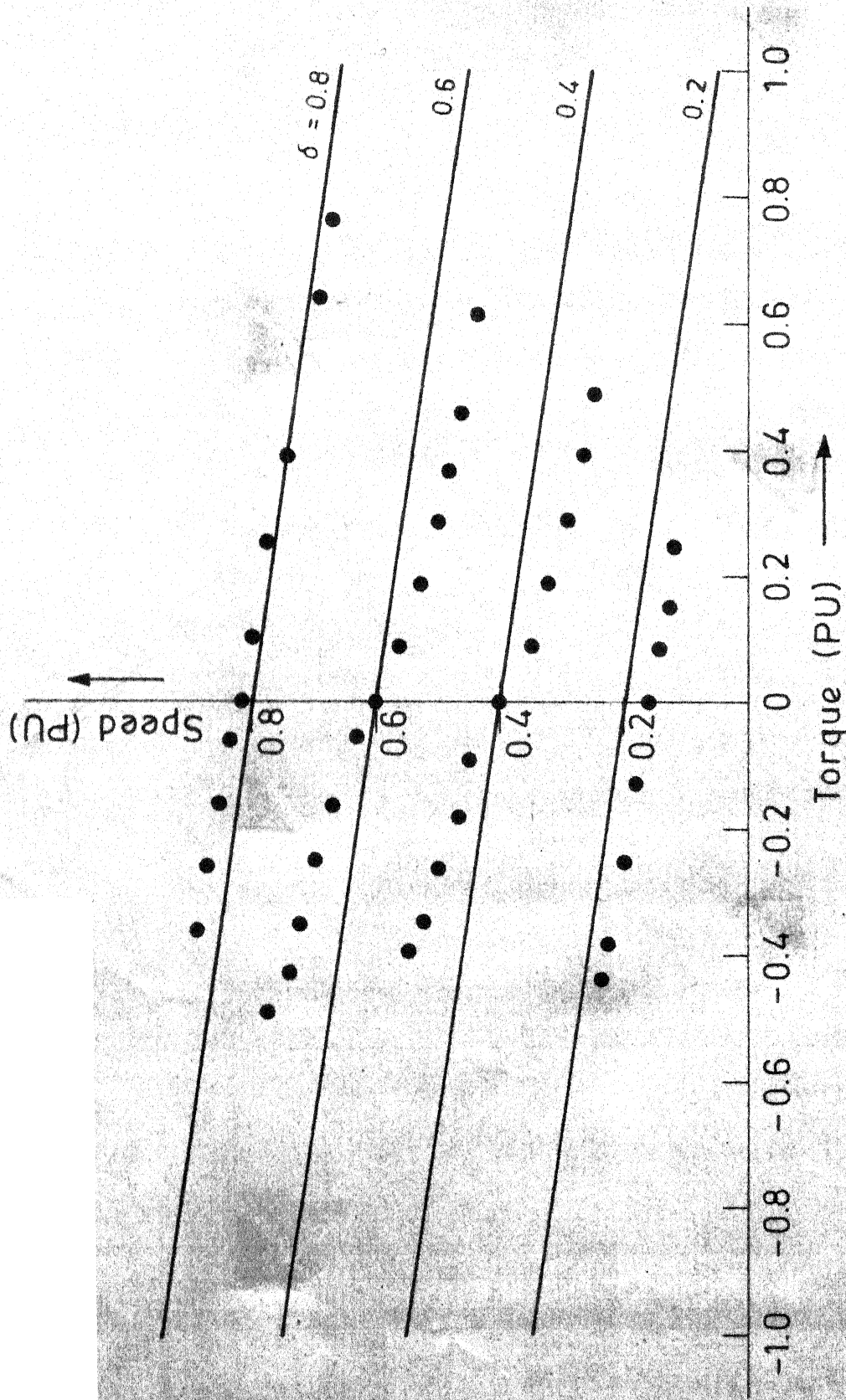


FIG. 2.11. SPEED-TORQUE CHARACTERISTIC OF THE MOTOR FED BY THE DEVELOPED CHOPPER.

explicit. Load current, current through diode D_4 and source current are shown in Fig. 2.9(d). During freewheeling the flux resetting in saturable reactor L_1 is also taking place, as voltage overshoot of capacitor is discharging through it, D_4 and the source. Therefore negative source current is found to be present. In Fig. 2.9(e), are shown current through load, D_4 and source for low load condition. As the load current goes negative here, thyristor T_2 will conduct for some time. Source current will be zero for this duration. Now this current is fed back to the source and correspondingly a dip in source current is observed. Current through D_3 , saturable inductor L_1 and the source current is shown in Fig. 2.9(f) current through D_3 indicates current fed back to the source.

2.7.3 Motor performance verification:

Oscillograms of the load voltage and current waveforms for $\delta = 0.16, 0.5$ and 0.8 are shown in Fig. 2.10. For light load condition and regeneration, voltage waveforms are found to be distorted. This is probably because of the saturable reactors L_1 and L_2 .

Further, torque-speed characteristics is drawn for the motor fed by this chopper (Fig. 2.11). Experimental results' variation from the calculated values for $\delta = 0.2, 0.4$ and 0.6 is large.

For $\delta = 0.8$ experimental results are in close proximity with the calculated values. The deviation can be attributed to the assumption taken about the variation of inductance of the saturable reactors. In practical, saturable reactor will need some current to go into saturation and there will be certain current flowing through it, when it is assumed to give infinite impedance. Further, magnetic characteristic is not linear, as assumed for the simplicity of analysis. Efforts were made to take nonlinearity of magnetic circuit into account, but due to complexities involved, simplifying assumptions had to be made. If actual nature of inductors is taken into account better results can be obtained.

2.8 Conclusions:

From the preceding discussions and the experimental results, it can be concluded that the proposed circuit has the following advantages and disadvantages.

2.8.1 Advantages:

1. Saturable reactors L_1 and L_2 support the dc bus voltage during commutation and thus reduce the energy trapped in the commutation circuit. Minimisation of trapped energy i.e. the energy stored in the commutation inductor at the end of the commutation interval, reduces the amount of energy

that needs to be pumped back to the supply. As a result of this losses are lower.

2. Commutation diodes D_1 and D_2 makes the circuit self healing, in case, nonrepeatitive misfiring occurs due to a wrong gate pulse or due to dv/dt triggering.

3. Load voltage is free from any overshoot because of diodes D_4 and D_3 , although the ringing capacitor voltage appear across T_1 and T_2 .

4. It is possible to turn off both the thyristors with the gate control circuit.

5. Capacitor voltage is always available as soon as the dc voltage is switched on, No special starting sequence is needed. Moreover there is no piling up of charge, as observed in the case of McMurrey's circuit and Laha's circuit [5].

6. No discontinuous conduction in motor operation , so even at light loads, good speed regulation and faster transient response are obtained.

7. Number of semiconductor devices and commutation circuit component is less, so cost is less and losses are low.

9. Mostly dual choppers suffer from the disadvantage of lower attainable frequency of operation. Proposed circuit uses only two thyristors which can be turned on simultaneously also. So higher frequency of operation is possible.

10. Firing circuit is simple.

2.8.2 Disadvantages:

1. Saturable inductors possess some resistance, so there will be some loss of energy in the form of heat.

2. If saturable reactors are not properly designed a direct short circuit may take place across the supply.

The developed circuit is superior to the existing chopper circuits. The commutation scheme, used in this chopper, makes it very attractive for the high power applications.

CHAPTER 3

COMPARATIVE STUDY OF CHOPPERS

3.1 Introduction:

A two quadrant chopper capable of operation with positive output current and voltage in either direction has been discussed in this chapter. This type of chopper is suitable for dc drives, for crane application, regenerative magnet power supplies, and a.c. drives using current source inverter. In present chapter, three control approaches are proposed for the power circuit configuration (Ref. Fig. 3.1(a)) of an ideal chopper capable of operation in first and fourth quadrant. A comparative study of all the three approaches has been carried out for a highly inductive load as well as a motoring load, with an objective to reach at the optimum control approach. All the performance curves and equations are presented in terms of the normalised quantities so that they can be utilised for any motor or highly inductive load, as the case may ^{be}. Boundaries between the continuous and discontinuous conduction for all the three approaches are given to facilitate design of filter inductance. It is shown that APPROACH-2 and APPROACH-3 give similar performances ^{and} both result in reduction in the output voltage harmonics, input current harmonics, and armature

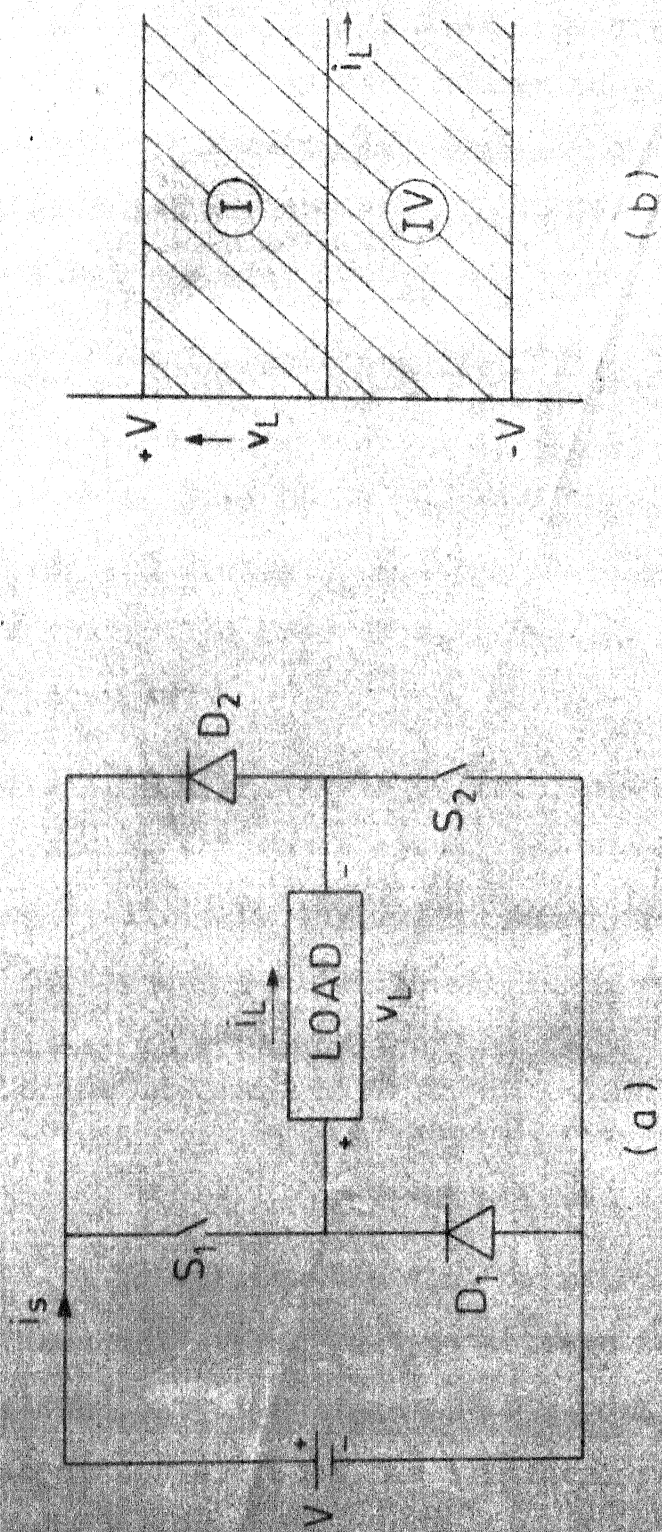


FIG 3.1. (a) POWER CIRCUIT CONFIGURATION FOR A TWO QUADRANT CHOPPER.
(b) QUADRANTS OF OPERATION ON v_L - i_L PLANE.

current ripple. They also give narrow zone of discontinuous conduction. They have lesser commutation losses. Further, APPROACH-2 results in reduction in switching frequency while APPROACH-3 has the advantages of lower cost and simpler control circuit.

3.2 Control Approaches:(Ref. Fig. 3.1(a))

The instantaneous output voltage V_L can have the value $+V$, zero or $-V$ depending upon the state of switches S_1, S_2 and diodes D_1 and D_2 . The average output voltage can be controlled from $-V$ to $+V$ by the following control approaches.

a) APPROACH-1: Double polarity simultaneous control: Switches S_1 and S_2 are to be opened and closed together. These switches are realised by thyristor, power transistor etc.. Assuming a continuous current in the load, the instantaneous output voltage is given by

$$\begin{aligned} v_L &= +V \text{ when } S_1 \text{ and } S_2 \text{ are closed} \\ &= -V \text{ when } S_1 \text{ and } S_2 \text{ are open} \end{aligned} \quad (3.1)$$

By varying the time duration for which switches are closed the average output voltage is varied. The instantaneous output voltage is both positive and negative in one output cycle. Both the switches are controlled simultaneously so the approach is termed as double polarity simultaneous control.

(b) APPROACH 2: Single Polarity simultaneous control: Switches S_1 and S_2 are controlled switches here also, so they are realised by thyristor, power transistor etc.. Switches S_1 and S_2 are operated with a time delay of half the time period. For continuous load current, instantaneous output voltage can be derived from the following equations

$$\begin{aligned}
 v_L &= +V \text{ when } S_1 \text{ and } S_2 \text{ are closed} \\
 &= 0 \text{ when } S_1 \text{ is closed and } S_2 \text{ is open} \\
 &= 0 \text{ when } S_1 \text{ is open and } S_2 \text{ is closed} \\
 &= -V \text{ when } S_1 \text{ and } S_2 \text{ are open}
 \end{aligned}
 \tag{3.2}$$

The instantaneous output voltage is either positive or negative depending upon on-time of switches. Both switches S_1 and S_2 are controlled simultaneously. So this approach is termed as single polarity simultaneous control.

(c) APPROACH 3: Single Polarity nonsimultaneous Control:

Variable positive output voltage is obtained by keeping S_1 closed all the time and operating S_2 periodically. Keeping S_1 open all the time and operating switch S_2 periodically as before, gives variable negative output voltage. Since S_1 is closed all the time for first quadrant of operation and open during fourth quadrant of operation, it can be an ordinary switch. Thus only one semiconductor switch is required. As only one switch is controlled at one time this approach is termed as single polarity nonsimultaneous control.

3.3 Chopper Performance Analysis for a Highly Inductive Load:

The dual chopper, feeding a highly inductive load is studied for output voltage ripple and input current harmonics, for each control approach. Load current is assumed to be ripple free. A.C. voltage ripple on output side or output voltage ripple is a measure of the harmonic content of the waveform which does not require the calculation of the individual harmonics.

3.3.1 APPROACH-1: Double polarity simultaneous control:

Figure 3.2(a) shows the output voltage waveform when both switches S_1 and S_2 are closed periodically at T seconds for a period of T_{on} seconds. Output voltage can be varied from $-V$ to $+V$ volts by varying the ratio t_{on}/T .

$$V_{av} = \text{Average output voltage} = 2V[\delta - 0.5] \quad (3.3)$$

where, δ = duty cycle of S_1 and $S_2 = t_{on}/T$

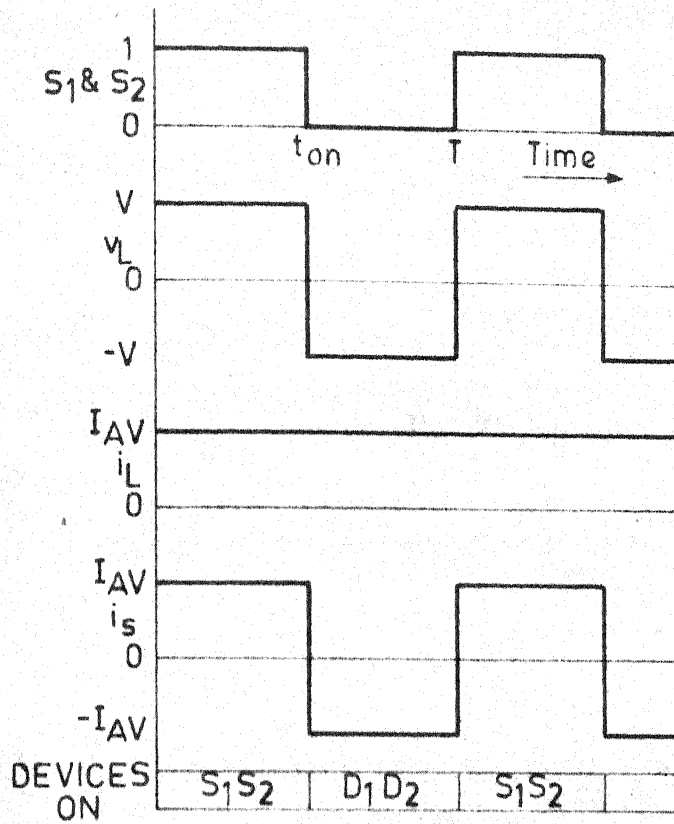
$$\text{output voltage ripple} = \sqrt{V_{rms}^2 - V_{av}^2} \quad (3.4)$$

where,

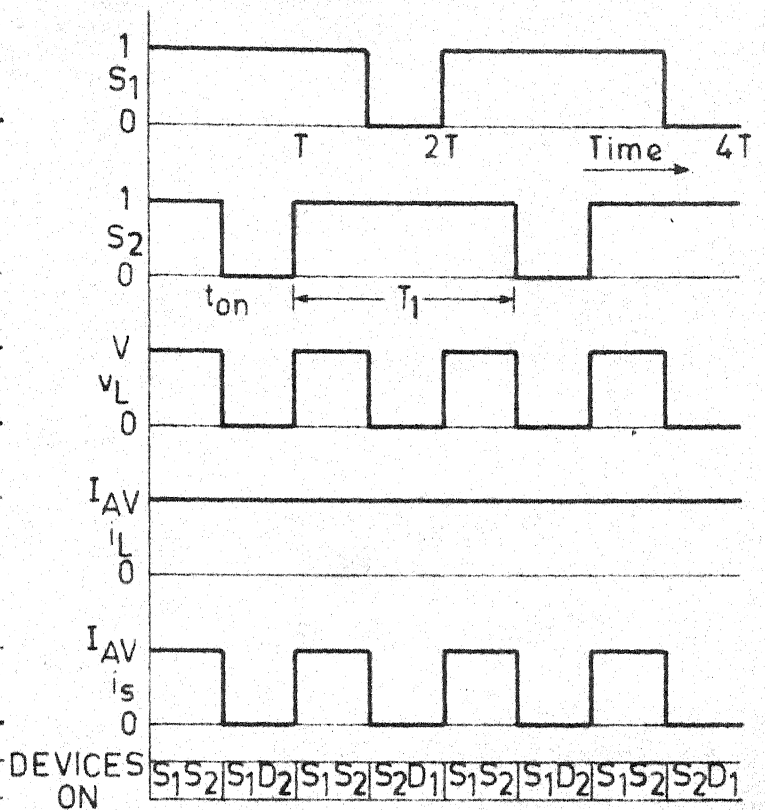
$$V_{rms} = \text{rms value of output voltage} = V$$

Substituting values of V_{rms} and V_{av} in (3.4) and taking input voltage V as base value, p.u. ripple voltage, for this case can be written as

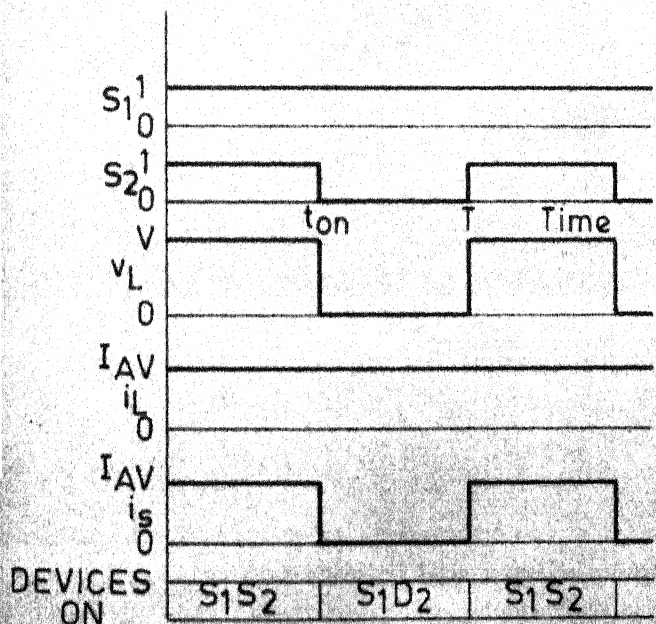
$$\text{output voltage ripple (pu)} = 2(\delta - \delta^2)^{1/2} \quad (3.5)$$



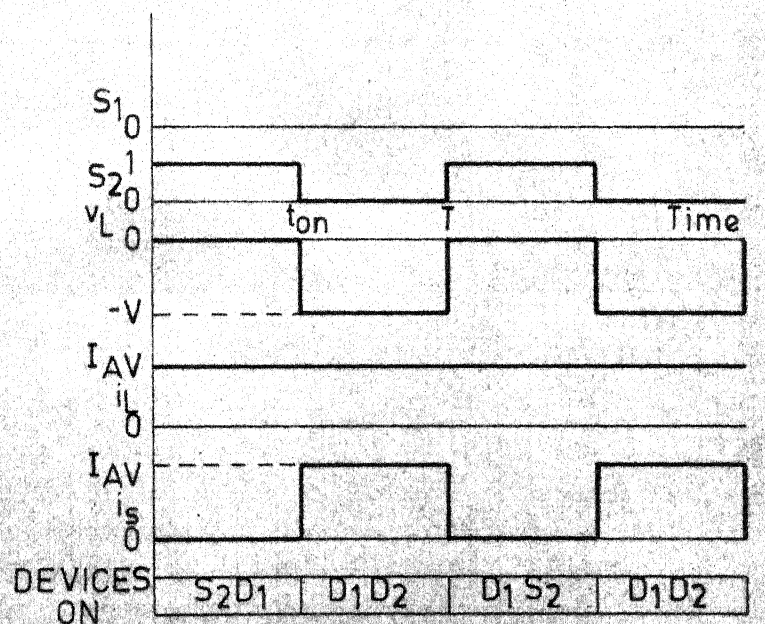
(a) Approach 1



(b) Approach 2



(c) Approach 3, motoring



(d) Approach 3, reverse regeneration

FIG. 3.2. CIRCUIT WAVEFORMS OF THE CHOPPER FOR DIFFERENT APPROACHES.

Waveform of the source current i_s is similar to that of the output voltage v_L , so equation (3.5) is also indicator of amount of source current harmonics and gives p.u. ripple of the input current, with I_{av} as base.

3.3.2 APPROACH-2: Single polarity simultaneous control: (Ref. Fig. 3.2(b)):

Switches S_1 and S_2 are operated periodically at $2T$ seconds with a time delay of T seconds between them. The average voltage is positive if the duty cycle of the switches δ is greater than 0.5 and negative if it is less than 0.5. Thus V_{av} can be varied from $+V$ to $-V$ by controlling the duty cycle of the switches S_1 and S_2 . Average output voltage for this is also given by equation (3.3).

$$\begin{aligned} V_{rms} &= V\sqrt{1-2\delta} & \delta < 0.5 \\ &= V\sqrt{(2\delta-1)} & \delta \geq 0.5 \end{aligned}$$

Substituting values of V_{rms} and V_{av} in Eqn. (3.4),

$$\begin{aligned} \text{p.u. output voltage ripple} &= (2\delta-4\delta^2)^{1/2} & \delta < 0.5 \\ &= (6\delta-2-4\delta^2)^{1/2} & \delta > 0.5 \end{aligned} \quad (3.6)$$

Equation (3.6) also indicates p.u. source current ripple with I_{av} as base current.

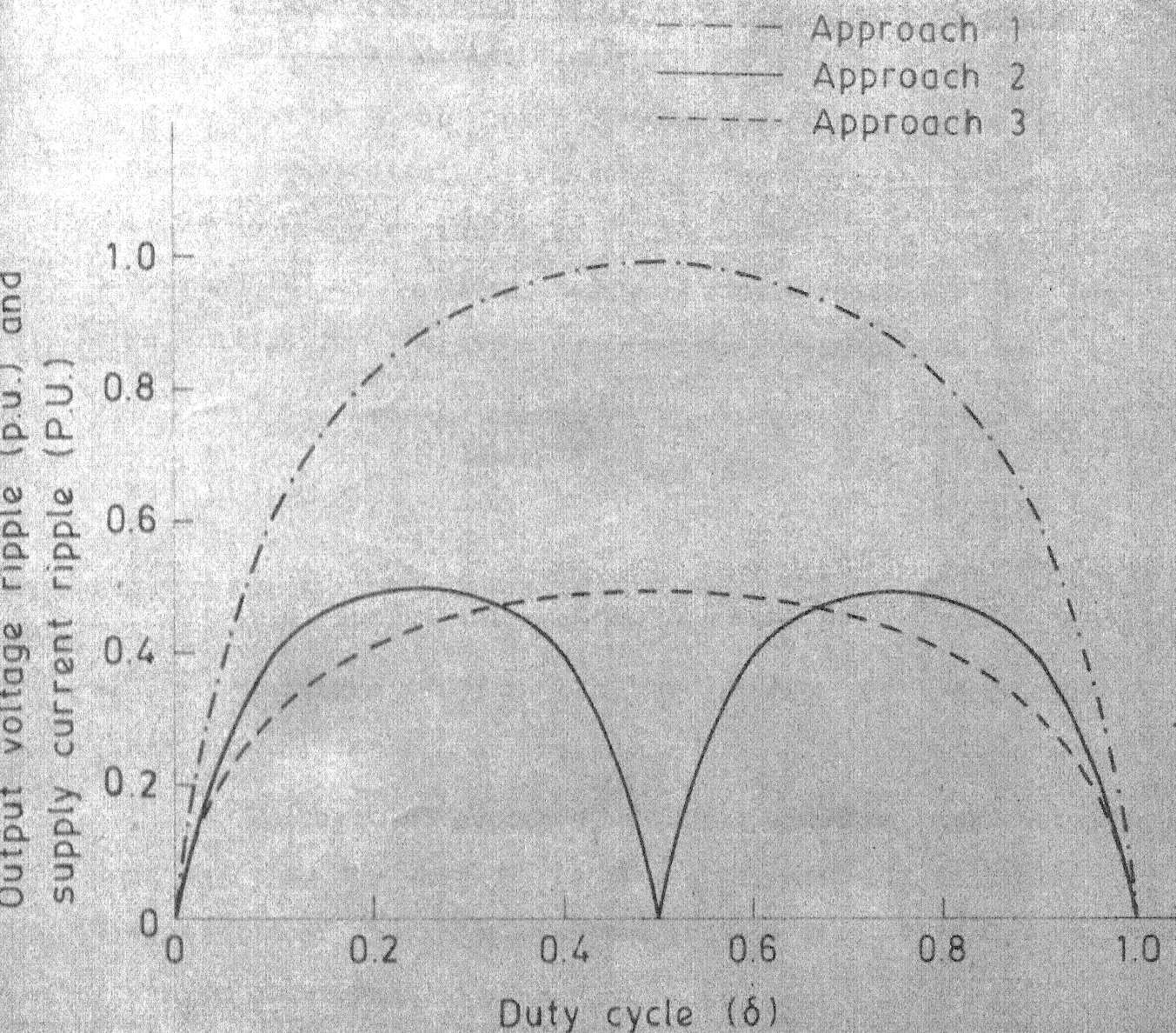


FIG. 3.3. OUTPUT VOLTAGE RIPPLE (p.u.) AND SUPPLY CURRENT RIPPLE (P.U.) vs DUTY CYCLE OF THE SWITCHES

3.3.3 APPROACH-3: Single polarity non-simultaneous control (Ref. Fig. 3.2(c and d)):

Switch S_1 is closed permanently and switch S_2 is operated periodically at T seconds for different values of t_{on}/T to get a variation of output voltage from 0 to $+V$. Average output voltage and p.u. output voltage ripple can be written for the first quadrant operation as follows:

$$V_{av} = \text{average output voltage} = V\delta \quad (3.7)$$

$$\text{and } V_{rms} = V\sqrt{\delta} \quad \text{where } \delta = t_{on}/T$$

so,

$$\text{p.u. output voltage ripple} = (\delta - \delta^2)^{1/2} \quad (3.8)$$

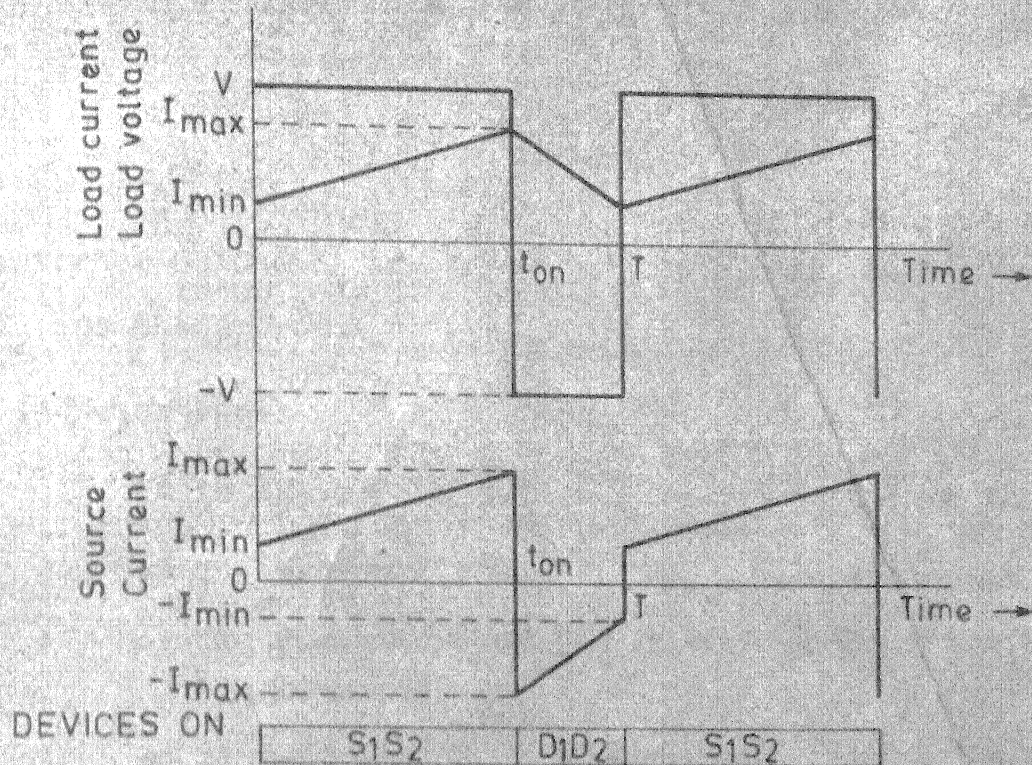
Equation (3.8) is also the indicator of source current harmonics (with I_{av} as base).

Keeping the switch S_1 open all the time, the variation of the time for which S_2 is closed periodically will give variation of the average output voltage from $-V$ to 0. It can be shown that

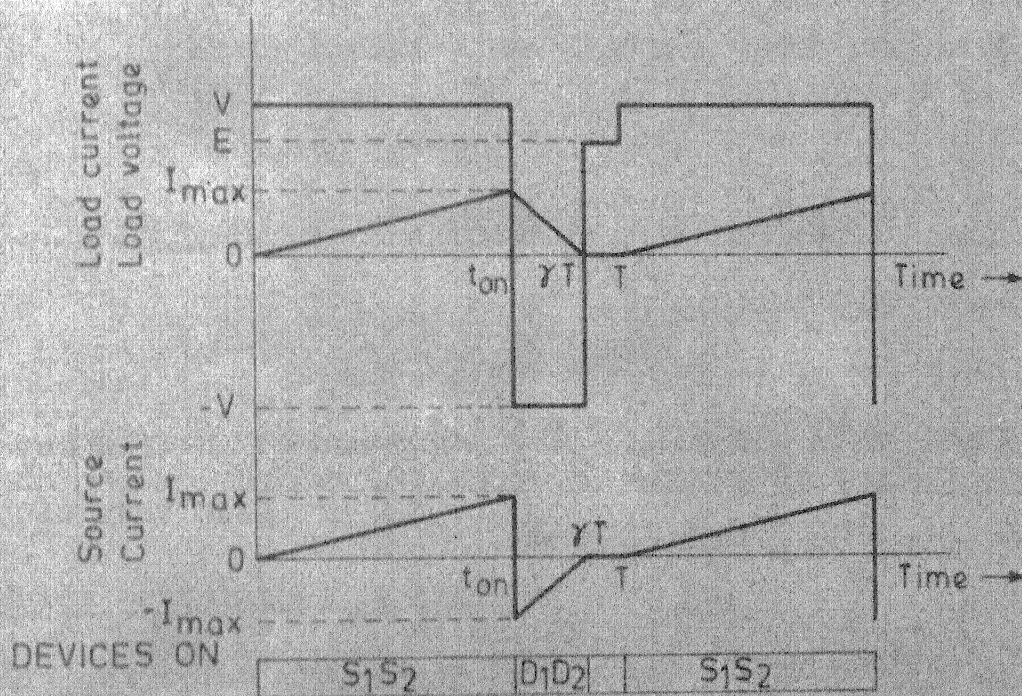
$$\text{Average output voltage} = -V(1-\delta) \quad (3.9)$$

$$\text{and } V_{rms} = V\sqrt{(1-\delta)}$$

p.u. output voltage ripple will be given by equation (3.8) for this case also. Fig. 3.3 shows the p.u. output voltage ripple (with V as base voltage) and p.u. input current ripple (with I_{av} as base current) vs. the duty cycle of the



(a) Continuous conduction



(b) Discontinuous conduction

switches S_1 and S_2 for first two approaches and of the switch S_2 for the Approach 3.

3.4 Motor Load:

It is assumed in the analysis which follows that

- a) The switches S_1 and S_2 and diodes are ideal switches.
- b) The resistance and inductance of the motor armature are constant.
- c) Since commutation pattern for S_1 and S_2 is not considered, so effect of commutation interval is overlooked.
- d) The motor speed is constant during a given steady state condition or in other words, the mechanical time constant is very large compared to chopping period.

3.4.1 APPROACH-1:

In this approach it is also assumed that there is no inherent time delay between operation of S_1 and S_2 . Motoring mode will be observed for $\delta > 0.5$ while reverse regeneration mode runs upto $\delta = 0.5$.

Motor performance analysis:

A. Continuous conduction (Ref. Fig. 3.4(a) and 3.5(a)): There are two possible intervals when the load current is continuous. Performance equations for motor in these intervals can be written as follows:

a) Interval-1: when both switches S_1 and S_2 are on.

$$V = L \frac{di_a}{dt} + Ri_a + E \text{ for } 0 \leq t \leq t_{on} \quad (3.10)$$

$$\text{and } i_a(0) = I_{min}$$

b) Interval-2: when both switches S_1 and S_2 are off

$$-V = L \frac{di_a}{dt} + Ri_a + E \text{ for } t_{on} \leq t \leq T \quad (3.11)$$

$$\text{and } i_a(t_{on}) = I_{max}$$

$$t_{on} = \delta T \text{ for this approach.}$$

Solving eqns.(3.10) and (3.11), one gets

$$i_a = \frac{V-E}{R}(1-e^{-t/\tau}) + I_{min} e^{-t/\tau} \text{ for } 0 \leq t \leq t_{on} \quad (3.12)$$

$$i_a = \frac{-(V+E)}{R} (1-e^{-(t-\delta T)/\tau}) + I_{max} e^{-(t-\delta T)/\tau} \quad (3.13)$$

for $t_{on} \leq t \leq T$

In steady state, from eqns. (3.12) and (3.13)

Since $i_a \big|_{t=t_{on}} = I_{max}$ in eqn. (3.12) and $i_a \big|_{t=T} = I_{min}$ in

eqn. (3.13). So on solving eqn. (3.12) and eqn. (3.13) and

taking input voltage V as normalising voltage, V/R as

normalising current, and τ as normalising time period,

normalised expressions for I_{max} and I_{min} can be written

as follows.

$$I_{max}(\text{norm.}) = \frac{(1+e^{-T_p} - 2e^{-\delta T_p})}{(1-e^{-T_p})} - m \quad (3.14)$$

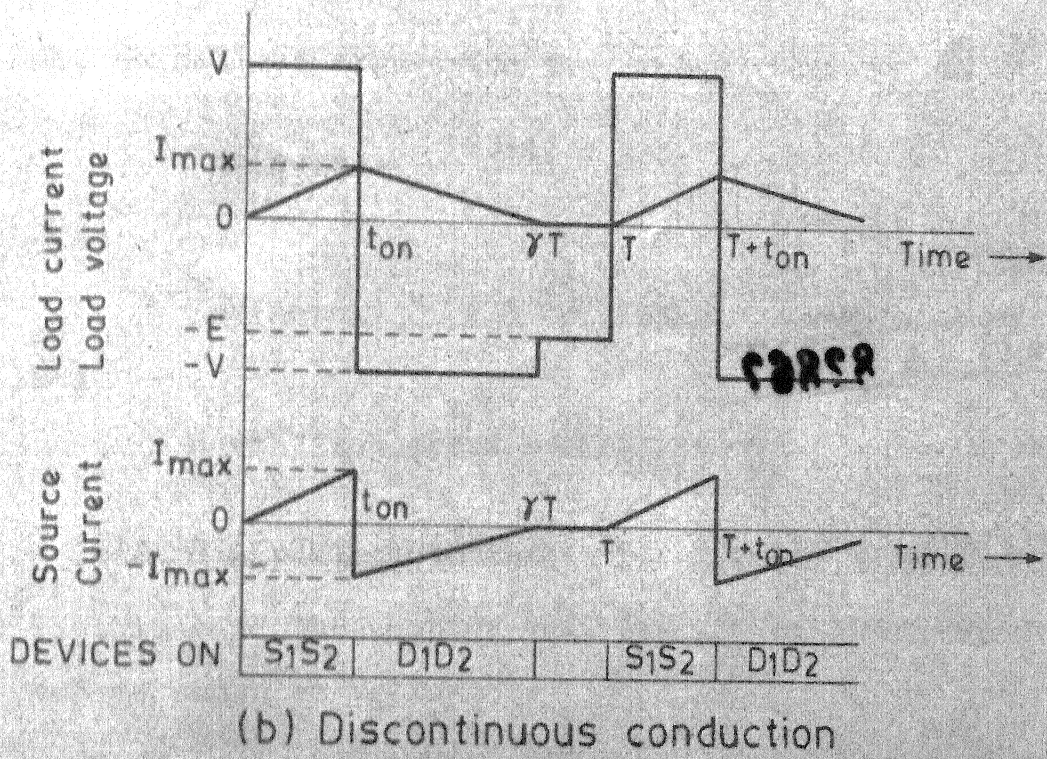
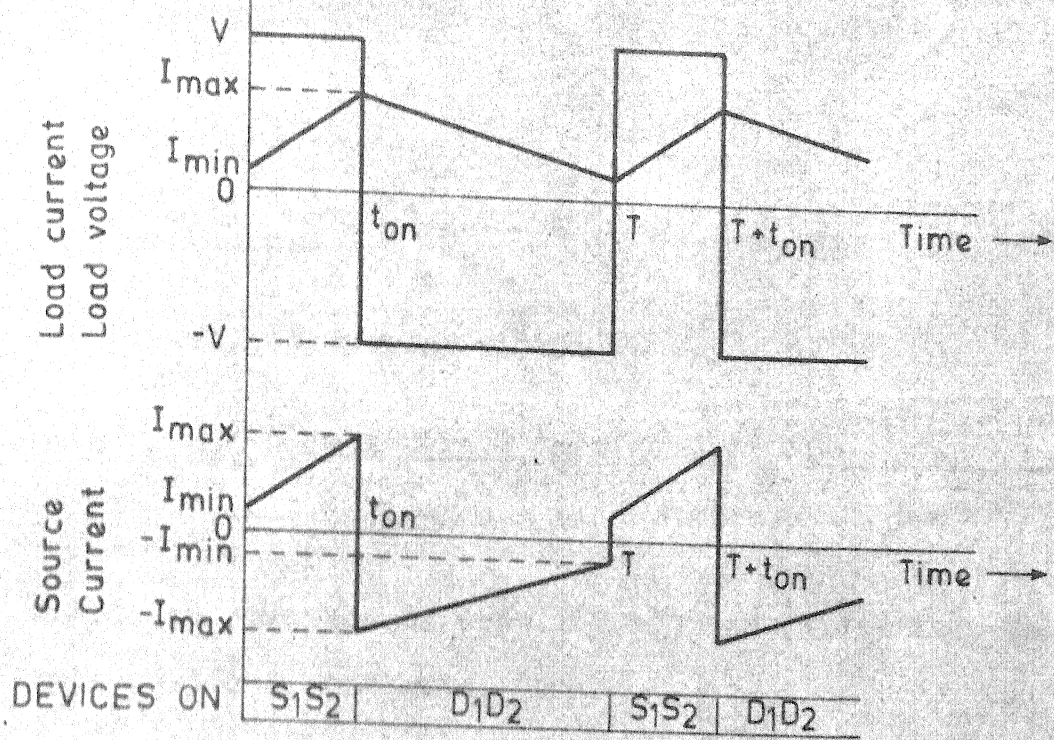


FIG. 3.5. APPROACH 1, REVERSE REGENERATION.

$$I_{\min(\text{norm.})} = \frac{2e^{\delta T_p} - e^{T_p} - 1}{e^{T_p} - 1} - m \quad (3.15)$$

The normalised current ripple is

$$\text{C.R. (norm.)} = \frac{I_{\max(\text{norm.})} - I_{\min(\text{norm.})}}{2} = \frac{1 - e^{-\delta T_p} - e^{-(1-\delta)T_p} - e^{-T_p}}{1 - e^{-T_p}} \quad (3.16)$$

Taking the average of eqns. (3.10) and (3.11) for the whole time period T , one gets

$$R \cdot I_{\text{av}} = V[2\delta - 1] - E \quad (3.)$$

so, normalised expression for average current is,

$$I_{\text{av}(\text{norm.})} = [2\delta - 1] - m \quad (3.17)$$

Thus,

$$T_{\text{av}(\text{norm.})} = K_T \cdot I_{\text{av}(\text{norm.})} \quad (3.18)$$

and

$$\text{normalised speed} = \omega_{\text{norm}} = \frac{m}{K_V} \quad (3.19)$$

B. Discontinuous conduction: (Ref. Fig. 3.4(b) and 3.5(b)):

In this case the chopper will operate in three modes which can be shown as follows:

a) Interval-1: when switches S_1 and S_2 are closed

$$L \frac{di_a}{dt} + R i_a + E = V \quad \text{for } 0 \leq t \leq t_{\text{on}} \quad (3.20)$$

$$i_a(0) = 0$$

b) Interval-2: when S_1 and S_2 are open.

$$L \frac{di_a}{dt} + R i_a + E = -V \quad \text{for } t_{\text{on}} \leq t \leq \gamma T \quad (3.21)$$

$$i_a(\delta T) = I_{\text{max}}$$

c) Interval-3: It can be termed as zero current interval also. Here

$$i_a = 0 \quad (3.22)$$

On solving eqn. (3.20) and eqn. (3.21),

$$i_a = \frac{V-E}{R} (1-e^{-t/\tau}) \quad \text{for } 0 \leq t \leq t_{\text{on}} \quad (3.23)$$

$$i_a = \frac{-(V+E)}{R} (1-e^{-(t-\delta T)/\tau}) + I_{\text{max}} e^{-(t-\delta T)/\tau} \quad \text{for } t_{\text{on}} \leq t \leq \gamma T \quad (3.24)$$

Since, $i_a \Big|_{t=\delta T} = I_{\text{max}}$ so in terms of normalised quantities

$$I_{\text{max}}(\text{norm.}) = (1-m)(1-e^{-\delta T_p}) \quad (3.25)$$

Let i_a be zero at time γT measured from the beginning of the interval-1, then from eqn. (3.24) γ can be written in terms of the normalised quantities.

$$\gamma = \frac{1}{T_p} \ln \left(\frac{2e^{\delta T_p} + m-1}{m+1} \right) \quad (3.26)$$

The critical speed ω_c , representing boundary between continuous and discontinuous conditions is obtained by letting $\gamma = 1$ in eqn. (3.26)

$$\omega_c(\text{norm.}) = \frac{m_c}{K_v} = \frac{1}{K_v} \left(\frac{2 e^{-(1-\delta)T_p} - e^{-T_p} - 1}{1 - e^{-T_p}} \right) \quad (3.27)$$

Taking the average of eqns. (3.20), (3.21) and (3.22) over the time period T , one gets

$$R.I_{av} + \gamma \cdot E = V.(2\delta - \gamma)$$

So, in terms of normalised quantities

$$I_{av}(\text{norm.}) = 2\delta - \gamma (1+m) \quad (3.28)$$

Eqns. (3.18) and (3.19) are applicable here as well.

$$C.R. (\text{norm.}) = \frac{I_{\max}(\text{norm.})}{2} = \frac{(1-m) \cdot (1 - e^{-\delta T_p})}{2} \quad (3.29)$$

All the above equations hold good both for motoring as well as reverse regeneration with slight modification. For the reverse regeneration operation, back emf E or normalised back emf m is replaced by $-E$ or $-m$ as the case may be. Eqn. (3.27) is applicable to both quadrants of operation.

Harmonics in supply current:

A. Continuous conduction: The waveform of supply current shown in Fig. 3.4(a) and Fig. 3.5(a) can be expressed mathematically as

$$i_s = (1-m) - K_1(\delta, T_p) e^{-t/\tau} \quad \text{for } 0 \leq t \leq t_{on} \quad (3.30)$$

$$\text{where, } K_1(\delta, T_p) = \frac{2(e^{T_p} - e^{\delta T_p})}{e^{T_p} - 1} \quad (3.31)$$

$$i_s = (1+m) - K_2(\delta, T_p) \cdot e^{-t/\tau} \quad \text{for } t_{on} \leq t \leq T \quad (3.32)$$

$$\text{where, } K_2(\delta, T_p) = \frac{2(e^{\delta T_p} - 1)}{1 - e^{-T_p}} \quad (3.33)$$

$K_1(\delta, T_p)$ and $K_2(\delta, T_p)$ are taken just to simplify the expressions for supply current and will be used also in the analysis that follows.

After doing Fourier analysis of above eqns., one gets the dc component of supply current as

$$a_0 = I_{av} = 1+m (1-2\delta) - \frac{K_1(\delta, T_p)}{T_p} \cdot (1 - e^{-\delta T_p}) + \frac{K_2(\delta, T_p)}{T_p} [e^{-T_p} - e^{-\delta T_p}] \quad (3.34)$$

Fourier constants are

$$a_n = -2.m. \frac{\sin 2\pi n\delta}{\pi n} - \frac{2}{T_p^2 + 4\pi^2 n^2} [e^{-\delta T_p} \{ -T_p \cdot \cos 2\pi n\delta + 2\pi n \cdot \sin 2\pi n\delta \} (K_1(\delta, T_p) - K_2(\delta, T_p)) + T_p \{ K_1(\delta, T_p) - K_2(\delta, T_p) \cdot e^{-T_p} \}] \quad (3.35)$$

and

$$b_n = \frac{-2.m.(1 - \cos 2\pi n\delta)}{\pi n} + \frac{2}{T_p^2 + 4\pi^2 n^2} [e^{-\delta T_p} \{ T_p \sin 2\pi n\delta + 2\pi n \cos 2\pi n\delta \} \cdot (K_1(\delta, T_p) - K_2(\delta, T_p)) - 2\pi n \{ K_1(\delta, T_p) - K_2(\delta, T_p) \cdot e^{-T_p} \}] \quad (3.36)$$

Hence, the rms value of nth harmonic of supply current will be

$$I_n = \sqrt{(a_n^2 + b_n^2)/2} \quad (3.37)$$

B. Discontinuous Conduction: The mathematical expression for this case (Ref. Fig. 3.4(b) and Fig. 3.5(b)) can be given as follows

$$\begin{aligned} i_s &= (1-m) (1-e^{-t/\tau}) & 0 \leq t \leq t_{on} \\ &= 1+m+(1-m-2e^{\delta T_p})e^{-t/\tau} & t_{on} \leq t \leq \gamma T \\ &= 0 & \gamma T \leq t \leq T \end{aligned} \quad (3.38)$$

The dc component will be

$$\begin{aligned} a_0 = I_{av} &= (1+m)(\gamma-\delta) + (1-m) \left\{ \delta + \frac{1}{T_p} (2e^{-\delta T_p} - e^{-\gamma T_p} - 1) \right\} \\ &\quad - \frac{2}{T_p} (1 - e^{-(\gamma-\delta)T_p}) \end{aligned} \quad (3.39)$$

The Fourier coefficients can be written as follows

$$\begin{aligned} a_n &= \frac{\sin 2\pi n \gamma}{\pi n} + \frac{m}{\pi n} (\sin 2\pi n \gamma - 2\sin 2\pi n \delta) - \frac{4}{T_p^2 + 4\pi^2 n^2} (1-m-e^{\delta T_p}) \\ &\quad \left\{ e^{-\delta T_p} (-T_p \cos 2\pi n \delta + 2\pi n \sin 2\pi n \delta) \right\} + \frac{2}{T_p^2 + 4\pi^2 n^2} [(m-1) \cdot T_p \\ &\quad + (1-m-2e^{\delta T_p}) \left\{ e^{-\gamma T_p} (-T_p \cos 2\pi n \gamma + 2\pi n \sin 2\pi n \gamma) \right\}] \end{aligned} \quad (3.40)$$

and

$$\begin{aligned}
 b_n = & \frac{(1 - \cos 2\pi n \gamma)}{\pi n} + \frac{m}{\pi n} \cdot (2 \cos 2\pi n \delta - \cos 2\pi n \gamma - 1) \\
 & - \frac{4\pi n}{T_p^2 + 4\pi^2 n^2} (1 - m) + \frac{4}{T_p^2 + 4\pi^2 n^2} \left\{ e^{-\delta T_p} (T_p \sin 2\pi n \delta \right. \\
 & \left. + 2\pi n \cos 2\pi n \delta) (1 - m - e^{\delta T_p}) \right\} - \frac{2}{T_p^2 + 4\pi^2 n^2} (1 - m - 2e^{\delta T_p}) \\
 & \left\{ e^{-\gamma T_p} (T_p \sin 2\pi n \gamma + 2\pi n \cos 2\pi n \gamma) \right\} \quad (3.41)
 \end{aligned}$$

Therefore the rms value of nth harmonic in the supply current is obtained from eqn. (3.37)

3.4.2 APPROACH-2:

Switches S_1 and S_2 are closed for T_1 seconds every $2T$ seconds with a time difference of T seconds between them. Motoring operation is achieved for $\delta > 0.5$ while values of δ from 0 to 0.5 give reverse regenerative operation.

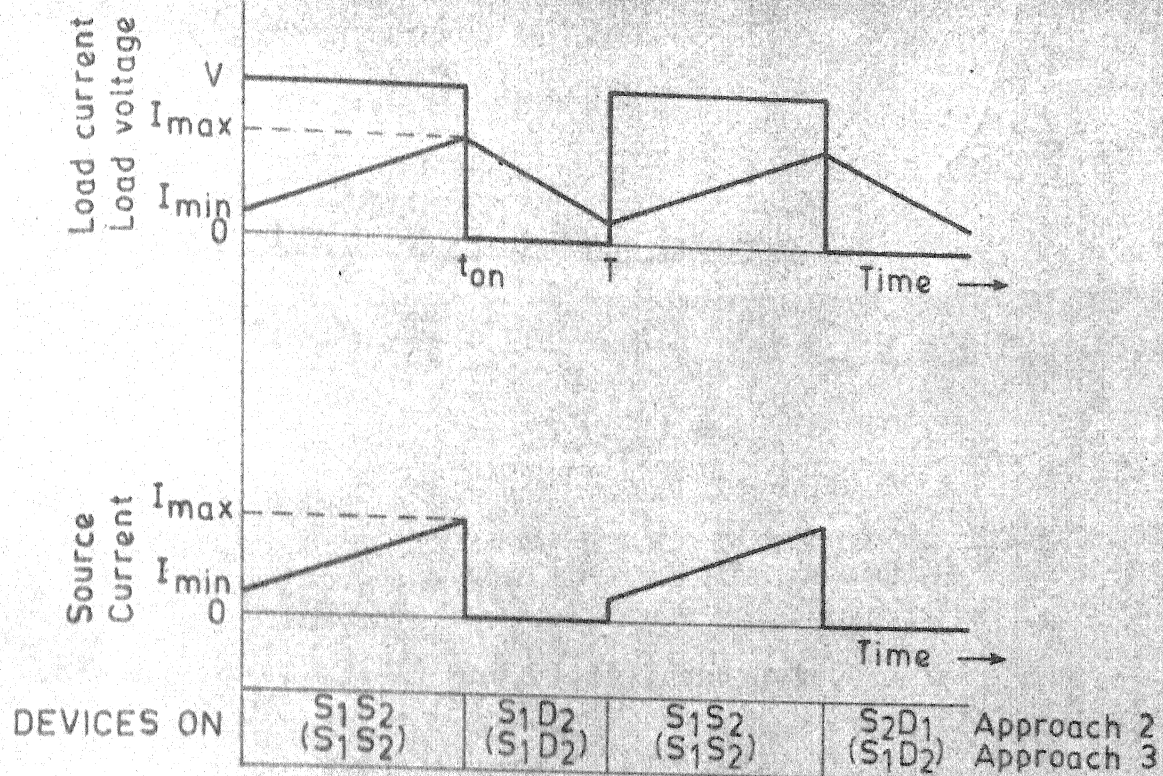
Motor performance analysis for motoring operation

A. Continuous conduction (Ref. Fig. 3.6(a)): There are two intervals in this mode of operation which can be expressed as follows with help of the corresponding mesh equations.

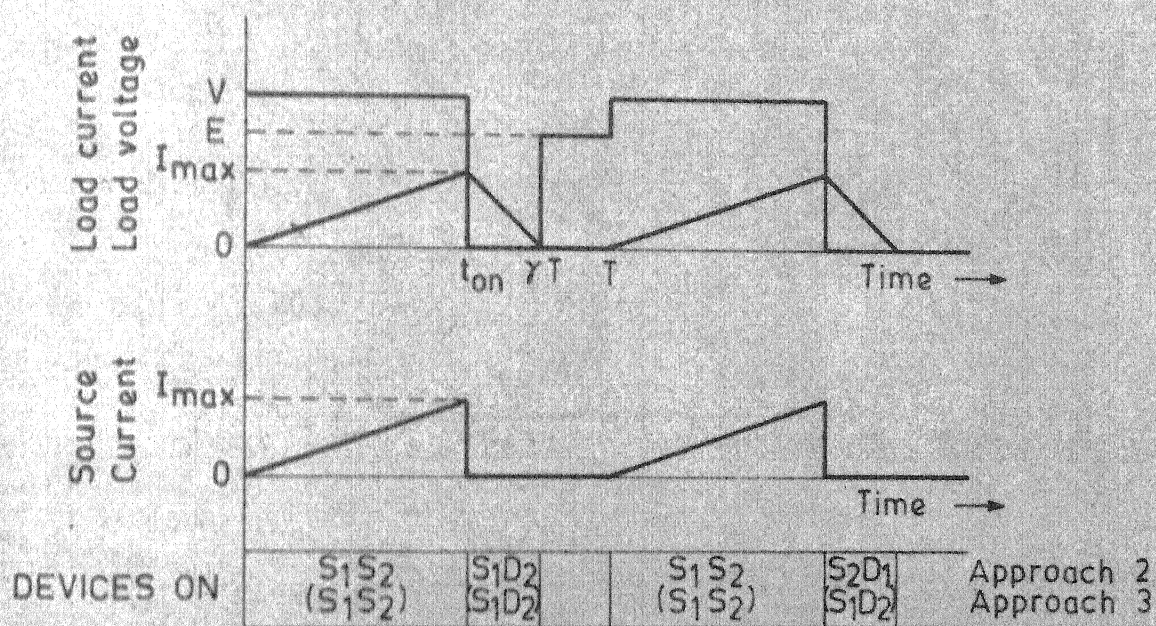
a) Interval-1 or Duty interval

$$V = L \frac{di_a}{dt} + R i_a + E \quad \text{for } 0 \leq t \leq t_{on} \quad (3.42)$$

$$\text{and } i_a(0) = I_{min}$$



(a) Continuous conduction



(b) Discontinuous conduction

FIG. 3.6. APPROACH 2 & 3, MOTORING OPERATION.

b) Interval-2 or Freewheeling interval:

$$0 = L \frac{di_a}{dt} + R i_a + E \quad \text{for } t_{on} \leq t \leq T \quad (3.43)$$

$$i_a(t_{on}) = I_{max}$$

For this approach

$$t_{on} = (2\delta - 1)T \quad (3.44)$$

Solving eqns. (3.42) and (3.43), one gets,

$$i_a = \frac{V-E}{R} (1 - e^{-t/\tau}) + I_{min} e^{-t/\tau} \quad \text{for } 0 \leq t \leq t_{on} \quad (3.45)$$

$$i_a = \frac{-E}{R} (1 - e^{-(t-t_{on})/\tau}) + I_{max} e^{-(t-t_{on})/\tau} \quad \text{for } t_{on} \leq t \leq T \quad (3.46)$$

Since $i_a \Big|_{t=t_{on}} = I_{max}$ in eqn. (3.45) and $i_a \Big|_{t=T} = I_{min}$ in eqn. (3.46), so

$$I_{max} = \frac{V}{R} \frac{(1 - e^{-t_{on}/\tau})}{1 - e^{-T/\tau}} - \frac{E}{R} \quad (3.47)$$

$$I_{min} = \frac{V}{R} \left(\frac{e^{t_{on}/\tau} - 1}{e^{T/\tau} - 1} \right) - \frac{E}{R} \quad (3.48)$$

Substituting value of t_{on} in eqn. (3.47) and eqn. (3.48) from eqn. (3.44), I_{max} and I_{min} can be rewritten in terms of normalised quantities as follows.

$$I_{\max}(\text{norm.}) = \frac{1 - e^{-(2\delta-1)T_p}}{1 - e^{-T_p}} - m \quad (3.49)$$

$$I_{\min}(\text{norm.}) = \frac{e^{(2\delta-1)T_p} - 1}{e^{T_p} - 1} - m \quad (3.50)$$

The normalised current ripple is

$$\begin{aligned} \text{C.R.}(\text{norm.}) &= \frac{I_{\max}(\text{norm.}) - I_{\min}(\text{norm.})}{2} \\ &= \frac{0.5 \cdot (1 - e^{-(2\delta-1)T_p} - e^{-2(1-\delta)T_p} + e^{-T_p})}{1 - e^{-T_p}} \end{aligned} \quad (3.51)$$

Taking the average of eqns. (3.42) and (3.43)

$$\frac{V \cdot t_{\text{on}}}{T} = R \cdot I_{\text{av}} + E \quad (3.52)$$

In steady state the average voltage across the inductor will be zero. So,

$$I_{\text{av}}(\text{norm.}) = 2\delta - (1+m) \quad (3.53)$$

Normalised torque and speed can be found out from eqns. (3.18) and (3.19)

B. Discontinuous conduction: (Ref. Fig. 3.6(b)): Three intervals present in this case can be expressed with the help of eqns. as follows.

a) Interval-1 or Duty interval

$$V = L \frac{di_a}{dt} + R i_a + E \quad \text{for } 0 \leq t \leq t_{on} \quad (3.54)$$

$$i_a(0) = 0$$

b) Interval-2 or Freewheeling interval

$$0 = L \frac{di_a}{dt} + R i_a + E \quad \text{for } t_{on} \leq t \leq \gamma T \quad (3.55)$$

$$i_a(t_{on}) = I_{max}$$

c) Interval-3 or Zero current interval

$$i_a = 0 \quad \text{for } \gamma T \leq t \leq T \quad (3.56)$$

On solving eqns. (3.54) and (3.55)

$$i_a = \frac{V-E}{R} (1 - e^{-t/\tau}) \quad \text{for } 0 \leq t \leq t_{on} \quad (3.57)$$

$$i_a = \frac{-E}{R} (1 - e^{-(t-t_{on})/\tau}) + I_{max} e^{-(t-t_{on})/\tau}$$

$$\text{for } t_{on} \leq t \leq \gamma T \quad (3.58)$$

From eqn. (3.57)

$$i_a \Big|_{t=t_{on}} = I_{max} = \frac{V-E}{R} (1 - e^{-t_{on}/\tau}) \quad (3.59)$$

Substituting value of t_{on} from eqn. (3.44) in eqn. (3.59) the normalised expression for I_{max} can be written as,

$$I_{max}(\text{norm.}) = (1-m) \cdot (1 - e^{-(2\delta-1)T_p}) \quad (3.60)$$

Let the current reduce to zero value at $t = \gamma T$, then

$$\gamma = \frac{1}{T_p} \ln \left[1 + \frac{e^{\frac{t_{on}}{T} \cdot T_p} - 1}{m} \right] \quad (3.61)$$

Substituting the value of t_{on} from eqn.(3.44) into (3.61)

$$\gamma = \frac{1}{T_p} \ln \left(1 + \frac{(e^{(2\delta-1)T_p} - 1)}{m} \right) \quad (3.62)$$

Normalised value of critical speed

$$\omega_c(\text{norm.}) = \frac{m_c}{K_v} = \frac{1}{K_v} \left(\frac{e^{\frac{t_{on}}{T} \cdot T_p} - 1}{e^{T_p} - 1} \right) \quad (3.63)$$

On substituting value of t_{on} from eqn.(3.44) in eqn.(3.63),

$$\omega_c(\text{norm.}) = \frac{m_c}{K_v} = \frac{1}{K_v} \left(\frac{e^{(2\delta-1)T_p} - 1}{e^{T_p} - 1} \right) \quad (3.64)$$

Taking the average of eqns. (3.54), (3.55) and (3.56) over the time period T

$$V \cdot \frac{t_{on}}{T} = R \cdot I_{av} + \gamma \cdot E \quad (3.65)$$

so, normalised value of I_{av}

$$I_{av}(\text{norm.}) = 2\delta - 1 - \gamma \cdot m \quad (3.66)$$

Eqn. (3.18) and (3.19) are used to find out $T_{av}(\text{norm.})$ and $\omega(\text{norm.})$ respectively.

$$C.R.(\text{Norm.}) = \frac{I_{\max}(\text{norm.})}{2} = \frac{(1-m)(1-e^{-(2\delta-1)T_p})}{2} \quad (3.67)$$

Motor performance analysis for reverse regenerative operation

A. Continuous conduction: (Ref. Fig. 3.7(a)): Respective mesh equations for the intervals present in this mode are written below

a) Interval-1 or Freewheeling interval

$$0 = L \frac{di_a}{dt} + R.i_a - E \quad \text{for } 0 \leq t \leq t_{on} \quad (3.68)$$

$$i_a(0) = I_{\min}$$

b) Interval-2 or Duty interval

$$-V = L \frac{di_a}{dt} + R.i_a - E \quad \text{for } t_{on} \leq t \leq T \quad (3.69)$$

$$i_a(t_{on}) = I_{\max}$$

On solving eqns. (3.68) and (3.69) one gets,

$$i_a = \frac{E}{R} (1 - e^{-t/\tau}) + I_{\min} e^{-t/\tau} \quad \text{for } 0 \leq t \leq t_{on} \quad (3.70)$$

$$i_a = \frac{E-V}{R} (1 - e^{-(t-t_{on})/\tau}) + I_{\max} e^{-(t-t_{on})/\tau} \quad \text{for } t_{on} \leq t \leq T \quad (3.71)$$

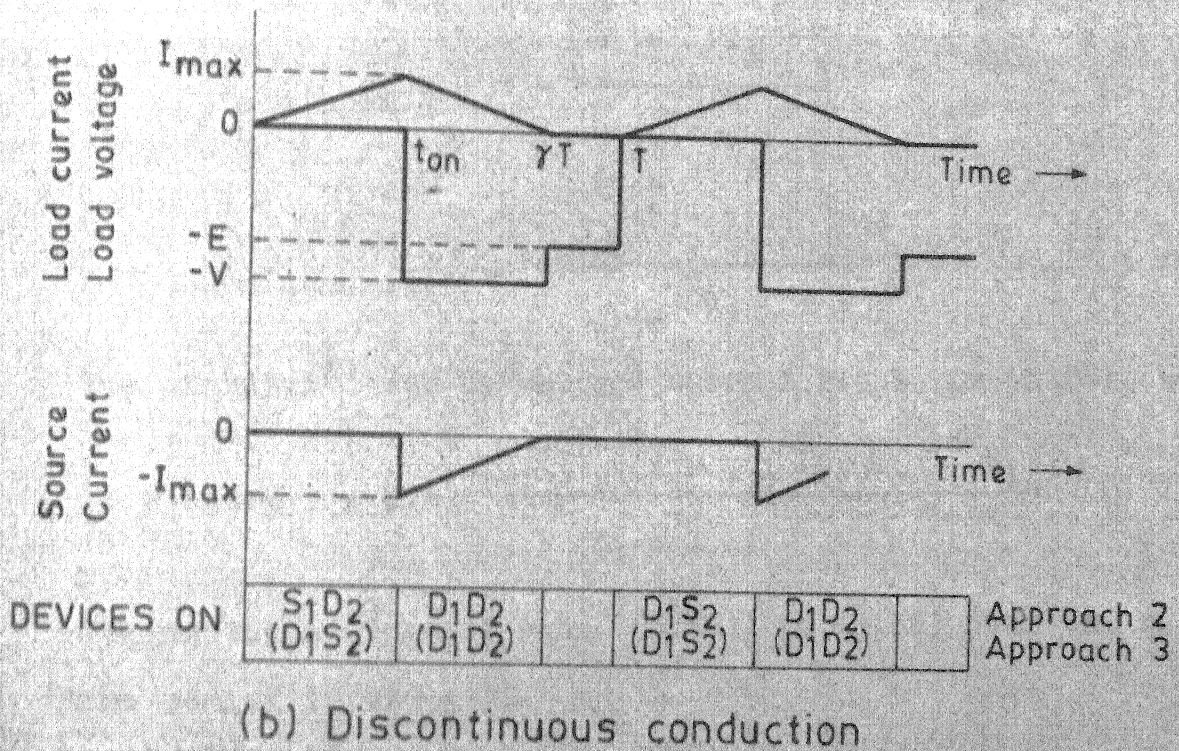
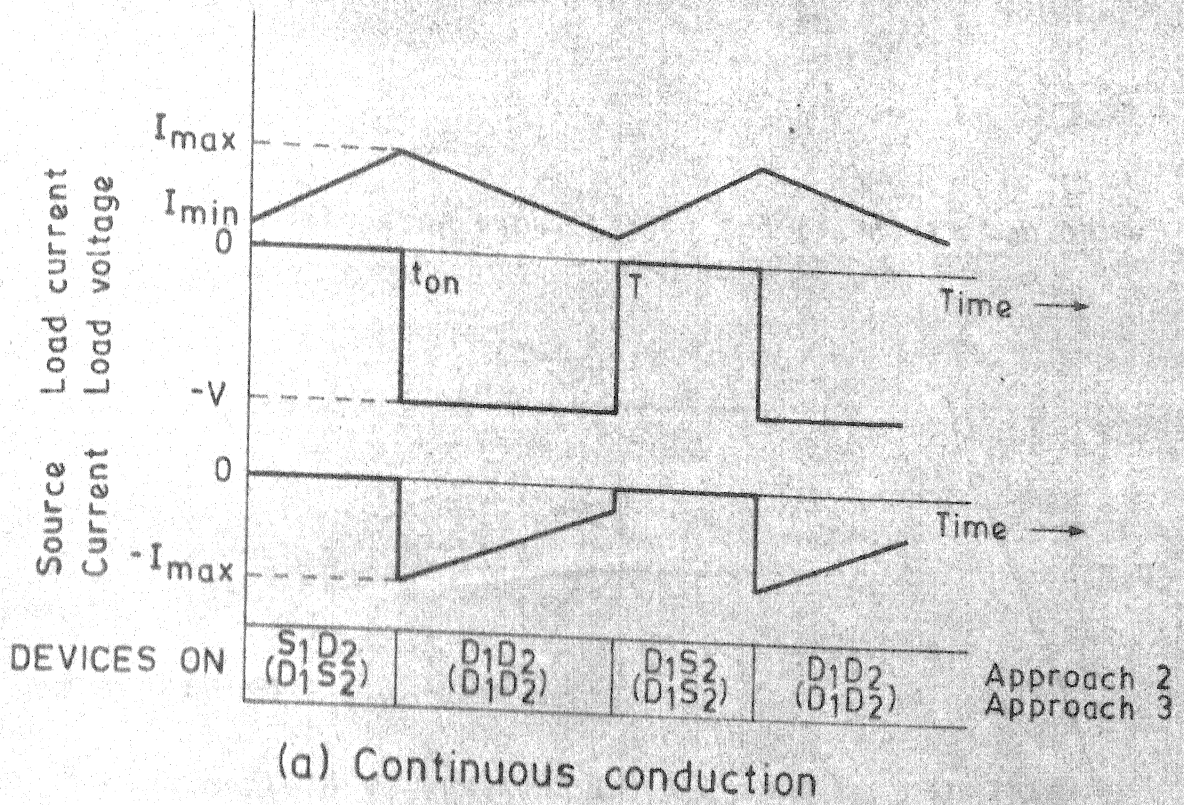


FIG. 3.7. APPROACH 2 & 3, REVERSE REGENERATION.

In steady state from eqns. (3.70) and (3.71) it can be written

$$I_{\max} = \frac{E}{V} - \frac{V}{R} \frac{(e^{(T-t_{\text{on}})/\tau} - 1)}{e^{T/\tau} - 1} \quad (3.72)$$

$$I_{\min} = \frac{E}{R} - \frac{V}{R} \frac{(1 - e^{-(T-t_{\text{on}})/\tau})}{(1 - e^{-T/\tau})} \quad (3.73)$$

$$\text{For this case } t_{\text{on}} = 2\delta T \quad (3.74)$$

The normalised expressions for I_{\max} and I_{\min} in this case are as follows:

$$I_{\max}(\text{norm.}) = m - \frac{e^{-(1-2\delta)T_p} - 1}{e^{T_p} - 1} \quad (3.75)$$

$$I_{\min}(\text{norm.}) = m - \frac{1 - e^{-(1-2\delta)T_p}}{1 - e^{-T_p}} \quad (3.76)$$

The expression for normalised current ripple is as follows:

$$\text{C.R.}(\text{norm.}) = 0.5 \frac{(1 - e^{-(1-2\delta)T_p} + e^{-T_p} - e^{-2\delta T_p})}{(1 - e^{-T_p})} \quad (3.77)$$

Taking the average of eqns. (3.68) and (3.69) over the full time period T , one gets

$$I_{\text{av}} = \frac{-V.(T-t_{\text{on}})/T + E}{R} \quad (3.78)$$

Normalised expression for I_{av} in this case is as follows.

$$I_{av}(\text{norm.}) = 2\delta - 1 + m \quad (3.79)$$

On replacing m by $-m$ in eqn. (3.54) one can derive eqn. (3.79).

Using eqns. (3.18) and (3.19) norm. torque and speed can be found out.

B. Discontinuous conduction (Ref. Fig. 3.7(b)): Following are the representative mesh eqns. for the three intervals present in this mode.

a) Interval-1 or Freewheeling interval

$$0 = L \frac{di_a}{dt} + R.i_a - E \quad \text{for } 0 \leq t \leq t_{on} \quad (3.80)$$

$$i_a(0) = 0$$

b) Interval-2 or Duty interval

$$-V = L \frac{di_a}{dt} + R.i_a - E \quad \text{for } t_{on} \leq t \leq \gamma T \quad (3.81)$$

$$i_a(t_{on}) = I_{max}$$

c) Interval-3 or Zero current interval

$$i_a = 0 \quad \text{for } \gamma T \leq t \leq T \quad (3.82)$$

On solving eqns. (3.80) and (3.81) one gets

$$i_a = \frac{E}{R} (1 - e^{-t/\tau}) \quad \text{for } 0 \leq t \leq t_{on} \quad (3.83)$$

$$i_a = \frac{(E-V)}{R} (1 - e^{-(t-t_{on})/\tau}) + I_{max} e^{-(t-t_{on})/\tau} \quad \text{for } t_{on} \leq t \leq \gamma.T \quad (3.84)$$

Let $i_a \Big|_{t=\gamma T} = 0$ in eqn. (3.84). Then γ can be written in terms of normalised quantities as follows

$$\gamma = \frac{1}{T_p} \ln \left[\frac{-m + e^{\frac{t_{on}}{T} \cdot T_p}}{1-m} \right] \quad (3.85)$$

Critical value of speed (i.e. speed at $\gamma = 1$) is obtained from eqn. (3.85)

$$\omega_{c(\text{norm.})} = \frac{m_c}{K_v} = \frac{1}{K_v} \left[\frac{1 - e^{-(1 - \frac{t_{on}}{T}) T_p}}{1 - e^{-T_p}} \right] \quad (3.86)$$

Substituting $t_{on} = 2\delta T$ in eqn. (3.85) and eqn. (3.86) γ and ω_c can be written as follows in terms of normalised quantities for this case.

$$\gamma = \frac{1}{T_p} \ln \left[\frac{e^{\frac{2\delta T_p}{1-m}} - m}{1-m} \right] \quad (3.87)$$

and

$$\omega_{c(\text{norm.})} = \frac{1}{K_v} \left[\frac{1 - e^{-(1-2\delta) T_p}}{1 - e^{-T_p}} \right] \quad (3.88)$$

I_{\max} in terms of normalised quantities,

$$I_{\max(\text{norm.})} = m \cdot \left(1 - e^{-\frac{t_{on}}{T} \cdot T_p} \right) \quad (3.89)$$

Substituting value of t_{on} from eqn. (3.74) in eqn. (3.89),

$I_{\max(\text{norm.})}$ is rewritten for this case

$$I_{\max(\text{norm.})} = m \cdot \left(1 - e^{-2\delta T_p} \right) \quad (3.90)$$

Thus

$$C.R.(norm.) = 0.5 m \cdot (1 - e^{-2\delta T_p}) \quad (3.91)$$

Taking the average of eqns. (3.80), (3.81) and (3.82) over the full time period T , I_{av} can be found as

$$I_{av} = \frac{V}{R} \cdot \frac{(t_{on} - \gamma T)}{T} + \frac{\gamma \cdot E}{R} \quad (3.92)$$

Substituting $t_{on} = 2\delta T$ in eqn. (3.92), $I_{av}(norm.)$ for this case will be,

$$I_{av}(norm.) = 2\delta - \gamma (1 - m) \quad (3.93)$$

Normalised torque and speed are calculated by substituting values of $I_{av}(norm.)$ and m in eqns. (3.18) and (3.19) respectively.

Harmonics in supply current for motoring operation

A. Continuous conduction: The waveform of the supply current as shown in Fig. 3.6(a) can be expressed mathematically as follows:

$$i_s = (1 - m) + K \left(\frac{t_{on}}{T}, T_p \right) e^{-\frac{t}{T} \cdot T_p} \quad \text{for } 0 \leq t \leq t_{on}$$

$$\text{where } K \left(\frac{t_{on}}{T}, T_p \right) = \frac{e^{\frac{t_{on}}{T} \cdot T_p} - e^{T_p}}{e^{T_p} - 1}$$

$$= 0 \quad \text{for } t_{on} \leq t \leq T \quad (3.94)$$

On doing Fourier analysis of eqn. (3.94), following expressions for dc component of supply current and for other Fourier coefficients, are obtained

$$a_0 = I_{av} = (1-m) \cdot \frac{t_{on}}{T} + \frac{K(\frac{t_{on}}{T}, T_p)}{T_p} (1 - e^{-\frac{t_{on}}{T} \cdot T_p}) \quad (3.95)$$

$$a_n = \frac{(1-m)}{\pi n} \cdot \sin(2\pi n \cdot \frac{t_{on}}{T}) + \frac{2K(\frac{t_{on}}{T}, T_p)}{T_p^2 + 4\pi^2 n^2} [T_p + e^{-\frac{t_{on}}{T} \cdot T_p} \{ 2\pi n \cdot \sin(2\pi n \cdot \frac{t_{on}}{T}) - T_p \cdot \cos(2\pi n \cdot \frac{t_{on}}{T}) \}] \quad (3.96)$$

and

$$b_n = \frac{(1-m)}{\pi n} \cdot (1 - \cos(2\pi n \cdot \frac{t_{on}}{T})) + \frac{2K(\frac{t_{on}}{T}, T_p)}{T_p^2 + 4\pi^2 n^2} [2\pi n - e^{-\frac{t_{on}}{T} \cdot T_p} \{ T_p \cdot \sin(2\pi n \cdot \frac{t_{on}}{T}) + 2\pi n \cdot \cos(2\pi n \cdot \frac{t_{on}}{T}) \}] \quad (3.97)$$

The rms value of nth harmonic component in supply current is obtained from eqns. (3.37), (3.96) and (3.97).

Since $t_{on} = (2\delta-1)T$ for this case ^{the} expressions for a_0 , a_n and b_n can be rewritten as follows:

$$a_0 = (1-m) \cdot (2\delta-1) + \frac{K((2\delta-1), T_p)}{T_p} (1 - e^{-(2\delta-1)T_p}) \quad (3.98)$$

$$a_n = \frac{(1-m)}{\pi n} \cdot \sin(2\pi n \cdot (2\delta-1)) + \frac{2K((2\delta-1), T_p)}{T_p^2 + 4\pi^2 n^2} \\ \left[T_p + e^{-(2\delta-1)T_p} \left\{ 2\pi n \cdot \sin(2\pi n \cdot (2\delta-1)) \right. \right. \\ \left. \left. - T_p \cos(2\pi n \cdot (2\delta-1)) \right\} \right] \quad (3.99)$$

and

$$b_n = \frac{(1-m)}{\pi n} \cdot (1 - \cos(2\pi n \cdot (2\delta-1))) + \frac{2K((2\delta-1), T_p)}{T_p^2 + 4\pi^2 n^2} \\ \left[2\pi n - e^{-(2\delta-1)T_p} \left\{ T_p \cdot \sin(2\pi n \cdot (2\delta-1)) \right. \right. \\ \left. \left. + 2\pi n \cdot \cos(2\pi n \cdot (2\delta-1)) \right\} \right] \quad (3.100)$$

where,

$$K((2\delta-1), T_p) = \frac{e^{(2\delta-1)T_p} - e^{T_p}}{e^{T_p} - 1}$$

B. Discontinuous conduction: The mathematical expressions for the supply current waveform, in this mode, shown in Fig. 3.6(b), are as follows.

$$i_s = (1-m) \left(1 - e^{\left\{ -t/T \right\} T_p} \right) \quad \text{for } 0 \leq t \leq t_{on} \\ = 0 \quad \text{for } t_{on} \leq t \leq T \quad (3.101)$$

On doing Fourier analysis of eqn. (3.101), one gets,

$$a_0 = (1-m) \left[\frac{t_{on}}{T} - \frac{1}{T_p} \cdot (1 - e^{-\frac{t_{on}}{T} \cdot T_p}) \right] \quad (3.102)$$

$$a_n = (1-m) \left[\frac{\sin(2\pi n(t_{on}/T))}{\pi n} - \frac{2}{T_p^2 + 4\pi^2 n^2} \right. \\ \left. \left\{ e^{-\frac{t_{on}}{T} T_p} (-T_p \cos(2\pi n \cdot t_{on}/T) + 2\pi n \sin(2\pi n \cdot t_{on}/T) + T_p) \right\} \right] \quad (3.103)$$

and

$$b_n = (1-m) \left[\frac{(1 - \cos(2\pi n(t_{on}/T)))}{\pi n} - \frac{2}{T_p^2 + 4\pi^2 n^2} \right. \\ \left. \left\{ 2\pi n e^{-\frac{t_{on}}{T} T_p} (T_p \sin(2\pi n \cdot (t_{on}/T)) + 2\pi n \cos(2\pi n \cdot (t_{on}/T)) \right\} \right] \quad (3.104)$$

The rms value of nth harmonic component of input current is obtained from eqn. (3.37), (3.103) and (3.104).

Since, $t_{on}/T = 2\delta - 1$ for this case, the expression for a_n and b_n can be w rewritten as

$$a_0 = (1-m) \left[2\delta - 1 - \frac{1}{T_p} (1 - e^{-(2\delta - 1)T_p}) \right] \quad (3.105)$$

$$a_n = (1-m) \left[\frac{\sin(2\pi n(2\delta - 1))}{\pi n} - \frac{2}{T_p^2 + 4\pi^2 n^2} \right. \\ \left. \left\{ e^{-(2\delta - 1)T_p} (-T_p \cos(2\pi n(2\delta - 1)) + 2\pi n \sin(2\pi n(2\delta - 1)) + T_p) \right\} \right] \quad (3.106)$$

and,

$$b_n = (1-m) \left[\frac{1 - \cos(2\pi n(2\delta-1))}{\pi n} - \frac{2}{T_p^2 + 4\pi^2 n^2} \right. \\ \left. \left\{ 2\pi n e^{-(2\delta-1)T_p} (T_p \cdot \sin(2\pi n(2\delta-1)) + 2\pi n \cdot \cos(2\pi n(2\delta-1))) \right\} \right] \quad (3.107)$$

Harmonics in supply current for reverse regenerative operation:

A. Continuous conduction: Supply current waveform in this mode, is as shown in Fig. 3.7(a) and can be expressed mathematically as follows:

$$i_s = 0 \quad \text{for } 0 \leq t \leq t_{on} \\ = (1-m) - K \left(\frac{t_{on}}{T}, T_p \right) e^{-\frac{t}{T} \cdot T_p} \quad \text{for } t_{on} \leq t \leq T \\ \text{where } K \left(\frac{t_{on}}{T}, T_p \right) = \frac{e^{(t_{on}/T)T_p} - 1}{1 - e^{-T_p}} \quad (3.108)$$

Fourier analysis of above eqn. results in the following expressions for a_0 , a_n and b_n .

$$a_0 = (1-m) \left(1 - \frac{t_{on}}{T} \right) + \frac{K(t_{on}/T, T_p)}{T_p} (e^{-T_p} - e^{-(t_{on}/T)T_p}) \quad (3.109)$$

$$a_n = \frac{(m-1)}{\pi n} \cdot \sin(2\pi n(\frac{t_{on}}{T})) + \frac{2K(t_{on}/T, T_p)}{T_p^2 + 4\pi^2 n^2} [T_p \cdot e^{-T_p} + e^{(t_{on}/T)T_p} \\ \left\{ -T_p \cdot \cos(2\pi n(\frac{t_{on}}{T})) + 2\pi n \cdot \sin(2\pi n(\frac{t_{on}}{T})) \right\}] \quad (3.110)$$

and

$$b_n = \frac{(m-1)}{\pi n} \cdot (1 - \cos(2\pi n(\frac{t_{on}}{T}))) + \frac{2K(t_{on}/T, T)}{T_p^2 + 4\pi^2 n^2} [2\pi n \cdot e^{-T_p} - e^{-(t_{on}/T) \cdot T_p} \{ T_p \cdot \sin(2\pi n(\frac{t_{on}}{T})) + 2\pi n \cdot \cos(2\pi n(\frac{t_{on}}{T})) \}] \quad (3.111)$$

The rms value of nth harmonic component of input current will be obtained using eqns. (3.37), (3.110) and (3.111).

Since, $\frac{t_{on}}{T} = 2\delta$, the expression for a_o , a_n and b_n can be rewritten as follows for this case. So,

$$a_o = (1-m) \cdot (1-2\delta) + \frac{K(2\delta, T_p)}{T_p} (e^{-T_p} - e^{-2\delta T_p}) \quad (3.112)$$

$$a_n = \frac{m-1}{\pi n} \cdot \sin 4\pi n\delta - \frac{2K(2\delta, T_p)}{T_p^2 + 4\pi^2 n^2} [-T_p \cdot e^{-T_p} - e^{-2\delta T_p} \{ -T_p \cdot \cos 4\pi n\delta + 2\pi n \cdot \sin 4\pi n\delta \}] \quad (3.113)$$

and,

$$b_n = \frac{(m-1)}{\pi n} \cdot (1 - \cos 4\pi n\delta) + \frac{2K(2\delta, T_p)}{T_p^2 + 4\pi^2 n^2} [2\pi n e^{-T_p} - e^{-2\delta T_p} \{ T_p \cdot \sin 4\pi n\delta + 2\pi n \cdot \cos 4\pi n\delta \}] \quad (3.114)$$

$$\text{where } K(2\delta, T_p) = \frac{e^{-2\delta T_p} - 1}{1 - e^{-T_p}}$$

B. Discontinuous conduction: The supply current waveform is shown in Fig. 3.7(b). This can be expressed mathematically as follows:

$$\begin{aligned}
 i_s &= 0 && \text{for } 0 \leq t \leq t_{on} \\
 &= (1-m)e^{(-t/T)T_p} (m-e^{(t_{on}/T)T_p}) && \text{for } t_{on} \leq t \leq \gamma T \\
 &= 0 && \text{for } \gamma T \leq t \leq T
 \end{aligned} \quad (3.115)$$

Fourier constants for this supply current function are obtained as follows:

$$a_0 = \left(\gamma - \frac{t_{on}}{T} \right) (1-m) + \frac{(m-e^{(t_{on}/T)T_p})}{T_p} \left\{ e^{-(t_{on}/T)T_p} - e^{-\gamma T_p} \right\} \quad (3.116)$$

$$\begin{aligned}
 a_n &= \frac{(1-m)}{\pi n} \left\{ \sin 2\pi n \gamma - \sin \left(2\pi n \left(\frac{t_{on}}{T} \right) \right) \right\} + \frac{2(m-e^{(t_{on}/T)T_p})}{T_p^2 + 4\pi^2 n^2} \\
 &\quad \left[e^{-\gamma T_p} \left\{ -T_p \cdot \cos 2\pi n \gamma + 2\pi n \cdot \sin 2\pi n \gamma \right\} - e^{-(t_{on}/T)T_p} \right. \\
 &\quad \left. \left\{ -T_p \cdot \cos \left(2\pi n \left(\frac{t_{on}}{T} \right) \right) + 2\pi n \cdot \sin \left(2\pi n \left(\frac{t_{on}}{T} \right) \right) \right\} \right] \quad (3.117)
 \end{aligned}$$

and,

$$\begin{aligned}
 b_n &= \frac{(1-m)}{\pi n} \left\{ \cos \left(2\pi n \left(\frac{t_{on}}{T} \right) \right) - \cos 2\pi n \gamma \right\} - \frac{2(m-e^{(t_{on}/T)T_p})}{T_p^2 + 4\pi^2 n^2} \\
 &\quad \left[e^{-\gamma T_p} \left\{ T_p \cdot \sin 2\pi n \gamma + 2\pi n \cdot \cos 2\pi n \gamma \right\} - e^{-(t_{on}/T)T_p} \right. \\
 &\quad \left. \left\{ T_p \cdot \sin \left(2\pi n \left(\frac{t_{on}}{T} \right) \right) + 2\pi n \cdot \cos \left(2\pi n \left(\frac{t_{on}}{T} \right) \right) \right\} \right] \quad (3.118)
 \end{aligned}$$

The rms value of nth harmonic content is obtained using eqns. (3.37), (3.117) and (3.118). Since $\frac{t_{on}}{T} = 2\delta$ for this case, so,

$$a_0 = (\gamma - 2\delta) \cdot (1-m) + \frac{(m-e)^{2\delta T_p}}{T_p} (e^{-2\delta T_p} - e^{-\gamma T_p}) \quad (3.119)$$

$$a_n = \frac{(1-m)}{\pi n} (\sin 2\pi n \gamma - \sin 4\pi n \delta) + \frac{2(m-e)^{2\delta T_p}}{T_p^2 + 4\pi^2 n^2} [e^{-\gamma T_p} \{ -T_p \cdot \cos 2\pi n \gamma + 2\pi n \sin 2\pi n \gamma \} - e^{-2\delta T_p} \{ -T_p \cdot \cos 4\pi n \delta + 2\pi n \cdot \sin 4\pi n \delta \}] \quad (3.120)$$

and,

$$b_n = \frac{(1-m)}{\pi n} (\cos 4\pi n \delta - \cos 2\pi n \gamma) - \frac{2(m-e)^{2\delta T_p}}{T_p^2 + 4\pi^2 n^2} \{ e^{-\gamma T_p} (T_p \cdot \sin 2\pi n \gamma + 2\pi n \cdot \cos 2\pi n \gamma) - e^{-2\delta T_p} (T_p \cdot \sin 4\pi n \delta + 2\pi n \cdot \cos 4\pi n \delta) \} \quad (3.121)$$

3.4.3 APPROACH-3: For motoring operation S_1 is kept closed all the time and switch S_2 is opened for t_{on} seconds every T seconds. If switch S_1 is open all the time and S_2 is operated as before, reverse regeneration is achieved.

Motor performance analysis for motoring operation:

A. Continuous conduction: (Ref. Fig. 3.6(a)) : Eqns. (3.42), (3.43), (3.45) to (3.48) and (3.52) are valid in this case also. For this case,

$$t_{on} = \delta T \quad (3.122)$$

From eqns. (3.47), (3.48) and (3.122), normalised expressions for I_{max} and I_{min} can be written as

$$I_{\max}(\text{norm}) = \frac{1 - e^{-\delta T_p}}{1 - e^{-T_p}} - m \quad (3.123)$$

$$I_{\min}(\text{norm.}) = \frac{e^{\delta T_p} - 1}{e^{T_p} - 1} - m \quad (3.124)$$

so,

$$\text{C.R.}(\text{norm.}) = 0.5 \frac{(1 - e^{-\delta T_p} + e^{-T_p} - e^{-(1-\delta)T_p})}{(1 - e^{-T_p})} \quad (3.125)$$

Substituting value of t_{on} from eqn. (3.122) to eqn. (3.52), normalised equation for I_{av} can be written as

$$I_{\text{av}}(\text{norm.}) = \delta - m \quad (3.126)$$

Normalised torque and speed can be found out from eqns.

(3.18), and (3.19) and (3.126)

B. Discontinuous conduction: (Ref. Fig. 3.6(b)): Eqns. (3.54) to (3.59), (3.61), (3.63) and (3.65) are valid in this case also.

Substituting value of t_{on} from eqn. (3.122) into (3.59), I_{\max} can be written for this case, in terms of normalised quantities as follows

$$I_{\max}(\text{norm.}) = (1-m) \cdot (1 - e^{-\delta T_p}) \quad (3.127)$$

so,

$$\text{C.R.}(\text{norm.}) = 0.5 I_{\max}(\text{norm.}) = 0.5(1-m)(1 - e^{-\delta T_p}) \quad (3.128)$$

Substituting value of t_{on} in eqn. (3.61) and putting all quantities in normalised form,

$$\gamma = \frac{1}{T_p} \ln \left[1 + \frac{e^{\frac{\delta T_p}{m}} - 1}{m} \right] \quad (3.129)$$

From eqns. (3.63) and (3.122) normalised critical speed

$$= \omega_c \text{ (norm.)} = \frac{1}{K_v} \left[\frac{e^{\frac{\delta T_p}{T_p}} - 1}{e^{\frac{\delta T_p}{T_p}} - 1} \right] \quad (3.130)$$

On substituting value of t_{on}/T in eqn. (3.65) and writing I_{av} in normalised form

$$I_{av} \text{ (norm.)} = \delta - \gamma m \quad (3.131)$$

torque and speed are calculated with help of eqns. (3.18) and (3.19).

Motor performance analysis for reverse regenerative operation:

A. Continuous conduction: (Ref. Fig. 3.7(a)): Eqns. (3.68)

to (3.73), eqn. (3.78) ^{and} eqn. (3.122) are valid here.
From eqns. (3.122), (3.72) and (3.73),

$$I_{\max} \text{ (norm.)} = m - \frac{e^{\frac{(1-\delta)T_p}{T_p}} - 1}{e^{\frac{(1-\delta)T_p}{T_p}} - 1} \quad (3.132)$$

$$I_{\min} \text{ (norm.)} = m - \frac{1 - e^{-\frac{(1-\delta)T_p}{T_p}}}{1 - e^{-\frac{(1-\delta)T_p}{T_p}}} \quad (3.133)$$

So,

$$C.R.(norm.) = 0.5 \frac{(1-e^{-(1-\delta)T_p} + e^{-T_p} - e^{-\delta T_p})}{(1-e^{-T_p})} \quad (3.134)$$

Substituting value of t_{on} from eqn. (3.122) into eqn. (3.78), the normalised expression of I_{av} for this case will be,

$$I_{av}(norm.) = \delta - 1 + m \quad (3.135)$$

Normalised torque and speed are obtained with the help of eqns. (3.18) and (3.19).

B. Discontinuous conduction: (Ref. Fig. 3.7(b)): Eqns. (3.80) to (3.86), (3.89), (3.92) and (3.122), are valid here too.

From eqns. (3.89) and (3.122)

$$I_{max}(norm.) = m \cdot (1-e^{-\delta T_p}) \quad (3.136)$$

Thus,

$$C.R.(norm.) = 0.5 \cdot m \cdot (1-e^{-\delta T_p}) \quad (3.137)$$

Substituting value of t_{on} in eqns. (3.85) and (3.86), from eqn. (3.122), one gets following expressions for γ and ω_c .

$$\gamma = \frac{1}{T_p} \ln \left[\frac{e^{\delta T_p} - m}{1-m} \right] \quad (3.138)$$

and

$$\omega_c = \frac{1}{K_v} \left[\frac{(1-e^{-(1-\delta)T_p})}{(1-e^{-T_p})} \right] \quad (3.139)$$

Substituting value of t_{on} from eqn. (3.122) into eqn. (3.92) I_{av} can be written for this case in the m normalised form as,

$$I_{av}(\text{norm.}) = \delta - \gamma (1-m) \quad (3.140)$$

Eqns. (3.18), (3.19) and (3.140) are used to calculate normalised torque and speed.

Harmonics in supply current for motoring operation

A. Continuous conduction: (Ref. Fig. 3.6(a)) : Mathematically representative expression for this waveform has already been analysed. Eqns. (3.37) and (3.94) to (3.97) are valid here too. Substituting value of t_{on} from eqn. (3.122) into eqns. (3.96) and (3.97), one gets

$$a_0 = I_{dc} = (1-m) \cdot \delta + \frac{K(\delta, T_p)}{T_p} (1 - e^{-\delta T_p}) \quad (3.141)$$

$$a_n = \frac{(1-m)}{\pi n} \cdot \sin 2\pi n \delta + \frac{2K(\delta, T_p)}{T_p^2 + 4\pi^2 n^2} [T_p + e^{-\delta T_p} \{ 2\pi n \cdot \sin 2\pi n \delta - T_p \cos \pi n \delta \}] \quad (3.142)$$

and

$$b_n = \frac{(1-m)}{\pi n} (1 - \cos 2\pi n \delta) + \frac{2K(\delta, T_p)}{T_p^2 + 4\pi^2 n^2} [2\pi n - e^{-\delta T_p} \{ T_p \cdot \sin 2\pi n \delta + 2\pi n \cdot \cos 2\pi n \delta \}] \quad (3.143)$$

$$\text{where, } K(\delta, T_p) = \frac{e^{\delta T_p} - e^{T_p}}{e^{T_p} - 1} \quad (3.144)$$

B. Discontinuous conduction: (Ref. Fig. 3.6(b)): This supply current waveform has already been analysed. Eqns. (3.37), (3.101) to (3.104) are valid in this case too. Substituting value of t_{on} into equations (3.102) to (3.104) from (3.122), one gets following eqns. for this case in particular.

$$\text{D.C. component} = a_0 = (1-m) \left[\delta - \frac{1}{T_p} (1 - e^{-\delta T_p}) \right] \quad (3.145)$$

$$a_n = (1-m) \left[\frac{\sin 2\pi n \delta}{\pi n} - \frac{2}{T_p^2 + 4\pi^2 n^2} \left\{ e^{-\delta T_p} (-T_p \cdot \cos 2\pi n \delta + 2\pi n \cdot \sin 2\pi n \delta) + T_p \right\} \right] \quad (3.146)$$

and

$$b_n = (1-m) \left[\frac{(1 - \cos 2\pi n \delta)}{\pi n} - \frac{2}{T_p^2 + 4\pi^2 n^2} \left\{ 2\pi n - e^{-\delta T_p} (T_p \cdot \sin 2\pi n \delta + 2\pi n \cdot \cos 2\pi n \delta) \right\} \right] \quad (3.147)$$

Harmonics in supply current for reverse regeneration

A. Continuous conduction (Ref. Fig. 3.7(a)) : Fourier analysis of the supply current waveform, expressed by eqn. (3.108), results in a_0 , a_n and b_n expressed as eqns. (3.109), (3.110) and (3.111) respectively. Substituting value of t_{on} from eqn. (3.122) into these eqns. one gets following expressions for a_0 , a_n and b_n for this case,

$$a_0 = (1-m)(1-\delta) + \frac{K(\delta, T_p)}{T_p} (e^{-T_p} - e^{-\delta T_p}) \quad (3.148)$$

$$a_n = \frac{(m-1)}{\pi n} \cdot \sin 2\pi n \delta + \frac{2K(\delta, T_p)}{T_p^2 + 4\pi^2 n^2} [T_p \cdot e^{-T_p} + e^{-\delta T_p} (-T_p \cdot \cos 2\pi n \delta + 2\pi n \sin 2\pi n \delta)] \quad (3.149)$$

and

$$b_n = \frac{(m-1)}{\pi n} (1 - \cos 2\pi n \delta) + \frac{2K(\delta, T_p)}{T_p^2 + 4\pi^2 n^2} [2\pi n e^{-T_p} - e^{-\delta T_p} (T_p \cdot \sin 2\pi n \delta + 2\pi n \cos 2\pi n \delta)] \quad (3.150)$$

$$\text{where } K(\delta, T_p) = \frac{e^{\delta T_p} - 1}{1 - e^{-T_p}} \quad (3.151)$$

B. Discontinuous conduction (Ref. Fig. 3.7(b)): Mathematically this supply current waveform is expressed by eqn. (3.115).

Fourier analysis of this eqn. results in a_0 , a_n and b_n given by eqns. (3.116), (3.117) and (3.118) respectively.

Substituting the value of t_{on} from eqn. (3.122) expressions for a_0 , a_n and b_n specific to this case can be written as follows:

$$I_{dc} = a_0 = (\gamma - \delta)(1-m) + \frac{(m-e^{\delta T_p})}{T_p} (e^{-\delta T_p} - e^{-\gamma T_p}) \quad (3.152)$$

$$a_n = \frac{(1-m)}{\pi n} (\sin 2\pi n \gamma - \sin 2\pi n \delta) + \frac{2(m-e^{\delta T_p})}{T_p^2 + 4\pi^2 n^2} [e^{-\gamma T_p} (-T_p \cdot \cos 2\pi n \gamma + 2\pi n \sin 2\pi n \gamma) - e^{-\delta T_p} (-T_p \cdot \cos 2\pi n \delta + 2\pi n \sin 2\pi n \delta)] \quad (3.153)$$

and

$$b_n = \frac{(1-m)}{\pi n} (\cos 2\pi n \delta - \cos 2\pi n \gamma) - \frac{2(m-e)^{\delta T_p}}{T_p^2 + 4\pi^2 n^2} [e^{-\gamma T_p} (T_p \cdot \sin 2\pi n \gamma + 2\pi n \cdot \cos 2\pi n \gamma) - e^{-\delta T_p} (T_p \cdot \sin \frac{\pi n}{\delta} + 2\pi n \cos 2\pi n \delta)] \quad (3.154)$$

3.5 Comparison between the Three different Control Approaches:

The comparison of the three control approaches has been carried out both for highly inductive load as well as motor load. For highly inductive load ripple free load current is assumed and output voltage ripple and supply current ripple are studied. For motor load the comparison has been done for the following aspects.

1. Nature of motor speed-torque characteristics
2. Maximum armature current ripple
3. Harmonics in supply current

For this study a generalised approach has been undertaken. All the aspects are studied in terms of the normalised quantities so that the results can be applied to any d.c. separately excited motor. Number of the commutation cycles per output cycle is also taken as a figure of merit for the comparison. It gives idea of the amount of the switching losses.

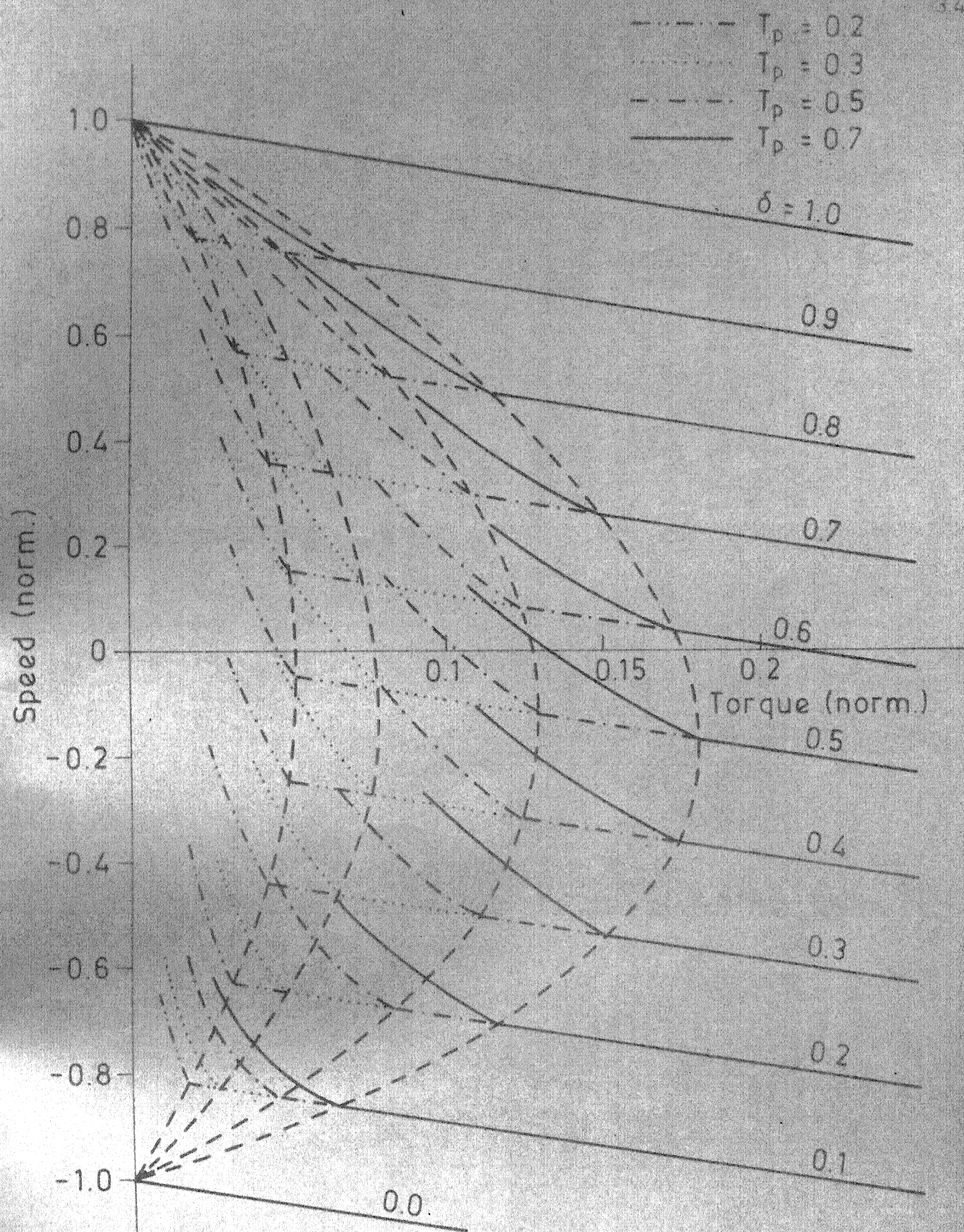


FIG. 3.8 SPEED-TORQUE CHARACTERISTICS FOR APPROACH 1.

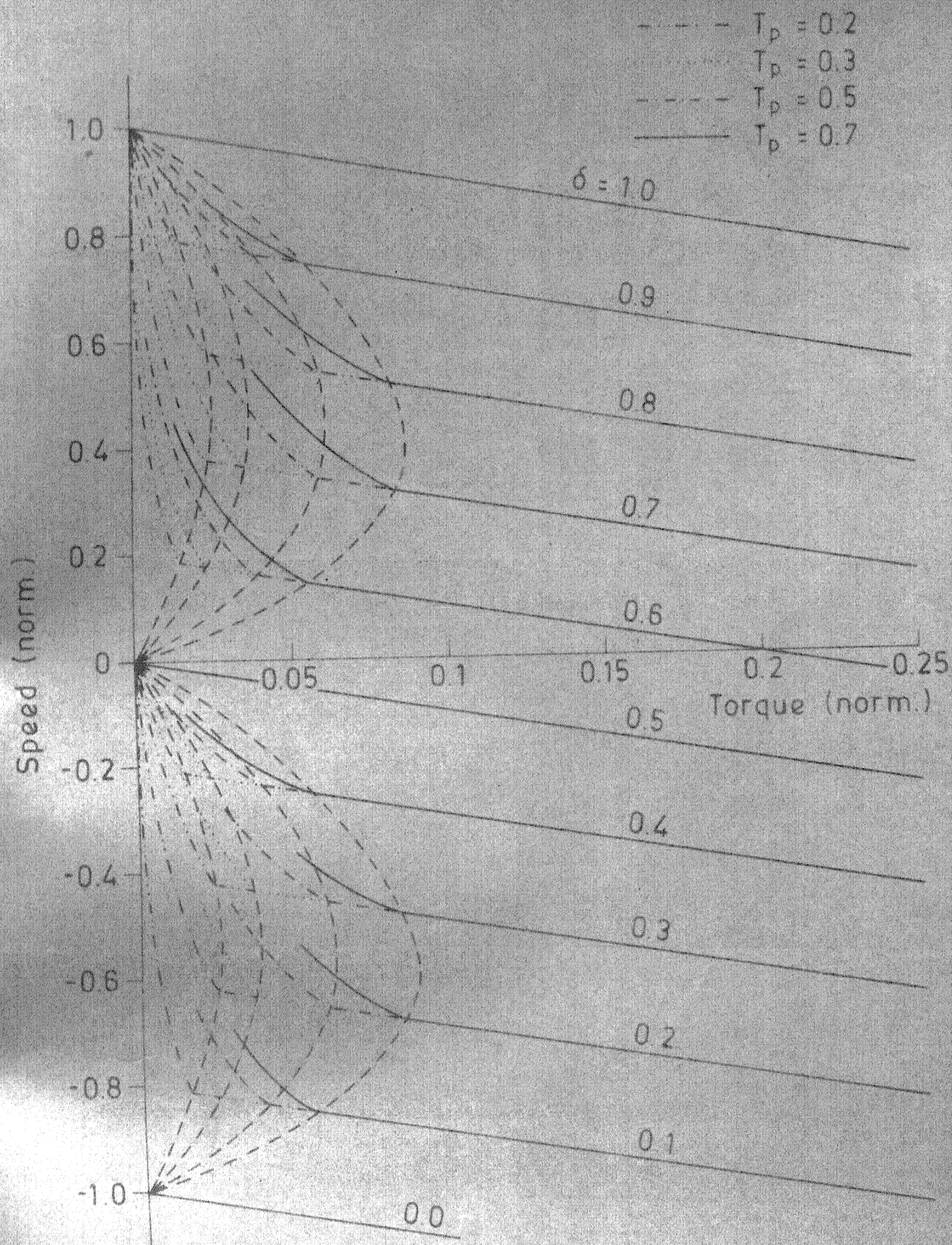


FIG. 3.9. SPEED-TORQUE CHARACTERISTICS FOR APPROACH 2

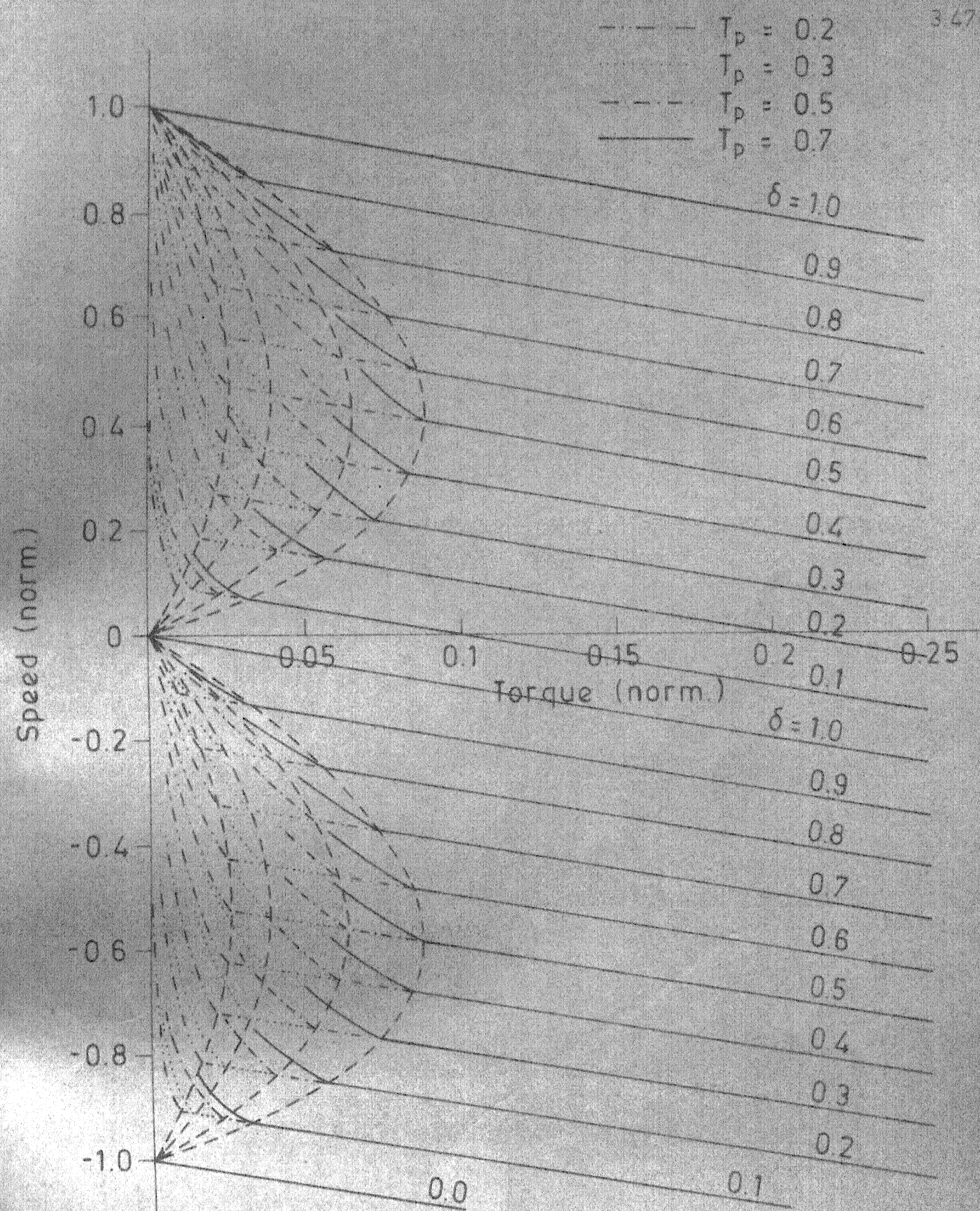


FIG. 3.10 SPEED-TORQUE CHARACTERISTICS FOR APPROACH 3.

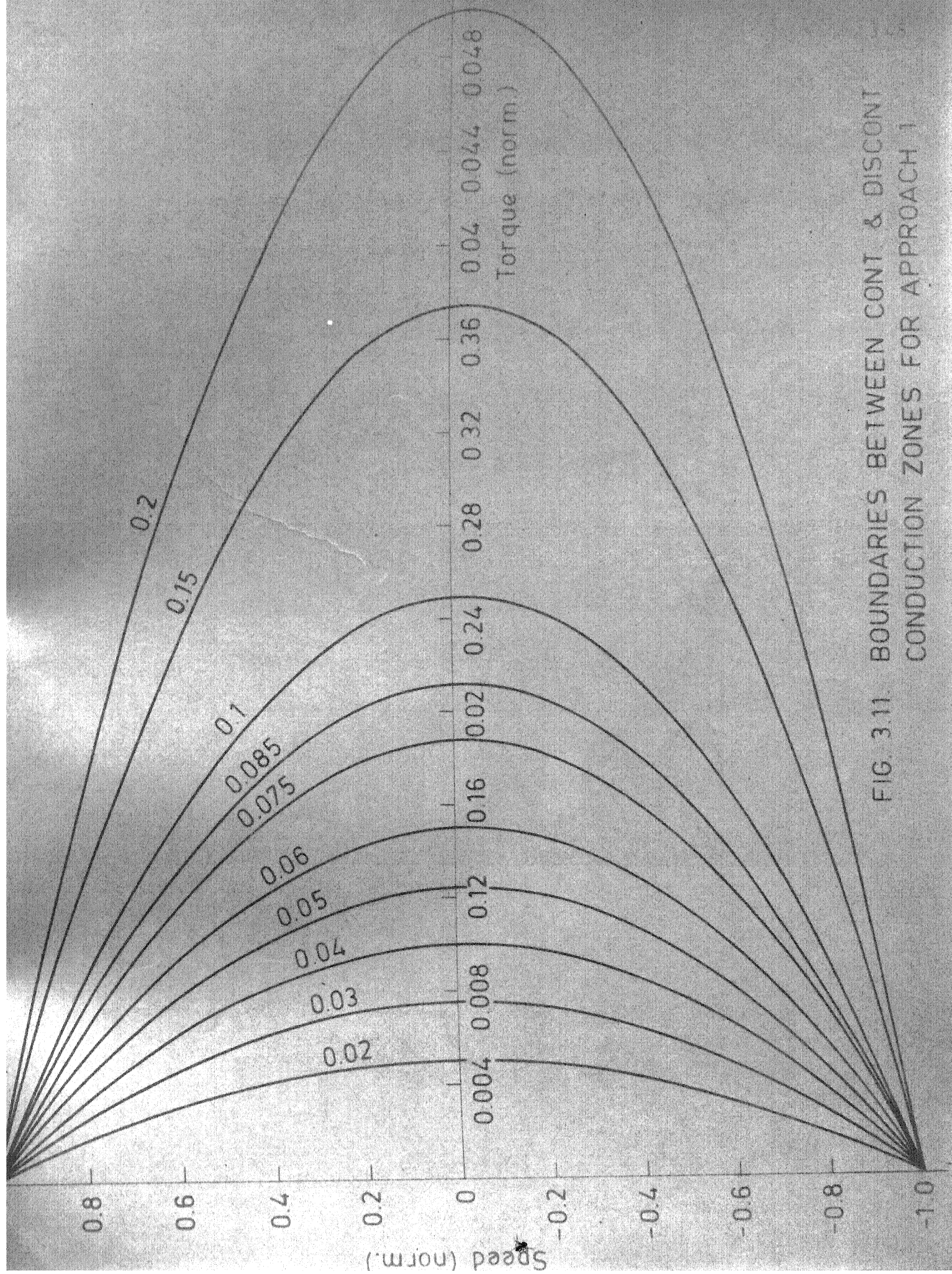


FIG. 3.11. BOUNDARIES BETWEEN CONT. & DISCONT. CONDUCTION ZONES FOR APPROACH 1

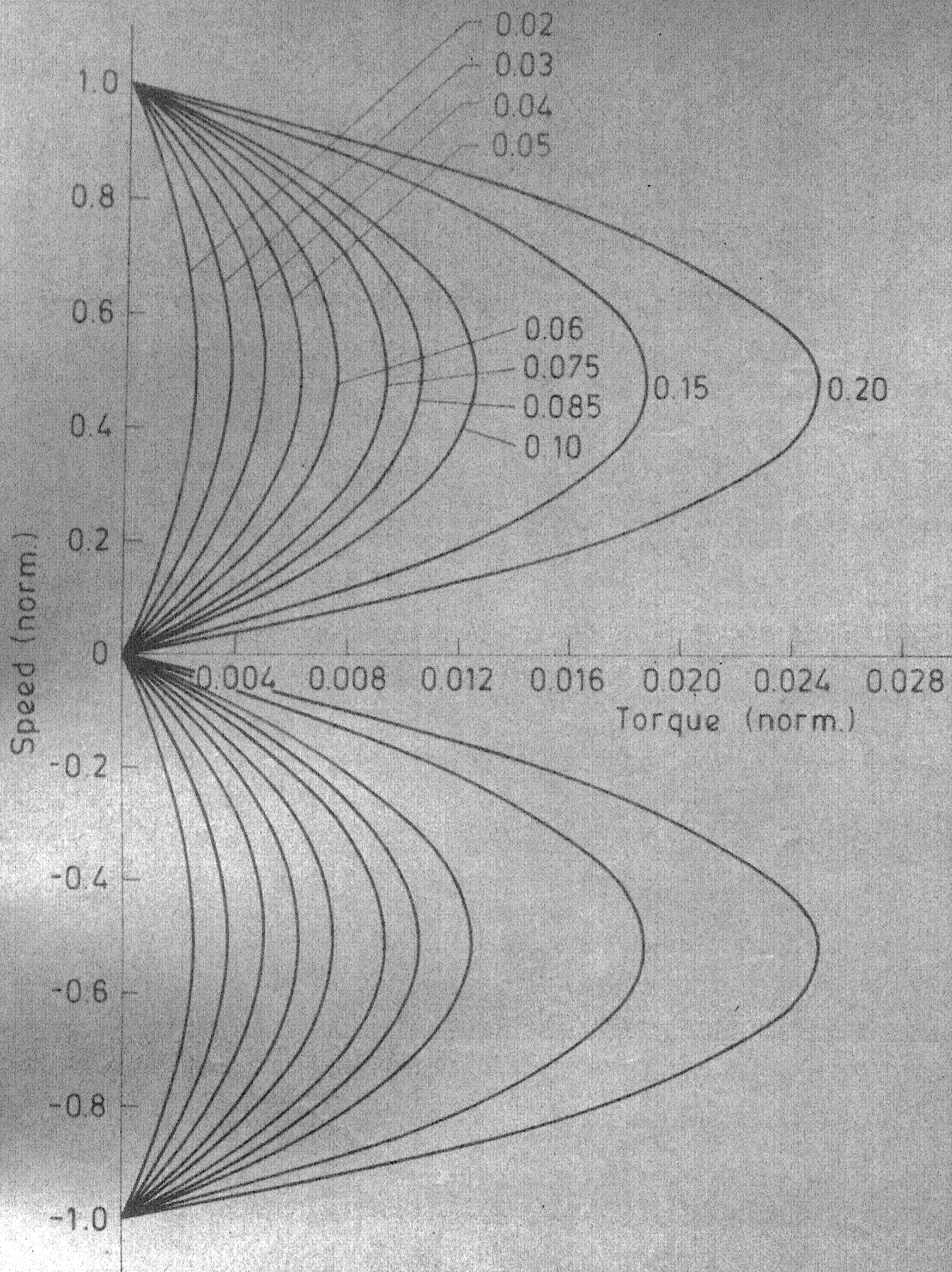


FIG. 3.12. BOUNDARIES BETWEEN ZONES OF CONT. & DISCONT. CONDUCTION FOR APPROACH 2 & 3

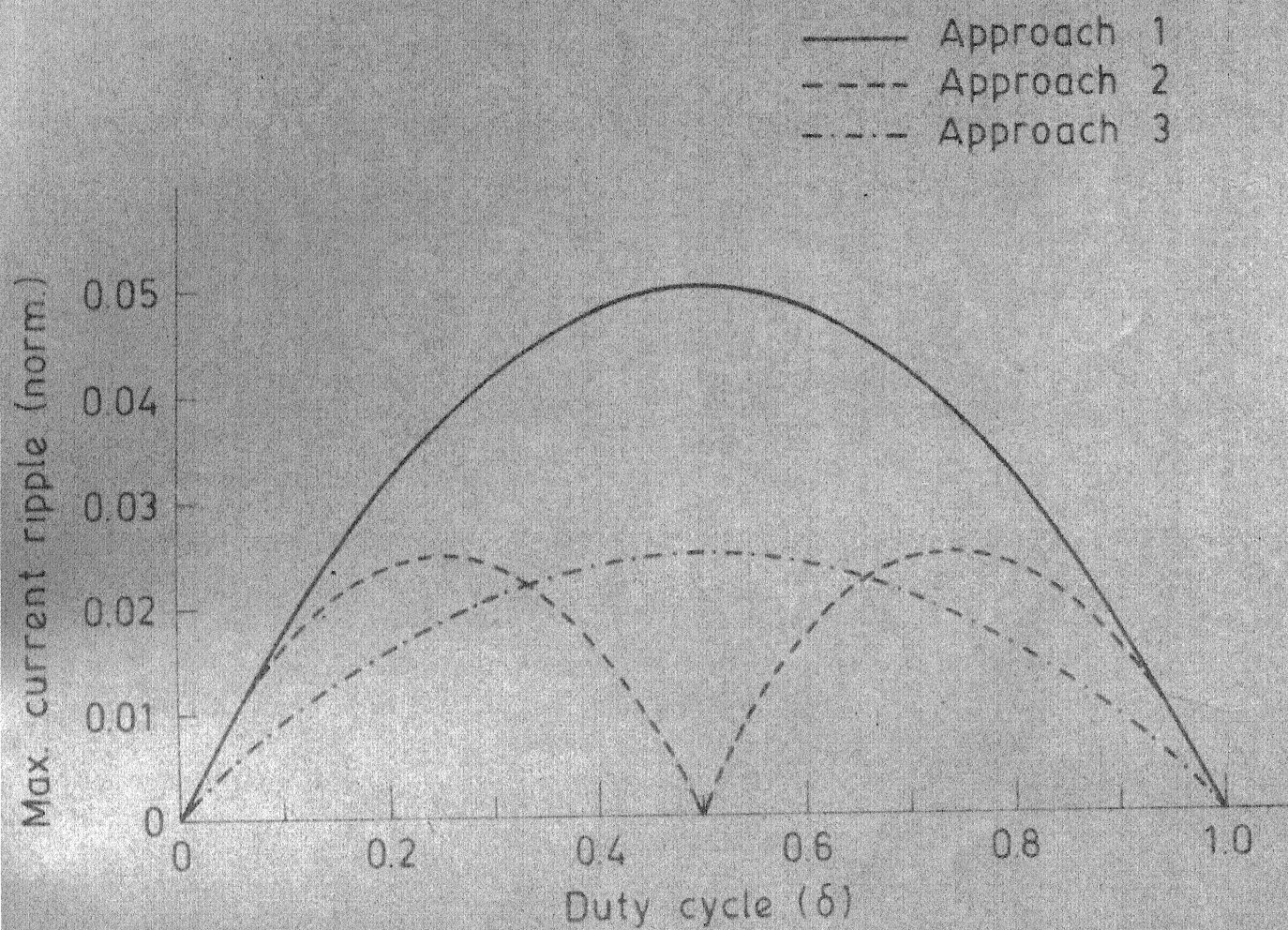


FIG. 3.13. NORMALISED MAX. CURRENT RIPPLE vs DUTY CYCLE.

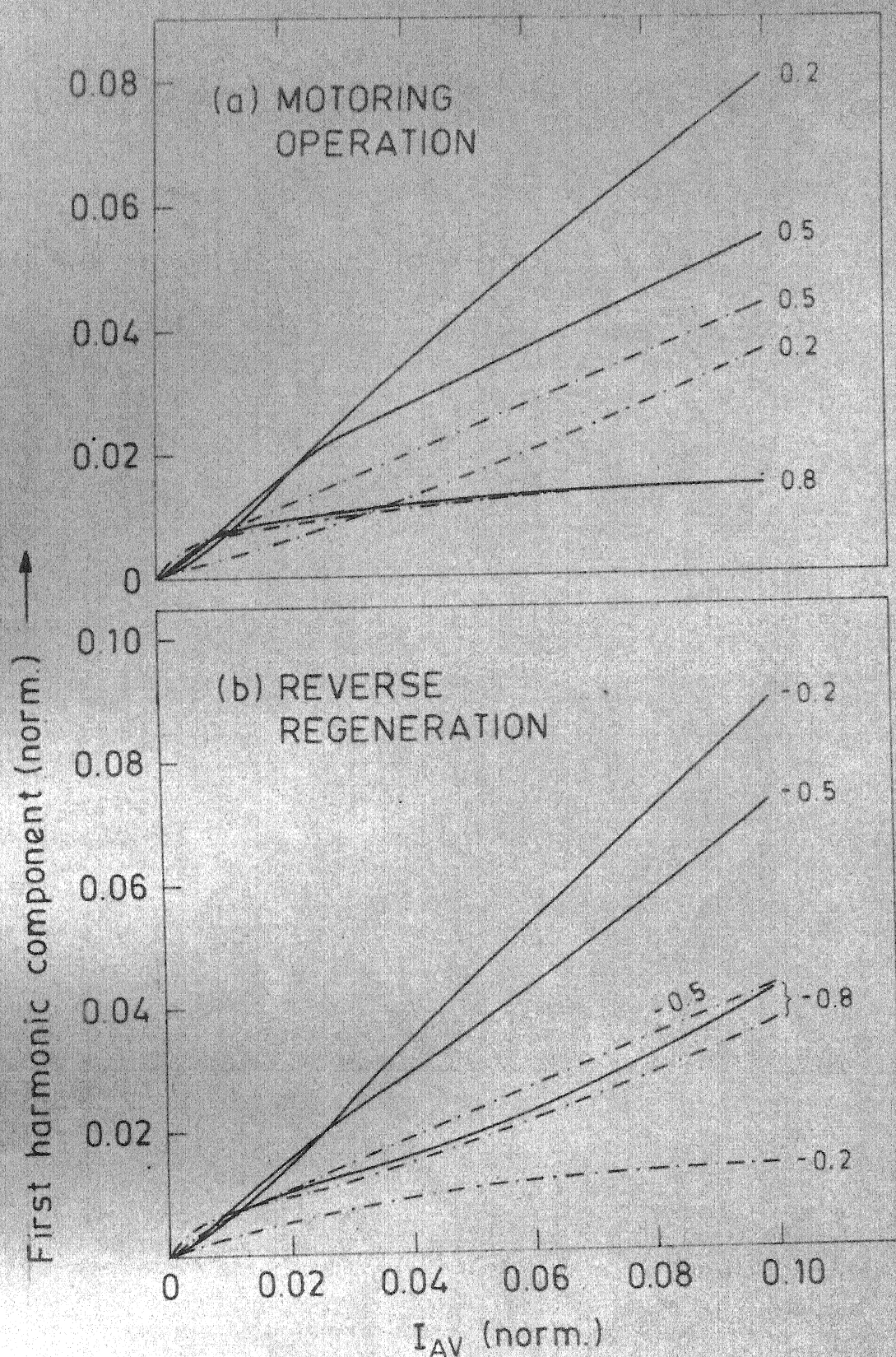
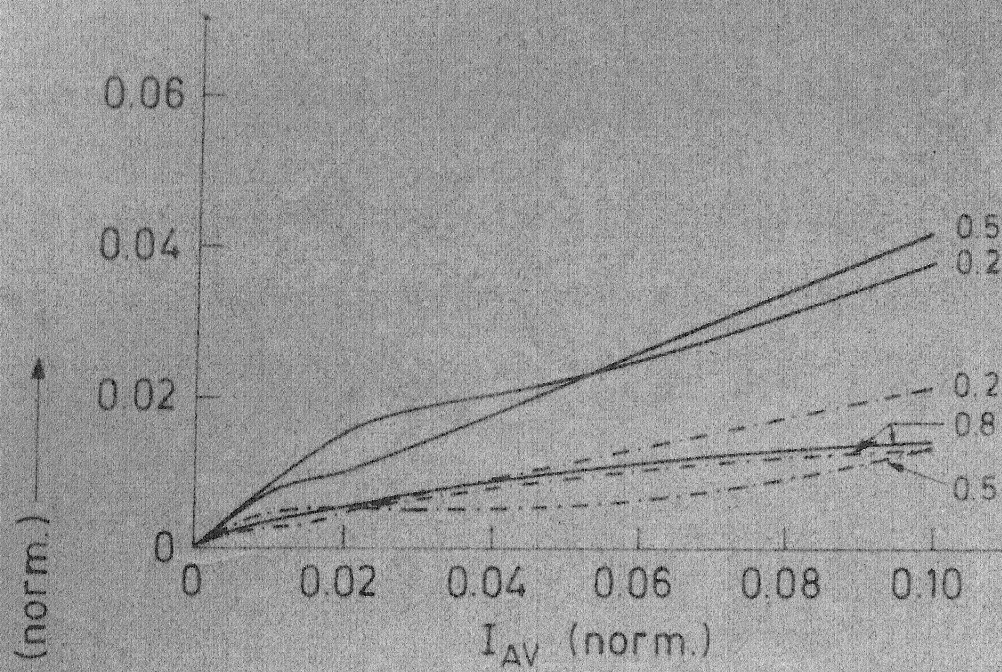
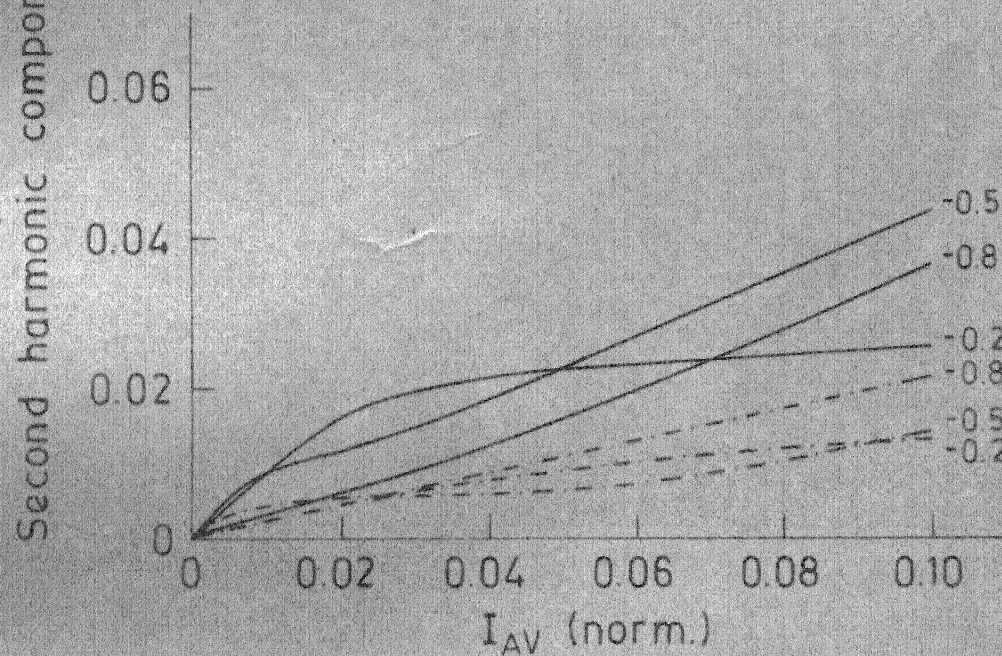


FIG. 3.14. NORMALISED FUNDAMENTAL COMPONENT OF SUPPLY CURRENT vs I_{AV} (NORM.) FOR $T_p = 0.2$ AND DIFFERENT VALUES OF BACK E.M.F.
 — Approach 1 - - - - - Approach 2 & 3



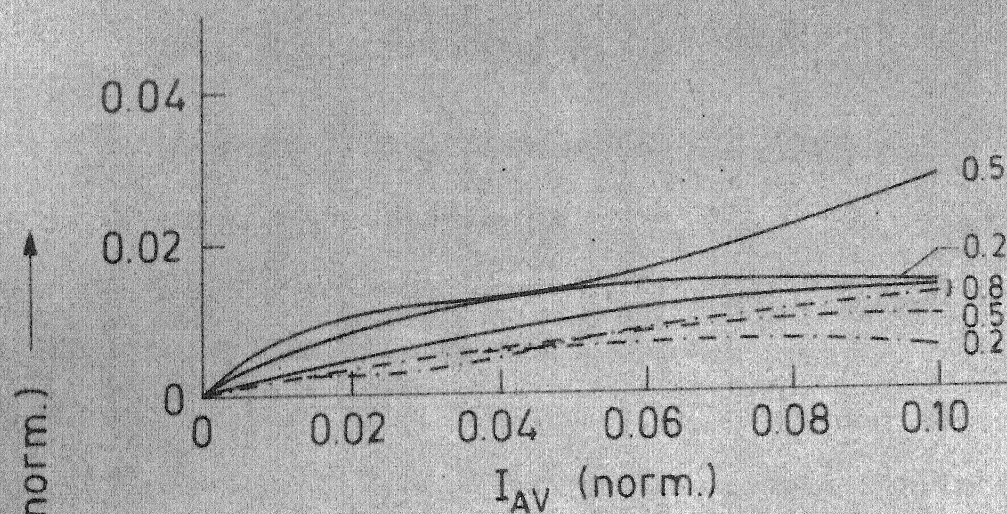
(a) Motoring operation



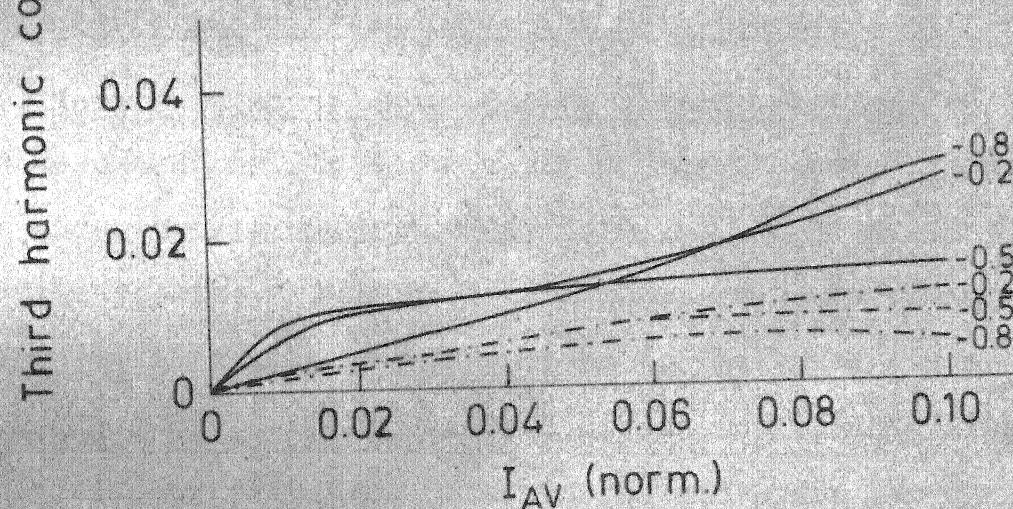
(b) Reverse regeneration

FIG. 3.15. NORMALISED SECOND HARMONIC COMPONENT OF SUPPLY CURRENT vs I_{AV} (NORM.) FOR $T_p=0.2$ AND DIFFERENT VALUES OF BACK E.M.F.

— Approach 1 - - - Approach 2 & 3



(a) Motoring operation



(b) Reverse regeneration

FIG. 3.16. NORMALISED THIRD HARMONIC COMPONENT OF SUPPLY CURRENT vs I_{AV} (NORM.) FOR $T_p = 0.2$ AND DIFFERENT VALUES OF BACK E.M.F.

— Approach 1 - - - Approach 2 & 3

3.5.1 Performance for a highly inductive load:

The p.u. a.c. ripple voltage at output vs. duty cycle has been shown in Fig. 3.3 for all the three approaches. It reveals that maximum a.c. ripple voltage at the output for APPROACH-2 and 3 is 50 percent to that in the APPROACH-1. If output current is assumed ripple free, the waveform of the supply current is similar to that of the output voltage. Thus APPROACH-2 and 3 will result in a 50 percent reduction in the input current harmonics.

3.5.2 Performance comparison for motor load:

1. Nature of motor speed-torque characteristics: The speed torque characteristics for three different control approaches are shown in Fig. 3.8, 3.9 and 3.10. APPROACH-2 and 3, give similar results. Zone of discontinuous conduction is almost twice for APPROACH-1 in comparison to that for the APPROACH-2 or 3. Discontinuous conduction is undesirable as it slows down transient response [4] and gives poor regulations of speed. As normalised time period T_p is increased, zone of discontinuous conduction becomes wider in all the cases. For different values of T_p , change in ches. is observed only in the discont. conduction zone. The characteristics for various values of δ are converging to point (0,1) for the APPROACH-1 while they are converging to (0,1)

in the first quadrant and (0,0) in the fourth quadrant for the APPROACH-3. For the APPROACH-2 characteristics for δ upto 0.5 are converging to (0,0). $\delta > 0.5$ in APPROACH-2 gives first quadrant operation and here characteristics converges to the point (0,1). For APPROACH-1, first and fourth quadrant operation are not distinct as they are in the case of the APPROACH-2 and 3.

2. Maximum armature current ripple: (Ref. Fig. 3.13):

Armature current ripple is a measure of motor heating and commutation problems. For the APPROACH-1 maximum current ripple is double to that for the APPROACH-2 and 3 and it takes place at $\delta = 0.5$ where changeover from one quadrant to another quadrant of operation is due. For APPROACH-2 and 3 there is no ripple at the instant of changeover.

3. Harmonics in supply current: (Ref. Fig. 3.14, 3.15 and 3.16):

Normalised values of first, second and third harmonic components of supply current are drawn against the normalised value of I_{av} for different sets of back emf. I_{av} (norm) upto 0.1 is considered as it covers the range of operation of a motor. As $E_b \cdot I_{av}$ is shaft power, so corresponding to different values of the shaft powers, input harmonics variation can be observed. Similar results were obtained for both the APPROACH-2 and 3. Harmonic content corresponding to a particular shaft power is more for APPROACH-1.

First harmonic content reduces as, speed increases in forward or reverse direction depending upon quadrant of operation for APPROACH-1. For higher values of speeds

harmonic content for APPROACH-1 is comparable to that for APPROACH-2 and 3. For APPROACH-2 and 3 first harmonic in supply current is maximum for mid-range of speeds but still it is quite low in comparison to that corresponding to the APPROACH-1.

Similarly second harmonic and third harmonic contents for all the three approaches are compared, APPROACH-1 has disadvantage of higher harmonic contents. Though for higher speed range in the first quadrant it gives comparable performance to that for the APPROACH-2 and 3.

Input current harmonics are undesirable because they interfere with the communication and other loads connected to the same supply. Third harmonic ^{component} specially becomes important from later consideration. If input voltage V is obtained from an ac source through a rectifier there is a further possibility of obtaining best frequencies in source current i_s . It is seen from Fig. 3.17 that APPROACH-2 and 3 gives better result in comparison to APPROACH-1.

4. Switching losses: Number of commutation cycles per output cycle gives an idea of the constraints over maximum APPROACH-1 has two commutations per output cycle while APPROACH-2 and 3 have one.

3.6 Conclusion:

1. APPROACH-2 and 3 give similar performance. For same output frequency, the frequency of operation of switches is half for APPROACH-2 while it is the same for APPROACH-1 and 3. So switching losses will be less for APPROACH-2.

2. costwise APPROACH-3 is attractive, as S_1 is an ordinary switch.

3. For a ripple free load current, p.u. input current ripple for APPROACH-2 and 3 is just 50 percent of that for the APPROACH-1. So use of APPROACH-2 and 3 reduces the size of the filter at the input terminals.

4. APPROACH-2 and 3 is preferable from the consideration of good speed regulation and faster transient response. Higher the value of T_p , wider is the zone of discontinuous conduction. So high frequency operation should be

preferred. As the output frequency is double the switching frequency for APPROACH-2, one can obtain narrow zone of discontinuous conduction easily by opting for this approach.

5 . A.C. ripple in armature current is reduced to 50 percent for APPROACH-2 and 3 as compared to APPROACH-1. Use of APPROACH-1 will result in more derating of motor and considerable reduction in its efficiency.

6 . For the same output frequency, more switching loss will occur in APPROACH-1.

7 . For APPROACH-1 input harmonic is considerably higher in comparison to APPROACH-2 and 3. These harmonics can interfere with communication system present around and other loads being fed by the same supply.

8 . Boundaries between continuous and discontinuous conduction have been drawn for different values of T_p . This is done to facilitate design of filter.

CHAPTER 4

CONCLUSIONS

The proposed two quadrant chopper with simultaneous control has the advantages of lower trapped energy, increased reliability, lower weight and less cost. No special sequence is required for the charging of capacitor, and there is no piling up of the energy. A spurious trigger on the blocking thyristor is self-healing. Both the thyristors can be turned off simultaneously by removing the gate pulses to them.

The performance of the chopper circuit fabricated has been found satisfactory. The oscillograms of the voltage and current waveforms reveal that only the load voltage and current waveforms show a deviation from the theoretically obtained nature. This deviation can be attributed to the effect of brush drops, armature reaction and the fact that the saturable reactors L_1 and L_2 do not offer negligible inductance under saturation, as assumed. The torque-speed characteristic has been drawn for the motor fed by this chopper in p.u. quantities. The experimental results deviate from the theoretical characteristic. This is probably because of the assumptions taken about the nature of the saturable reactors for the simplicity of analysis. It is confirmed from the oscillograms of the voltage and current waveforms and the

torque-speed characteristic obtained experimentally that the discontinuous conduction is not present. So fast transient response and good speed regulations are obtainable at all loads. Even better results can be obtained if saturable reactors L_1 and L_2 are designed more carefully. This chopper circuit has been tested for a frequency range of 200 to 600 Hz and the performance is found satisfactory. Such a high frequency of operation is usually not possible with dual chopper circuits.

The advantages in terms of lower trapped energy, reliable commutation with self healing capability, absence of discontinuous conduction, higher available frequency of operation, low weight and low cost make this circuit very attractive for the mainline traction and battery operated vehicle applications.

The following important conclusion can be drawn from the comparative study of two quadrant choppers capable of giving positive current and voltage in either direction:

1. For a highly inductive load, APPROACH-2 and 3 are found better than APPROACH-1 as they result in 50 percent reduction in input current ripple and the output voltage ripple.

2. For a motor load also, APPROACH-2 and 3 maintain their superiority over APPROACH-1. They result in 50 percent armature current ripple (maximum value), compared to the later.

3. Area of discontinuous conduction is almost 50 percent for the APPROACH-2 and 3 compared to APPROACH-1. So, better speed regulation and faster transient response are obtained in the former cases.

4. Number of commutation cycles per output cycle is two for APPROACH-1 and one for the other two cases. So switching losses are more in the former case.

5. Input current harmonics are less for APPROACH-2 and 3 compared to APPROACH-1. In higher speed range APPROACH-1 gives performance comparable to APPROACH-2 and 3. If further reduction in harmonics is necessary a cheaper filter will be required in the case of APPROACH-2 and 3.

6. For APPROACH-2, input frequency is half of the output frequency, while it is the same in other two cases. So for the same output frequency, the switching losses are minimum in this case.

7. Cost is the lowest for APPROACH-3, as switch S_1 is realised by an ordinary switch.

APPENDIX A

Details of dc separately excited motor used

Rated voltage	220V
Rated current	11.6A
Rated speed	1500 rpm
Armature resistance	2.08 Ω
Armature inductance	31.4 mH
Back emf constant K_V	1.11
Torque constant K_T	1.11

APPENDIX B

Details of components used in the developed chopper

Thyristors	T12F1000 (inverter grade), 25A, 1000V
Diodes	D_3 and D_4 - 6SM15
	D_1 and D_2 - EC1006, 6A, 1000V
C	8 μ F
L_c	120 μ H
Q	50
T	0.0025 sec.
Saturable chokes L_1 and L_2	75 mH, CRGO grade 51, T-3 stampings are used.

REFERENCES

1. S.M. Sriraghvan, B.D. Pradhan and G.N. Revankar, 'An improved complimentary impulse commutated inverter using saturable reactor', IEEE Trans. on IECI, vol. IECI-28, pp. 50-55, Feb. 1981.
2. S.B. Dewan and A. Straughen, 'Power semiconductor circuits', John Wiley and Sons, 1975, pp. 343-352.
3. G.K. Dubey, 'Calculation of filter inductance for chopper fed dc separately excited motor', Proc. IEEE, vol. 66, No. 12, pp. 1671-73, Dec. 1978.
4. G.K. Dubey and W. Shephard, 'Transient analysis of the dc motor controlled by power pulses', Proc. IEE vol. 124, No. 3, March, 1977, pp. 226-230.
5. A.K. Laha, 'Chopper fed dc motor drive for battery operated vehicle', M.Tech. thesis, IIT Kanpur, Dec. 1980.
6. G.K. Dubey, 'Classification of thyristor commutation methods', IEEE IA Soc. Annual Meeting, Philadelphia, Oct. 1981, pp. 895-905.
7. P.K. Saxena, 'Chopper control of dc separately excited motor', M.Tech., Thesis, IIT Kanpur, August, 1980.
8. Avinash Joshi and S.B. Dewan, 'Current commutated two quadrant thyristor chopper', Power Electronics Specialists conference, Syracuse, New York, 1978, pp. 1-8.
9. SCR manual, 5th Edition - Syracuse, N.Y. General Electric Company 1972.